Mechanics and energetics of walking with powered exoskeletons

by

Gregory Stephen Sawicki

A dissertation submitted in partial fulfillment
of the requirements for the degree of
Doctor of Philosophy
(Kinesiology and Mechanical Engineering)
at The University of Michigan
2007

Doctoral Committee:

Associate Professor Daniel P. Ferris, Chair
Associate Professor Richard B. Gillespie
Associate Professor M. Melissa Gross
Associate Professor Arthur D. Kuo

The picture you have in your mind of what you’re about will come true

-Bob Dylan (1941-)

This dissertation is dedicated to the five Poquott Sawicki's, who have always stood beside me, no matter what.

Acknowledgments

Most of what I learned in graduate school was from people and experiences, not books. So thank you all and stay in touch.

The fam- To this day I look forward to nothing more than spending time with Grandparents, Aunts, Uncles, Cousins and close friends who never pass judgment and simply enjoy each other's company around good food and drink. Thanks for the gatherings. Tent Weekend anyone?

The 'rents- Mom and Dad. I try to emulate the best parts of both of you. Thanks for your never ending interest and support in my work life. Thanks for your friendship. Thanks for your love. I'll be home soon.

The bro'- Brian. Thanks for opening my eyes to life beyond books. Thanks for the time in the mountains. Thanks for the laughs. See you more often?

The sis'- Sarah. You are an incredible teacher. Thanks for the daily lessons. Miss you;)

Habibti- Katia Koelle. Thanks for sharing your creative mind, passionate spirit and thirst for life. Can't wait until we are tenured and sitting in our rockers on the front porch. I love you very much.

dp- Daniel P. Ferris. My academic father. You have taught me many lessons. The most important is an equation: Enthusiasm + intelligence * humility =

dedication * success [respect]. I look forward to following the HNL. Thanks for giving me the opportunity to grow. I hope we continue to interact often.

Art Kuo- You convinced me of the power that simple models hold in parallel with simple experiments. Your fresh theoretical thinking style is enviable. Thanks for the constructive feedback.

Brent Gillespie- Thanks for serving on my committee. Your mechatronics class saved me >1 year in grad school. Thanks for encouraging me to use conceptual modeling and engineering principles to make my work stronger.

Melissa Gross- Thanks for serving on my committee. I will always think twice about my repeated measures ANOVA ;)

kg- Keith E. Gordon. You taught me much of what I know about being a scientist. The time we shared in the basement and the lab shaped my approach. Thanks for the incredible support. Thanks for the pranks. I hope we remain lifelong colleagues and good friends. See you in ChiTown.

Monica Daley- Glad I took five years and not four. The last year interacting with you has been great. You have a gifted mind and a super outlook to go with it. Thanks for trading ideas. Let's continue. See you in the UK ;)

Antoinette Domingo- Do work sista! Antoinette, you rock. I learned everything I know about clinical rehab from you. Your presence always made me more confident. Thanks for the collaboration. You're a great scientist. I hope we stay close colleagues.

Catherine Kinnaird- If evaRT was a virus, you'd be the cure. Thanks for all your help on data collections. Thanks for the snacks. And most of all, thanks for your great personality. I hope you had as much fun as I did on Fridays, fighting the ghost.

Steve Cain- Office mate extraordinaire. Thanks, Steve for sharing the white board and floor space in the office. Go hypergravity!

Jineane Shibuya- Thanks for helping in the lab, your time meticulously tracking data. And your great attitude.

Hnl'ers- Cara Lewis, Pei-Chun Kao, Helen Huang, Becca Stoloff, Evan Pelc, Kate Havens, Andrea Ikeda. Thanks to you all for help with my experiments and good clean intellectual exchange.

Neuromechanists- Peter Adamczyk, Jiro Doke, Jesse Dean, Mike Cherry. Thanks for the weekly forum and excellent critiques.

Felix Huang-The cat. Even-keeled, philosophical Felix. Thanks for supporting my abstract thinking and wacky ideas. You helped keep me a dreamer. See you in Chicago.

Brian Trease- Treaser. You live life more fully than anyone I know and your quest for knowledge goes unmatched. Thanks for showing me the limit. I'm trying to approach it. Chaockey rocks! Go build some robots with compliant brains. See you in Pasadena ;)

Sarah Calve- Thanks for all the chats over beer. Thanks for your incredible sense of humor. See you in Chicago. Go Big Red! See you in Chicago.

Doc Stockers- Steve Collins, Paul Griffiths, Brian Trease, Shawn O'Connor. Thanks for the motivation and deep intellectual discussions. You guys helped shape many of the ideas in this dissertation.

214 W. Ann'ers- Lulu, Kate and Dale. Thanks for being a second family.

Joaquin and Christine- Thanks for hosting Halloween, White Elephant, taco night, and other mini-celebrations. Joaquin, thanks for giving me hell on the basketball court and paying me all that money in lost bets. Christine, thanks for always listening. You guys are great. See you in Dublin?

Ross and Erin- Thanks for impromptu desserts, Trout Lake excursions and a dual shoulder to lean on. See you in Providence and beyond ;)

Annie and Nick- Thanks for hosting dinners, knitting caps and quality time. See you somewhere in the Midwest ;)

Espresso Royale Café- Thanks for fueling the fury.

Blue Room Karaoke- An effective stress relief venue. Thanks for the photo-ops.

UM Intramural Sports- We never took home the coveted T-shirts during my tenure. But good times played out. Go Kinball!

Summer BBQ's- Charcoal briquettes, bring your own grillables and we're good to go. Sunset and mosquitoes at Gallup Park cancel each other out.

Real Rhapsody- For constant musical accompaniment, thank you.

The work in this dissertation was supported by NSF BES-0347479.

Chapters 2, 3 and 4 have been prepared for publication in The Journal of Experimental Biology.

Sawicki GS, and Ferris DP. **Mechanics and energetics of level walking with powered ankle exoskeletons.** Journal of Experimental Biology. In review. 2007.

Sawicki GS, and Ferris DP. **Metabolic cost of ankle joint work during level walking with increasing step length.** Journal of Experimental Biology. To be Submitted. 2007.

Sawicki GS, and Ferris DP. **Mechanics and energetics of incline walking with robotic ankle exoskeletons.** Journal of Experimental Biology. To be Submitted. 2007.

Table of Contents

List of Figures

Figure

List of Tables

Tables

Abstract

Humans conserve energy during walking using an inverted pendulum mechanism during single-limb support. The step-to-step transition requires substantial muscle-tendon mechanical work by the trailing lower limb on the center of mass. Currently we have limited understanding of how the ankle, knee, and hip contribute to center of mass mechanical work and overall metabolic energy expenditure during human walking. I used lightweight bilateral robotic exoskeletons powered with artificial pneumatic muscles to replace ankle joint mechanical work and study changes in users' metabolic energy consumption during walking. First I studied walking on level ground at preferred step length. Ankle exoskeletons replaced 22% of the lower-limb joint positive mechanical power and users saved 10% net metabolic power. For each 1 J of exoskeleton mechanical assistance subjects saved ~1.6 J of metabolic energy. The 'apparent efficiency' of ankle joint muscle-tendon positive mechanical work (0.61) is much higher than for isolated muscle positive mechanical work (0.25). This suggests that Achilles tendon contributes ~60% of the ankle joint positive work, leaving ~40% to active muscle fiber shortening. The ankle joint, therefore, performs 35% of the total lower-limb positive mechanical work but consumes only 17%-20% of the total metabolic energy during level walking at the preferred step length. In the next two experiments I used the powered exoskeletons to study ankle mechanics

and energetics during walking with increasing step lengths and on increasing uphill inclines. Ankle joint 'apparent efficiency' decreased for walking with longer steps (0.39 at 140% of preferred step length) and on uphill gradients (0.38 at 15% grade). Thus, even when the demand for external positive mechanical work is high, the Achilles tendon still delivers 34% or more of the ankle joint positive work during walking. Overall these studies demonstrate that Achilles tendon elastic energy storage and return allows the ankle joint to perform positive mechanical work with very little metabolic cost. In contrast, knee and hip joint positive mechanical work performed by actively shortening muscle fibers likely exacts a much higher metabolic cost. Orthotic devices designed to reduce metabolic energy consumption during walking should target less efficient proximal joints (e.g. hip or knee).

Chapter I

Introduction

Robotic exoskeletons that can enhance human power capabilities are no longer limited to the realm of science fiction. Engineers have been working on exoskeletons to augment human power since the 1970's (Hughes, 1972; Ruthenberg et al., 1997; Seireg and Grundman, 1981; Vukobratovic et al., 1974; Zoss et al., 2006). Recently, the Defense Advanced Research Projects Agency (DARPA) initiated a project to build a lower-limb wearable robot capable of improving soldier endurance, speed, and load carrying ability (Fanelli, 2001; Lemley, 2002; Weiss, 2001). The DARPA project has helped renew interest in the development of robotic exoskeletons to assist locomotion, and recent advances in actuation technology, controls engineering and materials science have propelled the state-of the art quickly forward (Guizzo and Goldstein, 2005). Soldiers aren't the only ones who might benefit from exoskeletons aimed at augmenting human performance. Civilian laborers such as firefighters, construction workers and warehouse personnel could use exoskeletons to reduce the physical demands of climbing, heavy lifting, or long periods of sustained locomotion.

Lower-limb robotic exoskeletons could be a useful tool for conducting basic science research into the mechanics, energetics and control of human locomotion. Recent studies have begun to examine adaptations in electromyography and kinematics during walking with lower-limb powered assistance in both healthy and impaired populations (Dietz et al., 2004; Emken and Reinkensmeyer, 2005; Gordon and Ferris, 2007; Sawicki et al., 2005). But, surprisingly, we found only a single study that has examined the metabolic cost of walking with powered exoskeletons (Norris et al., 2007). This seems quite remarkable given that one of the primary goals of human augmentation technology is to decrease the energy expenditure of the human user.

Some open questions that deserve more attention include: (1) Is it possible to save metabolic energy by wearing a powered exoskeleton during walking? If so, (2) How much practice is required before the mechanical assistance leads to metabolic savings? (3) Would powered exoskeletons perform as well under conditions requiring increased power demands? and (4) How much bang-for-the-buck? i.e. Is there a relationship between the amount of mechanical energy supplied by powered exoskeletons and the amount of metabolic energy saved by the user? It is possible to answer these questions with carefully controlled experiments designed to address the biomechanics and energetics of humans walking with powered exoskeletons. Thus, the overall goal of this dissertation is to determine whether powered assistance at the ankle joint can reduce the metabolic cost of walking. The results will contribute to basic science by elucidating the contribution of ankle joint mechanical power to the metabolic

cost of walking. In addition, we will generate benchmark data that will inform future exoskeleton and prosthesis design.

Background

Biomechanists and physiologists have disputed the sources of metabolic energy expenditure in human locomotion for decades (Alexander, 1991; Cavanagh and Kram, 1985; Elftman, 1939b; Kram, 2000; Saunders et al., 1953; Taylor, 1994; Williams, 1985; Williams and Cavanagh, 1987). Muscles require fuel, or metabolic energy to produce force. Early studies showed that isolated muscle requires some energy during active lengthening contractions (i.e. to produce negative work), a little more energy during isometric contractions (i.e. to produce force but no work) and the most energy during active shortening contractions (i.e. to produce positive work) (Abbott et al., 1952; Bigland-Ritchie and Woods, 1976; Fenn, 1924; Hill, 1938; Hill, 1939; Rall, 1985). Furthermore, the metabolic energy consumption during all of these actions increases with increasing muscle force.

A ‘muscular efficiency’; or the ratio of mechanical energy output to metabolic energy input can be calculated for shortening or lengthening muscle contractions. Isolated muscle experiments have revealed ‘muscular efficiencies’ of approximately 25-30% for positive work and -120% for negative work (Heglund and Cavagna, 1985; Hill, 1939; Woledge, 1985). ‘Muscular efficiency’ can be useful for predicting the energetic cost of whole-body movements that require predominantly positive or negative mechanical power output (Abbott et al., 1952; Aura and Komi, 1986; Bobbert, 1960; Margaria, 1938; Margaria, 1976) but

locomotion is typically rhythmic with muscles performing a mixture of positive and negative work. As result, whole-body calculations of efficiency during human locomotion are extremely variable and can range from 10% to 80% depending on the task and the method of estimating mechanical work (Cavagna and Kaneko, 1977; Willems et al., 1995; Williams, 1985). Work-loop experiments that put muscle under stretch-shortening cycles tend to reflect *in vivo* muscle actions more accurately than purely concentric or purely eccentric experiments (Josephson, 1985; Josephson, 1989). Even measures of muscular efficiency during stretch-shortening actions are inconsistent, yielding efficiencies as low as 15% and as high as 52% (Barclay, 1994; Heglund and Cavagna, 1987). Furthermore, muscle actions *in vivo* are likely very different than those of isolated muscle.

In vivo muscle action is complicated by various aspects of musculoskeletal system organization. Compliance due to elasticity results in complex mechanical interactions between muscles and tendons in series (Roberts, 2002). Tendon stretch may allow overall muscle-tendon lengthening while muscles remain isometric or even shorten. Furthermore, the musculoskeletal system has many more muscles than joints and some muscles cross more than one joint. Thus, knowledge of how a joint is moving may not reflect how the underlying muscles are operating (Prilutsky et al., 1996). These complications make accurate predictions of individual muscle forces and displacements extremely difficult. Ultimately, the relative amounts of positive work, negative work, and isometric

activation summed over all of the muscles must be known to accurately predict the metabolic energy expenditure of a given task.

The link between mechanical energy production and metabolic energy expenditure is tenuous for whole-body movements precisely because it is exceedingly difficult to know the exact actions of muscles *in vivo*. Measurements of metabolic energy expenditure from methods of open-circuit spirometry have been validated and are relatively consistent across the literature (Bertram and Ruina, 2001; Brooks et al., 1996; Elftman, 1966; Zarrugh et al., 1974). In contrast, measurements of muscle mechanical energy production are limited to estimates that can be made from gross movement patterns of the body. External mechanical work done on the center of mass can be estimated using a force platform as an ergometer during gait (Cavagna, 1975; Cavagna et al., 1963). This combined limbs method (CLM) may underestimate muscle mechanical work in two ways: (1) it does not account for mechanical energy used to move segments relative to the center of mass and (2) it does not account for simultaneous mechanical work done on the center of mass by each limb when they are both in contact with the ground. To address energy relative to the center of mass a method was developed to calculate internal work by summing segment energies computed from motion capture techniques through time (Winter, 1979). To address simultaneous work done by the limbs on the center of mass the individual limbs method (ILM) was developed (Donelan et al., 2002a; Donelan et al., 2002b). Other variations using either or both segment energies and force platforms have been demonstrated (Cappozzo et al., 1976; Craik and Oatis,

1995; Elftman, 1939a; Robertson and Winter, 1980). The technique of inverse dynamics was developed to estimate the net muscle moments acting at the joints using force platform data and motion capture data together with a linked segment model of the body and Newton-Euler mechanics (Winter, 1990). With estimated net muscle moments and joint angular velocities the net muscle power (and therefore work) produced by muscles at a joint can be computed (Joint Power Method (JPM)). The joint work can then be summed over all joints to estimate the total net mechanical energy performed by muscles (Winter, 1990). One drawback of inverse dynamics is that it fails to account for muscles that work against each other during movement (co-contractions) and thus may still underestimate the actual work produced by muscles *in vivo*. In addition, it is difficult to account for energy transfer via biarticular muscles. More recently, computer simulations of walking gait that include models of individual muscle-tendon actuators acting at the joints have been used to estimate *in-vivo* muscle work and power (Anderson and Pandy, 2001; Neptune et al., 2004b; Pandy, 2001). In summary, there are many techniques for estimating the mechanical energy produced by muscles, but they are each closely tied to underlying models that may be plagued by unrealistic assumptions.

Despite the difficulties in estimating the mechanical energy production of muscles *in-vivo*, biomechanists have been able to partition the energetic cost of walking and running into factors such as leg swing, body-weight support, forward propulsion, and center of mass movement (Doke et al., 2005; Gottschall and Kram, 2003; Gottschall and Kram, 2005; Grabowski et al., 2005; Griffin et al.,

2003; Hardt and Mann, 1980; Kram, 2000; Myers et al., 1993; Neptune et al., 2001; Neptune et al., 2004a; Neptune et al., 2004b; Saunders et al., 1953; Taylor, 1994). A number of experimental paradigms have been useful in this partitioning of energetic cost. Simulated reduced gravity (Cavagna et al., 2000; Farley and McMahon, 1992; Griffin et al., 1999; Newman et al., 1994), horizontal forces (Boyne et al., 1981; Chang and Kram, 1999; Donovan and Brooks, 1977; Gottschall and Kram, 2003; Lloyd and Zacks, 1972), inclines (Margaria, 1938; Minetti et al., 1993; Pimental and Pandolf, 1979) and added loads (Grabowski et al., 2005; Griffin et al., 2003; Soule et al., 1978) can all perturb locomotion mechanics at the whole-body level to provide insight into the relative metabolic costs of different factors. The findings from these studies have provided many perspectives and a lot of data, but there is still considerable debate about the relative metabolic costs of different biomechanical functions during walking and running.

One aspect of walking mechanics that is not debated is that the majority of the positive mechanical work done on the center of mass is observed at the end of the double-support phase during trailing limb push-off (Donelan et al., 2002a; Donelan et al., 2002b; Kuo et al., 2005). Inverse dynamics can be used to get at possible sources of this push-off power burst by partitioning center of mass work into contributions from the hip, knee, and ankle. Although few studies have quantified joint work directly, estimates from inverse dynamics power curves over a full walking stride suggest that the ankle joint supplies up to half of the total positive mechanical work summed over the lower-limb joints for level, preferred

speed walking (Winter, 1991). Furthermore, during the double support phase of walking, ankle joint positive work accounts for up to 70% of the positive work summed across the joints (Meinders et al., 1998). Thus, the ankle joint extensors may be the primary power source during the trailing limb push-off in level walking (Gitter et al., 1991; Gottschall and Kram, 2003; Kuo et al., 2005).

In this dissertation, I employed a new experimental paradigm that can alter the mechanical work required by muscle-tendon at the level of the joints. The paradigm is novel because previous studies have only perturbed center of mass level mechanics and thus have not been able to isolate the contributions of muscle-tendons at a single joint to the metabolic cost of locomotion. We have developed a pneumatically powered lower-limb orthosis (i.e. exoskeleton) that humans can comfortably wear during relatively long periods of treadmill locomotion (Ferris et al., 2005; Ferris et al., 2006; Gordon et al., 2006). It consists of a lightweight carbon fiber shell with a hinge joint at the ankle and a single artificial pneumatic muscle that can provide high power outputs while adding minimal weight. The artificial pneumatic muscle is activated using proportional myoelectrical control. Air pressure in the muscle is adjusted based on the amplitude of the surface electromyography (EMG) signal generated by the soleus muscle from the person wearing the exoskeleton. This results in a very natural and physiologically relevant means of exoskeleton control to which humans quickly adapt (Gordon and Ferris, 2007). Our powered ankle exoskeletons can reach a maximum of 50% of the net muscle moment and can

produce ~65%-75% of the positive work (12-14 J unilateral) observed at the ankle during normal locomotion (i.e. without the exoskeleton) at 1.25 m/s.

If the ankle joint produces the majority of the lower-limb positive mechanical work during push-off then it should be possible to reduce metabolic cost of walking with an external power source at the ankle. Inverse dynamics analyses indicate that 35%-50% of the positive work during a walking step is observed at the ankle joint (Eng and Winter, 1995). Our previous work indicates that our exoskeletons can supply 12-14 J or ~75% of the total ankle positive work over a step. Furthermore, with practice, the exoskeletons deliver mechanical power at the right time during gait (i.e. exoskeletons do not absorb energy). Therefore, if ankle joint positive work constitutes 35%-50% of the total positive work done across the joints, and we can supply up to 75% of that ankle work with our exoskeletons in each step, the positive muscle-tendon work required by the user's ankle joint would be reduced by 25%-38%. If we accept that lower-limb joint mechanical work is proportional to net metabolic cost, and that most of the ankle joint work is performed by active muscles, then metabolic energy consumption during powered walking should decrease by up to 38% when comparing powered to unpowered walking. On the other hand, it could be that humans have adopted optimal walking mechanics such that powered assistance cannot reduce the metabolic cost of walking at all (Alexander, 2002; Bertram, 2005; Bertram and Ruina, 2001; Kuo, 2001; Srinivasan and Ruina, 2006).

In Chapter II, I examine whether bilateral powered ankle exoskeletons can reduce the metabolic cost of level preferred step length walking at 1.25 m/s.

In the next two chapters I study the effect of increasing center of mass mechanical workload on exoskeleton performance. In Chapter III, I examine the effect of walking step length on the performance of powered ankle exoskeletons to reduce the metabolic cost of walking. In Chapter IV, I study the effect of surface incline on the performance of powered ankle exoskeletons to reduce the metabolic cost of walking.

In each chapter I estimate the ankle joint 'apparent efficiency' of positive muscle-tendon mechanical work by computing the ratio of exoskeletons' average positive mechanical power to subjects' reduction in net metabolic power. If all of the positive mechanical work produced by the ankle exoskeletons goes to reduce underlying positive *muscle* work at the ankle joint, the reduction in net metabolic cost should be four times the amount of exoskeleton mechanical assistance (i.e. 'apparent efficiency' of ankle positive mechanical work of ~0.25). If however, part of the work at the joint is produced by recoiling Achilles tendon, the reduction in net metabolic cost might be less than four times the amount of exoskeleton mechanical assistance, yielding 'apparent efficiency' of ankle positive mechanical work > 0.25. Therefore, a measure of the efficiency at which mechanical power is transferred from a powered ankle exoskeleton to the biological ankle muscle-tendon system is an indicator of the relative contribution of elastic energy storage and return versus active muscle shortening to total ankle joint positive mechanical work under different walking conditions.

In summary, we know that ankle exoskeletons can produce mechanical power when attached to a walking human. The physiological response of the

human user to exoskeleton mechanical assistance is difficult to predict because a consistent relationship between the mechanics and energetics of human walking has not been established. This dissertation will examine the contribution of ankle joint positive mechanical work to the metabolic cost of human walking by adding powered assistance at the ankle while directly monitoring metabolic energy expenditure through oxygen uptake measurements. The results will give insight into the relative distribution of mechanical and metabolic energy expenditure across the lower-limb joints during human walking and inform future designs for robotic exoskeletons and powered prostheses.

References

Abbott, B. C., Bigland, B. and Ritchie, J. M. (1952). The physiological cost of negative work. *Journal of Physiology (London)* **117**, 380-390.

Alexander, R. M. (1991). Energy-saving mechanisms in walking and running. *Journal of Experimental Biology* **160**, 55-69.

Alexander, R. M. (2002). Energetics and optimization of human walking and running: The 2000 Raymond Pearl Memorial Lecture. *American Journal of Human Biology* **14**, 641-648.

Anderson, F. C. and Pandy, M. G. (2001). Dynamic optimization of human walking. *Journal of Biomechanical Engineering* **123**, 381-90.

Aura, O. and Komi, P. V. (1986). Mechanical Efficiency of Pure Positive and Pure Negative Work with Special Reference to the Work Intensity. *International Journal of Sports Medicine* **7**, 44-49.

Barclay, C. J. (1994). Efficiency of fast- and slow-twitch muscles of the mouse performing cyclic contractions. *Journal of Experimental Biology* **193**, 65-78.

Bertram, J. E. (2005). Constrained optimization in human walking: cost minimization and gait plasticity. *J Exp Biol* **208**, 979-91.

Bertram, J. E. and Ruina, A. (2001). Multiple walking speed-frequency relations are predicted by constrained optimization. *J Theor Biol* **209**, 445-53.

Bigland-Ritchie, B. and Woods, J. J. (1976). Integrated electromyogram and oxygen uptake during positive and negative work. *Journal of Physiology (London)* **260**, 267-77.

Bobbert, A. C. (1960). Physiological comparison of three types of ergometry. *Journal of Applied Physiology* **15**, 1007-1014.

Boyne, A. W., Brockway, J. M., Ingram, J. F. and Williams, K. (1981). Modification, by tractive loading, of the energy cost of walking in sheep, cattle and man. *Journal of Physiology (London)* **315**, 303-16.

Brooks, G. A., Fahey, T. D. and White, T. G. (1996). Exercise physiology: human bioenergetics and its applications. Mountain View, Calif.: Mayfield.

Cappozzo, A., Figura, F. and Marchetti, M. (1976). The interplay of muscular and external forces in human ambulation. *J Biomech* **9**, 35-43.

Cavagna, G. A. (1975). Force platforms as ergometers. *J. Appl. Physiol.* **39**, 174-179.

Cavagna, G. A. and Kaneko, M. (1977). Mechanical work and efficiency in level walking and running. *Journal of Physiology (London)* **268**, 647-681.

Cavagna, G. A., Saibene, F. P. and Margaria, R. (1963). External work in walking. *J. Appl. Physiol.* **18**, 1-9.

Cavagna, G. A., Willems, P. A. and Heglund, N. C. (2000). The role of gravity in human walking: pendular energy exchange, external work and optimal speed. *Journal of Physiology (London)* **528**, 657-668.

Cavanagh, P. R. and Kram, R. (1985). Mechanical and muscular factors affecting the efficiency of human movement. *Med Sci Sports Exerc* **17**, 326-31.

Chang, Y. H. and Kram, R. (1999). Metabolic cost of generating horizontal forces during human running. *Journal of Applied Physiology* **86**, 1657-62.

Craik, R. L. and Oatis, C. A. (1995). Gait Analysis: Theory and Application. St. Louis, MO: Mosby.

Dietz, V., Colombo, G. and Muller, R. (2004). Single joint perturbation during gait: neuronal control of movement trajectory. *Experimental Brain Research* **158**, 308-16.

Doke, J., Donelan, J. M. and Kuo, A. D. (2005). Mechanics and energetics of swinging the human leg. *Journal of Experimental Biology* **208**, 439-45.

Donelan, J. M., Kram, R. and Kuo, A. D. (2002a). Mechanical work for step-to-step transitions is a major determinant of the metabolic cost of human walking. *Journal of Experimental Biology* **205**, 3717-27.

Donelan, J. M., Kram, R. and Kuo, A. D. (2002b). Simultaneous positive and negative external mechanical work in human walking. *J Biomech* **35**, 117-24.

Donovan, C. M. and Brooks, G. A. (1977). Muscular efficiency during steady-rate exercise. II. Effects of walking speed and work rate. *Journal of Applied Physiology* **43**, 431-9.

Elftman, H. (1939a). Forces and energy changes in the leg during walking. *American Journal of Physiology* **125**, 339-356.

Elftman, H. (1939b). The function of muscles in locomotion. *American Journal of Physiology* **125**, 357-366.

Elftman, H. (1966). Biomechanics of muscle with particular application to studies of gait. *J Bone Joint Surg Am* **48**, 363-77.

Emken, J. L. and Reinkensmeyer, D. J. (2005). Robot-enhanced motor learning: accelerating internal model formation during locomotion by transient dynamic amplification. *IEEE Transactions on Neural Systems and Rehabilitation Engineering* **13**, 33-9.

Eng, J. J. and Winter, D. A. (1995). Kinetic analysis of the lower limbs during walking: what information can be gained from a three-dimensional model? *J Biomech* **28**, 753-758.

Fanelli, S. (2001). Power dressing. *New Scientist*, 33-35.

Farley, C. T. and McMahon, T. A. (1992). Energetics of walking and running: insights from simulated reduced-gravity experiments. *Journal of Applied Physiology* **73**, 2709-2712.

Fenn, W. O. (1924). The relation between the work performed and the energy liberated in muscular contraction. *Journal of Physiology, London* **58**, 373-395.

Ferris, D. P., Czerniecki, J. M. and Hannaford, B. (2005). An ankle-foot orthosis powered by artificial pneumatic muscles. *J Appl Biomech* **21**, 189-197.

Ferris, D. P., Gordon, K. E., Sawicki, G. S. and Peethambaran, A. (2006). An improved powered ankle-foot orthosis using proportional myoelectric control. *Gait and Posture* **23**, 425-8.

Gitter, A., Czerniecki, J. M. and DeGroot, D. M. (1991). Biomechanical analysis of the influence of prosthetic feet on below-knee amputee walking. *American Journal of Physical Medicine and Rehabilitation* **70**, 142-8.

Gordon, K. E. and Ferris, D. P. (2007). Learning to walk with a robotic ankle exoskeleton. *J Biomech* **in press**.

Gordon, K. E., Sawicki, G. S. and Ferris, D. P. (2006). Mechanical performance of artificial pneumatic muscles to power an ankle-foot orthosis. *J Biomech* **39**, 1832-41.

Gottschall, J. S. and Kram, R. (2003). Energy cost and muscular activity required for propulsion during walking. *J Appl Physiol* **94**, 1766-72.

Gottschall, J. S. and Kram, R. (2005). Energy cost and muscular activity required for leg swing during walking. *J Appl Physiol* **99**, 23-30.

Grabowski, A., Farley, C. T. and Kram, R. (2005). Independent metabolic costs of supporting body weight and accelerating body mass during walking. *J Appl Physiol* **98**, 579-83.

Griffin, T. M., Roberts, T. J. and Kram, R. (2003). Metabolic cost of generating muscular force in human walking: insights from load-carrying and speed experiments. *Journal of Applied Physiology* **95**, 172-83.

Griffin, T. M., Tolani, N. A. and Kram, R. (1999). Walking in simulated reduced gravity: mechanical energy fluctuations and exchange. *Journal of Applied Physiology* **86**, 383-90.

Guizzo, E. and Goldstein, H. (2005). The rise of the body bots. *IEEE Spectrum* **42**, 50-56.

Hardt, D. E. and Mann, R. W. (1980). A five body--three dimensional dynamic analysis of walking. *J Biomech* **13**, 455-7.

Heglund, N. C. and Cavagna, G. A. (1985). Efficiency of vertebrate locomotory muscles. *Journal of Experimental Biology* **115**, 283-292.

Heglund, N. C. and Cavagna, G. A. (1987). Mechanical work, oxygen consumption, and efficiency in isolated frog and rat muscle. *American Journal of Physiology* **253**, C22-29.

Hill, A. V. (1938). The heat of shortening and the dynamic constants of muscle. *Proceedings of the Royal Society of London: Biological Sciences* **B126**, 136-195.

Hill, A. V. (1939). The mechanical efficiency of frog's muscle. *Proceedings of the Royal Society of London: Biological Sciences* **127**, 434-451.

Hughes, J. (1972). Powered lower limb orthotics in paraplegia. *Paraplegia* **9**, 191-193.

Josephson, R. K. (1985). Mechanical power output from striated muscle during cyclic contraction. *Journal of Experimental Biology* **114**, 493-512.

Josephson, R. K. (1989). Power Output From Skeletal Muscle During Linear and Sinusoidal Shortening. *Journal Of Experimental Biology* **147**, 533-537.

Kram, R. (2000). Muscular force or work: what determines the metabolic energy cost of running? *Exerc Sport Sci Rev* **28**, 138-43.

Kuo, A. D. (2001). A simple model of bipedal walking predicts the preferred speed-step length relationship. *Journal of Biomechanical Engineering* **123**, 264-9.

Kuo, A. D., Donelan, J. M. and Ruina, A. (2005). Energetic consequences of walking like an inverted pendulum: step-to-step transitions. *Exerc Sport Sci Rev* **33**, 88-97.

Lemley, B. (2002). Future tech: really special forces. *Discover* **23**, 25-26.

Lloyd, B. B. and Zacks, R. M. (1972). The mechanical efficiency of treadmill running against a horizontal impeding force. *Journal of Physiology (London)* **223**, 355-63.

Margaria, R. (1938). Sulla fisiologia e specialmente sul consumo energetico della marcia e della corsa a varie velocita ed inclinazioni del terreno. *Atti Accad. Naz. Lincei Memorie, serie VI* **7**, 299-368.

Margaria, R. (1976). Biomechanics and energetics of muscular exercise. Oxford: Clarendon Press.

Meinders, M., Gitter, A. and Czerniecki, J. M. (1998). The role of ankle plantar flexor muscle work during walking. *Scandinavian Journal of Rehabilitation Medicine* **30**, 39-46.

Minetti, A. E., Ardigo, L. P. and Saibene, F. (1993). Mechanical determinants of gradient walking energetics in man. *Journal of Physiology (London)* **472**, 725-35.

Myers, M. J., Steudel, K. and White, S. C. (1993). Uncoupling the correlates of locomotor costs: a factorial approach. *J Exp Zoolog A Comp Exp Biol* **265**, 211-23.

Neptune, R. R., Kautz, S. A. and Zajac, F. E. (2001). Contributions of the individual ankle plantar flexors to support, forward progression and swing initiation during walking. *J Biomech* **34**, 1387-98.

Neptune, R. R., Zajac, F. E. and Kautz, S. A. (2004a). Muscle force redistributes segmental power for body progression during walking. *Gait and Posture* **19**, 194-205.

Neptune, R. R., Zajac, F. E. and Kautz, S. A. (2004b). Muscle mechanical work requirements during normal walking: the energetic cost of raising the body's center-of-mass is significant. *J Biomech* **37**, 817-25.

Newman, D. J., Alexander, H. L. and Webbon, B. W. (1994). Energetics and mechanics for partial gravity locomotion. *Aviation Space and Environmental Medicine* **65**, 815-823.

Norris, J. A., Granata, K. P., Mitros, M. R., Byrne, E. M. and Marsh, A. P. (2007). Effect of augmented plantarflexion power on preferred walking speed and economy in young and older adults. *Gait Posture* **25**, 620-7.

Pandy, M. G. (2001). Computer modeling and simulation of human movement. *Annual Review of Biomedical Engineering* **3**, 245-73.

Pimental, N. A. and Pandolf, K. B. (1979). Energy expenditure while standing or walking slowly uphill or downhill with loads. *Ergonomics* **22**, 963-73.

Prilutsky, B. I., Petrova, L. N. and Raitsin, L. M. (1996). Comparison of mechanical energy expenditure of joint moments and muscle forces during human locomotion. *J Biomech* **29**, 405-15.

Rall, J. A. (1985). Energetic aspects of skeletal muscle contraction: implications of fiber types. *Exerc Sport Sci Rev* **13**, 33-74.

Roberts, T. J. (2002). The integrated function of muscles and tendons during locomotion. *Comparative Biochemistry and Physiology A: Molecular and Integrative Physiology* **133**, 1087-99.

Robertson, D. G. and Winter, D. A. (1980). Mechanical energy generation, absorption and transfer amongst segments during walking. *J Biomech* **13**, 845-854.

Ruthenberg, B. J., Wasylewski, N. A. and Beard, J. E. (1997). An experimental device for investigating the force and power requirements of a powered gait orthosis. *Journal of Rehabilitation Research and Development* **34**, 203-213.

Saunders, J. B., Inman, V. T. and Eberhart, H. D. (1953). The major determinants in normal and pathological gait. *Journal of Bone and Joint Surgery* **35**, 543-558.

Sawicki, G. S., Gordon, K. E. and Ferris, D. P. (2005). Powered lower limb orthoses: applications in motor adaptation and rehabilitation. In *IEEE International Conference on Rehabilitation Robotics*. Chicago, IL: IEEE.

Seireg, A. and Grundman, J. G. (1981). Design of a multitask exoskeletal walking device for paraplegics. In *Biomechanics of Medical Devices*, (ed. D. N. Ghista), pp. 569-639. New York: Marcel Dekker, Inc.

Soule, R. G., Pandolf, K. B. and Goldman, R. F. (1978). Energy expenditure of heavy load carriage. *Ergonomics* **21**, 373-81.

Srinivasan, M. and Ruina, A. (2006). Computer optimization of a minimal biped model discovers walking and running. *Nature* **439**, 72-5.

Taylor, C. R. (1994). Relating mechanics and energetics during exercise. *Advances in Veterinary Science and Comparative Medicine* **38A**, 181-215.

Vukobratovic, M., Hristic, D. and Stojiljkovic, Z. (1974). Development of active anthropomorphic exoskeletons. *Medical & Biological Engineering* **12**, 66-80.

Weiss, P. (2001). Dances with robots. *Science News* **159**, 407-408.

Willems, P. A., Cavagna, G. A. and Heglund, N. C. (1995). External, internal and total work in human locomotion. *Journal of Experimental Biology* **198**, 379-393.

Williams, K. R. (1985). The relationship between mechanical and physiological energy estimates. *Med Sci Sports Exerc* **17**, 317-25.

Williams, K. R. and Cavanagh, P. R. (1987). Relationship between distance running mechanics, running economy, and performance. *Journal of Applied Physiology* **63**, 1236-45.

Winter, D. A. (1979). A new definition of mechanical work done in human movement. *Journal of Applied Physiology* **46**, 79-83.

Winter, D. A. (1990). Biomechanics and Motor Control of Human Movement. New York: John Wiley & Sons.

Winter, D. A. (1991). The biomechanics and motor control of human gait: normal, elderly and pathological. Waterloo, Ontario: Waterloo Biomechanics.

Woledge, R. C. (1985). Energetic aspects of muscle contraction. London: Academic Press.

Zarrugh, M. Y., Todd, F. N. and Ralston, H. J. (1974). Optimization of energy expenditure during level walking. *Eur J Appl Physiol Occup Physiol* **33**, 293-306.

Zoss, A. B., Kazerooni, H. and Chu, A. (2006). Biomechanical Design of the Berkeley Lower Extremity Exoskeleton (BLEEX). *IEEE/ASME Transactions on Mechatronics* **11**, 128-138.

Chapter II

Mechanics and energetics of level walking with powered ankle exoskeletons

Summary

Robotic lower-limb exoskeletons that can alter joint mechanical power output are novel tools for studying the relationship between the mechanics and energetics of human locomotion. We built pneumatically-powered ankle exoskeletons controlled by the user's own soleus electromyography (i.e. proportional myoelectric control) to determine whether mechanical assistance at the ankle joint could reduce the metabolic cost of level, steady-speed human walking. We hypothesized that subjects would reduce their net metabolic power in proportion to the average positive mechanical power delivered by the bilateral ankle exoskeletons. Nine healthy individuals completed three 30 minute sessions walking at 1.25 m/s while wearing the exoskeletons. Over the three sessions, subjects' net metabolic energy expenditure during powered walking progressed from +7% to -10% of that during unpowered walking. With practice, subjects significantly reduced soleus muscle activity (by ~28% RMS EMG, $p < 0.0001$) and negative exoskeleton mechanical power (-0.09 W/kg at the beginning of session 1 and -0.03 W/kg at the end of session 3; ($p = 0.005$)). Ankle joint

kinematics returned to similar patterns as unpowered walking. At the end of the third session, the powered exoskeletons delivered ~63% of the average ankle joint positive mechanical power and ~22% of the total positive mechanical power generated by all of the joints summed (ankle, knee and hip) during unpowered walking. Decreases in total joint positive mechanical power due to powered ankle assistance (~22%) were not proportional to reductions in net metabolic power (~10%). The 'apparent efficiency' of the ankle joint muscle-tendon system was >0.25 (~0.61) during human walking suggesting that recoiling Achilles tendon contributes a significant amount of ankle joint positive power during push-off.

Keywords: Locomotion, walking, metabolic cost, exoskeletons, ankle, human, efficiency, inverse dynamics, joint power

Introduction

Humans are adept at harnessing the passive dynamics of their lower limbs to save energy during each walking step (Alexander, 1991; Cavagna et al., 2002; Kuo et al., 2005). During the single support phase, the center of mass trajectory approximates that of an energy conserving inverted pendulum (Alexander, 1995; Cavagna and Margaria, 1966; Kuo et al., 2005). As the center of mass moves upward then downward along a curved arc, gravitational potential energy and kinetic energy cycle nearly out of phase so that, in theory, zero mechanical work is required to sustain motion (Cavagna et al., 1976). The swing leg also behaves like a pendulum and will oscillate freely near its natural frequency with very little energy input (Mochon and McMahon, 1980). If swing and stance leg dynamics

are matched so that they share a common cycle period, very little mechanical energy is required over a step. However, despite the available energy saving pendular mechanisms, walking still requires a significant amount of metabolic energy (Kuo et al., 2005).

Walking like an inverted pendulum has energetic consequences. Pendular exchange can only occur within a single step. At the end of each step, the leading leg collides into the ground, negative work is performed on the center of mass and energy is lost. In order to maintain steady walking, (i.e. zero net work on the center of mass over a stride) the lost energy must be exactly replaced. Active muscle work is required to redirect the velocity of the center of mass from the downward portion of one inverted pendulum to the upward portion of the next. Donelan et al. examined the mechanics of the step to step transition in detail using two force platforms to simultaneously record the ground reaction forces exerted by each limb during the double support phase of walking. They found that while the leading limb performs negative work during the collision the trailing limb performs simultaneous positive work to restore most of the energy of the center of mass (Donelan et al., 2002b). For walking at 1.25 m/s ~70% of the positive work performed on the center of mass is performed during double support (15.4 J of 21.7 J total). Furthermore, the mechanical work performed during double support increases with increasing step length and exacts a proportional metabolic cost (Donelan et al., 2002a). The combined results of these studies indicate that step-to-step transitions are a major determinant of the

metabolic cost during level walking (Donelan et al., 2002a; Donelan et al., 2002b; Kuo et al., 2005).

Other studies combining measurements of oxygen consumption and center of mass level mechanics support the idea that step-to-step transitions are costly. Gottschall et al. studied the cost of propulsion during walking using a horizontal pulling apparatus to apply aiding and impeding forces via a harness attached to the waist (Gottschall and Kram, 2003). When subjects walked at 1.25 m/s with an optimal aiding force of 10% bodyweight, forward directed impulse on the ground was minimized (21% of normal) and net metabolic cost decreased to 53% of normal walking. These results indicate that the propulsive push-off phase of walking could account for 47% of the metabolic cost of walking. In another study employing center of mass level perturbations, Grabowski et al. examined the relative costs of supporting bodyweight versus accelerating the center of mass during walking (Grabowski et al., 2005). They added weight to the hips and used an upward directed force to offset the additional load and isolate the effects of added mass only. They determined that the cost of mechanical work to redirect the center of mass velocity comprises ~45% of the metabolic cost of normal walking and is almost twice as great as the cost to support bodyweight.

One considerable drawback to studies employing center of mass level mechanical analyses is that they cannot directly address the relative roles of the lower-limb joints in generating mechanical power during walking. Although it is clear that a substantial amount of work is done by the trailing limb during double support, our understanding of how the ankle, knee, and hip joints generate that

energy is limited. Inverse dynamics can be used to get at possible sources of the push-off power burst by partitioning joint work into contributions from the hip, knee, and ankle (Winter, 1990). Few studies have quantified joint work directly, but estimates from single limb joint power curves over a full walking stride at 1.6 m/s suggest that the ankle (~38%) and hip (~50%) combine to generate the majority of the positive work summed over the lower-limb joints (Eng and Winter, 1995). However, when viewing only the push-off period of double support, it is evident that the ankle joint contributes more power than either the hip or knee (Kuo et al., 2005; Winter, 1991). Without direct *in vivo* measurements of triceps surae-Achilles tendon dynamics, it is difficult to assess whether the majority of ankle joint push-off power is generated by positive work performed by muscle or by tendon recoil.

Elastic energy released from a recoiling Achilles tendon may be a critical power source during human walking. Recent advances in ultrasonography have facilitated examination of muscle-tendon interaction dynamics during walking (Fukunaga et al., 2001; Ishikawa et al., 2005; Lichtwark and Wilson, 2006). Results between studies are consistent and indicate that both soleus and gastrocnemius muscles perform some but not all of the ankle joint positive work during push-off. Furthermore, the Achilles tendon undergoes a substantial amount of displacement and recoils in a ‘catapult action’, allowing muscles to remain nearly isometric, at an operating point favoring efficient force production.

Powered lower-limb exoskeletons offer a novel means to alter the mechanics of walking at the level of the joints (rather than the center of mass)

and study the human physiological response. Recently, Gordon et al. used a unilateral powered lower-limb orthosis to study motor adaptation during walking. The results showed that humans can rapidly learn to walk with ankle joint mechanical assistance controlled by their own soleus muscle (i.e. under proportional myoelectric control) (Gordon and Ferris, 2007). Over two thirty minute powered walking practice sessions individuals altered their soleus muscle activation to command distinct bursts of exoskeleton power focused at the push-off phase of walking. Although these results suggest that the human nervous system can selectively alter muscle activation patterns to produce efficient exoskeleton mechanics, measurements of the user's metabolic energy expenditure were not taken to assess changes in metabolic cost.

The purpose of the present study was to quantify the metabolic cost of ankle joint work during level walking. We used bilateral powered exoskeletons to alter joint level mechanics in order to answer two questions: (1) How much can powered plantar flexion assistance during push-off reduce the metabolic cost of walking? (2) What is the 'apparent efficiency' of ankle joint work? Isolated muscles generate positive mechanical work with an efficiency of 0.25 (i.e. 1 J positive mechanical energy consumes 4 J metabolic energy) (Fenn, 1924; Hill, 1938). We assumed that the positive mechanical work delivered by the powered exoskeletons' artificial muscles would directly replace biological ankle extensor positive muscle work. Thus, we hypothesized that for every 1 Joule of positive work the exoskeletons delivered, the user would save 4 Joules of metabolic energy. Further, we expected that the net metabolic power would be reduced in

proportion to the relative contribution of exoskeleton positive work to the summed positive joint work (ankle + knee +hip) over a stride. Stated differently, we hypothesized that ankle joint work is performed with an 'apparent efficiency' equal to 0.25, reflecting underlying positive work performed by ankle extensor muscles. We also expected reduced muscle activation amplitudes in the triceps surae group during powered walking. To test these ideas we compared subjects' net metabolic power and electromyography amplitudes with exoskeletons powered versus unpowered during level, steady-speed walking. In addition, for powered walking we used measurements of artificial muscle forces and moment arm lengths to compute the average mechanical power delivered by the exoskeletons over a stride. With simultaneous measurements of the mechanics and energetics of powered walking we computed the 'apparent efficiency' of ankle joint positve work to gain insight into underlying ankle extensor muscle-tendon function. Studying the relationship between the mechanics and energetics at the level of the joints is an important step in integrating results from isolated muscle experiments with whole-body locomotion.

Materials and methods

Subjects. We recruited nine (4 males, 5 females) healthy subjects (body mass = 77.8 ± 12.4 kg; height = 179 ± 9 cm; leg length = 93 ± 5 cm (mean ± s.d.)) who exhibited no gait abnormalities and had not previously walked with powered exoskeletons. Each participant read and signed a consent form prepared according the Declaration of Helsinki and approved by the University of Michigan Institutional Review Board for human subject research.

Exoskeletons. We constructed bilateral, custom-fitted ankle-foot orthoses (i.e. exoskeletons) for each subject (**Figure 2.1**). Details on the design and performance of the exoskeletons are documented elsewhere (Ferris et al., 2005; Ferris et al., 2006; Gordon et al., 2006). Briefly, the lightweight exoskeletons (mass = 1.21 ± 0.12 kg each) consisted of a polypropylene foot section attached to a carbon fiber shank with a hinge joint that allowed free motion about the ankle flexion-extension axis of rotation. We attached artificial pneumatic muscles (length = 46.0 ± 1.7 cm) along the posterior shank between two stainless steel brackets (moment arm = 10.4 ± 1.2 cm) to provide augmented plantar flexor torque. A physiologically-inspired controller incorporated the user's own soleus electromyography to dictate the timing and amplitude of mechanical assistance (i.e. proportional myoelectric control) (Gordon and Ferris, 2007).

Protocol. Subjects practiced walking with bilateral ankle exoskeletons on a motorized treadmill set to 1.25 m/s during three separate practice sessions (**Session 1**, **Session 2**, **Session 3**) (**Figure 2.1**). Our previous work with a unilateral exoskeleton showed that changes in kinematics and electromyography reached steady-state after two thirty minute practice sessions. We chose three sessions based on pilot studies that indicated no further reduction in net metabolic power during powered walking with an additional practice during a fourth session (n = 3, ANOVA p = 0.97). Thus, we considered data from the end of the third practice session as representative of adapted powered walking. The practice sessions were separated by three to five days to allow for motor

consolidation (Gordon and Ferris, 2007; Shadmehr and Holcomb, 1997). Each session followed the same walking timeframe (**Figure 2.1**).

At the start of the session subjects walked for 10 minutes wearing bilateral ankle exoskeletons unpowered (**Unpowered**). Subjects then completed 30 minutes of walking with the exoskeletons powered (**Powered**). Finally, subjects walked for 15 minutes with exoskeletons unpowered (**Unpowered**). Subjects chose their preferred step length, step width, and step frequency throughout. We tuned the gain and threshold of the proportional myoelectric controller during the initial unpowered walking bout so that the control signal saturated for at least five consecutive steps. We then doubled the gain to encourage reduction in soleus muscle recruitment (Gordon and Ferris, 2007).

We collected ten second trials (~7 full strides) of kinematic, electromyographic and artificial muscle force data at the beginning of each minute during each practice session. Metabolic data were collected continuously. For analysis, we averaged data from minutes 7-9 of the first unpowered bout (**Unpowered Beginning**), minutes 3-5 (**Powered Beginning**) and 27-29 (**Powered End**) of the powered bout and minutes 12-14 of the second unpowered bout (**Unpowered End**).

Metabolic Cost. We used an open-circuit spirometry system (Physiodyne Instruments, Quogue, NY, USA) to record O_2 and CO_2 flow rates (Blaxter, 1989; Brooks et al., 1996). We converted averaged flow rates for each of the two minute analysis intervals to units of metabolic power (Watts) using the standard equations documented by Brockway (Brockway, 1987). To obtain the net

metabolic power we averaged data from minutes 4-6 of a seven minute quiet standing trial and subtracted it from the gross metabolic power (Griffin et al., 2003; Poole et al., 1992). Net metabolic power values were then divided by subject mass. Throughout each session, care was taken to monitor the respiratory exchange ratio (RER) and ensure that subjects stayed in their aerobic range (RER < 1) (Brooks et al., 1996). We used the net metabolic power from the **Unpowered Beginning** interval to compute percentage differences between unpowered and powered walking during each session.

Kinematics. We used an 8-camera video system (frame rate 120 Hz, Motion Analysis Corporation, Santa Rosa, CA, USA) and placed twenty-nine reflective markers on the subjects' pelvis and lower limbs and recorded their positions during treadmill walking. We used custom software (Visual 3D, C-Motion, Rockville, MD) to apply a 4^{th}-order Butterworth low-pass filter (cutoff frequency 6 Hz) and smooth raw marker data. Using the smoothed marker data, we calculated joint angles (relative to neutral standing posture) and angular velocities (ankle, knee, hip) for both legs. We marked heel-strike and toe-off events using footswitches (1200 Hz, B & L Engineering, Tustin, CA, USA) and calculated the step period (time from heel-strike of one leg to heel-strike of the other leg) and double support period (time from heel-strike of one leg to toe-off of the other). To calculate step length and step width we computed the fore-aft and lateral distances between calcaneus markers at heel-strike. Joint angles for the right and left legs were averaged from heel-strike (0%) to heel-strike (100%) to get the stride cycle average joint kinematics profiles.

Joint Mechanics. To establish baseline joint mechanical power output we collected seven overground trials at 1.25 m/s for each subject walking with unpowered exoskeletons. To ensure that trials were within ± 0.05 m/s of the target speed, we used infrared timers triggered at beginning and end of the walkway. We used two force platforms (sampling rate 1200Hz, Advanced Mechanical Technology Inc., Watertown, MA, USA) to record ground reaction forces under each foot (left then right). Combining force platform and marker data we used inverse dynamics to calculate ankle, knee, and hip mechanical power over the stride for each leg (Visual3D software, C-Motion, Rockville, MD, USA). We used standard regression equations to estimate subjects' anthropometry (Zatsiorsky and Seluyanov, 1983) and adjusted foot and shank parameters to account for added exoskeleton mass and inertia. We averaged joint powers for the right and left legs (from heel-strike to heel-strike for each leg) and divided by subject mass to get the stride cycle average exoskeleton mechanical power.

We quantified the average rate of joint positive and negative mechanical work over a stride. For each joint, we integrated only the positive (or negative) portions of both the left and right mechanical power curves (from right heel-strike to left heel-strike to capture simultaneous trailing and leading limb joint powers), summed them, and divided the total by the average step period.

Exoskeleton Mechanics. We used single-axis compression load transducers (1200Hz, Omega Engineering, Stamford, CT, USA) to record the forces produced by the artificial pneumatic muscles during powered walking. We measured the artificial muscle moment arm with the ankle joint in the neutral

position during upright standing posture (moment arm = 10.4 ± 1.2 cm). We multiplied moment arm measurements and smoothed artificial muscle force data (low-pass filtered, 4th order Butterworth, cutoff frequency 6 Hz) to compute the exoskeleton torque for each leg. To determine the mechanical power delivered by the exoskeletons we multiplied the torque and ankle joint angular velocity (from motion capture). We averaged the exoskeleton power for the right and left legs (from heel-strike to heel-strike for each leg) and divided by subject mass to get the stride cycle average exoskeleton mechanical power.

We quantified the average rate of exoskeleton positive and negative mechanical work over a stride for comparisons with net metabolic power and baseline joint mechanics. We integrated only the positive (or negative) portions of both the left and right exoskeleton mechanical power curves (from left heel-strike to left heel-strike), summed them, and divided the total by the average stride period.

Electromyography. We recorded bilateral lower-limb surface electromyography (EMG) (1200 Hz, Konigsberg Instruments, Inc., Pasadena, CA, USA) from soleus (Sol), tibialis anterior (TA), medial gastrocnemius (MG) and lateral gastrocnemius (LG) using bipolar electrodes (inter-electrode distance = 3.5 cm) centered over the belly of the muscle along its long axis. EMG amplifier bandwidth filter was 12.5 Hz – 920 Hz. We placed electrodes to minimize cross-talk and taped them down to minimize movement artifact. We marked the locations of the electrodes on the skin so we could place them in the same position from session to session. We high-pass filtered (4th order Butterworth,

cutoff frequency 20 Hz), rectified and low-pass filtered (4^{th} order Butterworth, cutoff frequency 10 Hz) each of the EMG signals (i.e. linear envelope). We averaged the linear enveloped EMG for the right and left legs (from heel-strike to heel-strike for each leg) to get stride cycle averages. We normalized the curves using the peak value (average of left and right) for each muscle during the first unpowered walking bout (**Unpowered Beginning**) during each session.

To quantify changes in EMG amplitudes we computed stance phase root mean square (RMS) average EMG amplitudes from the high-pass filtered, rectified EMG data of each leg. We averaged RMS EMG values from each leg and normalized using the average RMS value from the **Unpowered Beginning** interval.

Exoskeleton Performance Index. We combined mechanical and metabolic analyses to determine the exoskeleton performance index. First, we calculated metabolic power savings due to the exoskeletons by subtracting the net metabolic power during the first unpowered walking interval in each session from the net metabolic power during each of the powered walking intervals in that session. Computing this difference provides a valid method of testing metabolic efficiency (Gaesser and Brooks, 1975). This method accounts for the fact that some metabolic cost during locomotion can be attributed to sources other than limb muscle energetics (e.g. breathing, circulation, digestion, etc.), resulting in whole-body metabolic power calculations that parallel direct lower-limb metabolic power across different workloads (Poole et al., 1992). We assumed that changes in metabolic cost would reflect the cost of the biological muscle positive work

replaced by the powered exoskeletons. Muscles perform positive mechanical work with a 'muscular efficiency' of 0.25 (Fenn, 1924; Hill, 1938). Thus, we multiplied changes in net metabolic power by 0.25 to yield the expected amount of positive mechanical power delivered by exoskeletons. Then we divided the measured by the expected average positive mechanical power delivered by the exoskeletons to yield the exoskeleton performance index (Equation 1). A performance index of 1.0 would suggest that exoskeleton assistance completely replaced underlying biological muscle positive mechanical work.

$$\text{Exoskeletons Performance Index} = \frac{\Delta \text{ Net Metabolic Power} * 0.25}{\text{Average Exoskeletons Positive Mechanical Power}} \quad (1)$$

An equivalent 'apparent efficiency' (Asmussen and Bonde-Petersen, 1974) can be computed by taking the reciprocal of four times the performance index (i.e. performance index = 1.0 is equivalent to 'apparent efficiency' = 0.25) (Equation 2).

$$\text{Ankle Joint Apparent Efficiency} = \frac{1}{4 * \text{Exoskeletons Performance Index}} = \frac{\text{Average Exoskeletons Positive Mechanical Power}}{\Delta \text{ Net Metabolic Power}} \quad (2)$$

We chose this performance index as the primary metric for two reasons: (1) as change in net metabolic power approaches zero, 'apparent efficiency' approaches infinity non-linearly (biasing means and preventing linear statistical analyses) whereas performance index approaches zero nearly linearly and (2) performance index may be more intuitive than the 'apparent efficiency' because it

approaches unity from below rather than 0.25 from above as reductions in metabolic cost increase.

Statistical Analyses. We used JMP statistical software (SAS Institute, Inc. Cary, NC, USA) to perform repeated measures analysis of variance tests (ANOVAs). When we found a significant effect ($p < 0.05$) we used post-hoc Tukey Honestly Significant Difference (THSD) tests to determine specific differences between means. Statistical power analyses were done for tests yielding significance ($p < 0.05$).

In the first two analyses (one for powered walking data, one for unpowered walking data) we assessed the effects of practice session (**Session 1, Session 2, Session 3**) and period (**Beginning, End**) on net metabolic power, exoskeleton mechanics, stance phase RMS EMG and gait kinematics metrics (three-way ANOVA (subject, session, period)).

In the other three ANOVA analyses (one for Session 1, Session 2 and Session 3) we assessed the effect of exoskeleton condition (**Unpowered, Powered**) on net metabolic power, stance phase RMS EMG and gait kinematics metrics (three-way ANOVA (subject, condition, period)).

Results

Joint Kinematics. During powered walking, subjects initially (**Powered Beginning Session 1**) walked with increased ankle plantar flexion throughout the stride. By the end of the third practice session (**Powered End Session 3**) stance phase ankle joint kinematics returned closer to the unpowered condition, but push-off started earlier in stance and peak plantar flexion angle was larger

(**Figure 2.2**). With practice, powered swing phase ankle kinematics became similar to the pattern observed during unpowered walking.

Knee and hip joint kinematics were not altered by exoskeleton powering and there were no changes in unpowered ankle, knee, or hip joint kinematics over the practice sessions (**Figure 2.2**).

Exoskeleton Mechanics. Ankle exoskeletons produced passive torques near zero during unpowered walking. During the beginning of the first powered interval (**Powered Beginning Session 1**) the exoskeletons produced plantar flexor torque over most of the stance phase. Exoskeletons also produced some extensor torque during the swing phase. With practice, exoskeleton torque became narrowly focused near the push-off phase of stance and was absent during swing. At the end of the third powered session (**Powered End Session 3**) peak exoskeleton torque reached ~0.47 N-m/kg or ~37% of the peak ankle joint moment from overground trials during unpowered walking.

Changes in exoskeleton torque were reflected in the mechanical power they delivered to the users' ankle joints. Because exoskeleton torque was initially spread over the stride there were periods of negative mechanical work done (i.e. energy absorption) by the mechanical assistance during early stance and in swing (**Figure 2.3**). The exoskeletons absorbed -0.09 ± 0.03 W/kg (mean ± s.e.) average negative mechanical power and delivered 0.29 ± 0.02 W/kg average positive mechanical power over the stride at the beginning of the first powered session (**Powered Beginning Session 1**). As torque became more focused near push-off, negative mechanical work done during both swing and early stance was

reduced. By the end of the third powered session (**Powered End Session 3**) exoskeleton average negative mechanical power was ~70% lower than during the initial powered interval (**Powered Beginning Session 1**) (ANOVA, $p = 0.005$; THSD, Session 3 < Session 1). Exoskeleton average positive mechanical power was not different across practice sessions (ANOVA, $p = 0.29$), but was significantly lower at the end of each session when compared to the beginning of each session (ANOVA, $p = 0.001$; THSD, End < Beginning). At the end of the third practice session, (**Powered End Session 3**) the exoskeletons delivered 0.23 ± 0.02 W/kg average positive mechanical power over a stride. This was 63% of unpowered ankle joint average positive mechanical power and 22% of unpowered average positive joint mechanical power summed across the joints (ankle + knee + hip) (**Figure 2.5**).

Metabolic Cost. As exoskeletons absorbed less mechanical energy from the user, the net metabolic power during powered walking decreased to levels below unpowered walking. Initially, powered assistance increased net metabolic power by 0.26 ± 0.28 W/kg (**Powered Beginning Session 1**) (**Figure 2.4 A)**. This was ~7% higher than the net metabolic power during unpowered walking (**Unpowered Beginning Session 1**). With practice, subjects reduced net metabolic power significantly both across (ANOVA, $p = 0.0001$; THSD, Session 3 < Session 2, Session 3 < Session 1) and within sessions (ANOVA, $p = 0.006$; THSD, End < Beginning) (**Table 2.1**). The net metabolic power at the beginning of the first powered session (**Powered Beginning Session 1**) was 3.84 ± 0.30 W/kg but was reduced by 22% (2.99 ± 0.17 W/kg) by the end of the third

powered session (**Powered End Session 3**). Further, the net metabolic power was significantly lower (-10%) with exoskeletons powered (2.99 ± 0.17 W/kg; **Powered End Session 3**) versus unpowered (3.31 ± 0.11 W/kg; **Unpowered Beginning Session 3**), by the end of the third practice session (ANOVA, p = 0.03; THSD, Powered < Unpowered) (**Figure 2.4 A, Table 2.1**).

The metabolic cost of unpowered walking decreased across sessions (ANOVA, p = 0.001; THSD, Session 2 < Session 1, Session 3 < Session 1) but was not different within sessions (ANOVA, p = 0.34) (**Table 2.1**). Unpowered net metabolic power was ~8% lower during **Session 3** when compared to **Session 1**.

Exoskeleton Performance Index. The metabolic benefit of powered ankle assistance increased with practice. Exoskeleton performance was significantly higher within practice sessions (ANOVA, p = 0.004; THSD, End > Beginning) and followed an increasing trend across practice sessions (ANOVA, p = 0.05) (**Figure 2.4 B**). Initially, powered assistance perturbed gait, net metabolic cost was elevated, and exoskeletons performance index was negative (-0.14 ± 0.19 during **Powered Beginning Session 1**). By the end of session three (**Powered End Session 3**) exoskeletons average positive mechanical power (0.24 ± 0.02 W/kg) reduced the net metabolic power by 0.32 ± 0.12 W/kg and performance index was positive (0.41 ± 0.19) (**Figure 2.4 B**). A performance index of 0.41 is equivalent to ankle joint 'apparent efficiency' of 0.61.

Electromyography. Subjects immediately reduced their soleus muscle activation during powered walking and continued to do so with practice (**Figure**

2.6, Table 2.2). By the end of the third practice session, stance phase soleus RMS EMG amplitude was 28% lower in the powered (**Powered End Session 3**) versus unpowered (**Unpowered Beginning Session 3**) condition (ANOVA, $p < 0.0001$; THSD, Powered < Unpowered) when compared to the unpowered condition (**Unpowered Beginning Session 3**). Soleus RMS was lower at the end when compared to the beginning of the powered interval during each practice session (ANOVAs, $p = 0.01$ in Session 1, $p = 0.007$ in Session 2 $p = 0.004$ in Session 3; THSD, all End < Beginning).

Initially subjects increased activity in their tibialis anterior muscle throughout the stride providing a reaction torque in response to powered assistance. With practice, activity patterns returned to normal (**Figure 2.7, Table 2.2**). During the beginning of powered walking (**Powered Beginning Session 1**), tibilais anterior stance phase RMS EMG was 52% higher than the unpowered condition (**Unpowered Beginning Session 1**) (ANOVA, $p = 0.001$; THSD, Powered > Unpowered). During powered walking, tibialis anterior activity decreased both across (ANOVA, $p = 0.001$; THSD, Session 3 < Session 1) and within (ANOVA, $p = 0.001$; THSD, End < Beginning) practice sessions (**Figure 2.7, Table 2.2**). By the third session, there was no significant difference between unpowered and powered walking tibilais anterior RMS amplitudes (ANOVA, $p = 0.05$).

At the end of the third powered session (**Powered End Session 3**), lateral gastrocnemius RMS EMG amplitude was ~10% lower than unpowered walking (**Unpowered Beginning Session 3**). Medial gastrocnemius amplitude was

reduced as well, but only by ~4%. However, none of the observed reductions in stance phase RMS EMG amplitudes for medial or lateral gastrocnemius during powered walking were statistically significant (ANOVA, $p = 0.52$ for medial gastrocnemius and $p = 0.09$ for lateral gastrocnemius) (**Table 2.2**).

Gait Kinematics. Initially subjects took shorter and wider steps during powered versus unpowered walking. Step length was 724 ± 9 mm during unpowered walking (**Unpowered Beginning Session 1**) and 713 ± 10 mm during powered walking (**Powered Beginning Session 1**) (ANOVA, $p = 0.006$; THSD, Powered < Unpowered). At the beginning of session one, step width was 105 ± 10 mm during unpowered walking and 127 ± 8 mm during powered walking (ANOVA, $p < 0.0001$; THSD, Powered > Unpowered). By the end of the third session, subjects' step width during powered walking (120 ± 12 mm) (**Powered End Session 3**) was not different than during unpowered walking (123 ± 11 mm) (**Unpowered Beginning Session 3**) (ANOVA, $p = 0.05$). In the third session, step length remained slightly shorter in powered (717 ± 14 mm) versus unpowered (732 ± 14 mm) walking (ANOVA, $p = 0.01$; THSD, Powered < Unpowered). There were no significant changes in step period or double support period due to powered assistance.

Discussion

In this study we quantified the metabolic cost of ankle joint work during level, steady-speed walking. We used bilateral powered exoskeletons to alter joint level mechanics and answer two questions. (1) Does powered plantar flexion assistance during push-off reduce the metabolic cost of walking? (2) What

is the ‘apparent efficiency’ of ankle joint work? Our results indicate that when powered ankle exoskeletons deliver 22% of the positive work generated by the joints (ankle + knee + hip) users reduce net metabolic power by ~10%. We determined that the ‘apparent efficiency’ of ankle joint work is 0.61, that is, for every 1 Joule of positive mechanical work delivered by ankle exoskeletons, users save ~1.6 Joules of metabolic energy.

We are aware of only one other study reporting oxygen consumption during walking with powered lower-limb exoskeletons. Norris et al. built bilateral powered ankle-foot orthoses with hardware based on our previous designs (Ferris et al., 2005; Ferris et al., 2006) but using an alternative control scheme based on ankle joint kinematics rather than soleus EMG (Norris et al., 2007). They examined the effects of augmented plantar flexion power on the economy and preferred walking speed in younger and older adults (Norris et al., 2007). Norris et al. found that when young adults walked with powered assistance, gross metabolic energy per stride was ~8% lower and preferred walking speed ~7% higher when compared to unpowered walking. Because they used a different type of exoskeleton controller (kinematic based timing rather than proportional myoelectric control), did not keep speed constant in their comparisons, had subjects complete only a very short period of training (less than 20 minutes), and did not measure inverse dynamics of their subjects, it is difficult to make comparisons between their findings and ours.

Our results are consistent with previous studies from our own laboratory using a unilateral powered ankle exoskeleton under soleus proportional

myoelectric control. Gordon et al. (Gordon and Ferris, 2007) found that within two 30 minute practice sessions (~45 minutes cumulative powered walking), humans reduced soleus activation by ~35%, returned to near normal ankle joint kinematics, eliminated exoskeleton negative mechanical power generation, and delivered positive exoskeleton mechanical power focused at push-off (~0.13-0.15 W/kg for 12-14 J). As expected, with practice, our bilateral exoskeletons delivered nearly twice the average positive mechanical power (0.24 ± 0.02 W/kg) when compared to the single unilateral exoskeleton in the study of Gordon et al. We also observed similar changes in ankle joint kinematics, soleus electromyography (~28% reduction), and exoskeleton average negative mechanical power (~70% reduction) over three training sessions. Gordon et al. quantified the time for key metrics (e.g. soleus RMS amplitude, exoskeleton positive and negative work, and ankle joint angle correlation common variance) to reach steady values. For the metrics they studied, they observed no further changes after ~45 minutes of cumulative powered walking. In the current study, we did not assess the rate of motor adaptation during powered walking, but data on three subjects showed no further reductions in net metabolic power during a fourth day of practice. Both tibialis anterior root mean square activation and step width remained elevated and did not return to baseline values observed in unpowered walking until the end of the third session. These results indicate that motor adaptation to bilateral powered assistance is not complete until ~90 minutes of practice. Thus, learning to walk with bilateral exoskeletons appears to be a more challenging task than learning to walk with a unilateral exoskeleton.

Our results also suggest that changes in net metabolic power may occur more slowly than changes in joint kinematics and muscle activation patterns during adaptation to powered walking.

Although net metabolic power was reduced by powered assistance, the reduction was not as large as expected. Contrary to our hypothesis, net metabolic power did not decrease in proportion to the contribution of the average positive mechanical power delivered by the exoskeletons to the total positive mechanical power generated by the ankle knee and hip. Powered ankle exoskeletons delivered 22% of the total (ankle + knee + hip) positive mechanical power across the lower-limb joints, but the net metabolic cost of walking decreased by only 10%.

It was possible that differences in net metabolic power between powered and unpowered conditions could have been confounded by differences in gait kinematics. Studies have demonstrated that the metabolic cost of walking increases with increasing step length (Donelan et al., 2002a), step width (Donelan et al., 2001) and step frequency (Bertram and Ruina, 2001). We compared step length, step width, double support period and step period between powered and unpowered walking in all three sessions. Initially subjects took wider and shorter steps during powered walking. By the end of the third session there were no differences in step width between powered and unpowered walking. Subjects took shorter steps (~2%) during powered compared to unpowered walking but these changes are too small to appreciably affect net metabolic cost (Donelan et al., 2002a).

Metabolic cost of walking with the powered exoskeletons could also have been affected by a number of other factors. Co-activation about a joint can be very costly metabolically. Added dorsiflexor reaction torque during stance would lead to smaller reductions in net metabolic power when using the exoskeletons. We reject this possibility because by the end of three practice sessions, tibialis anterior activation was not significantly different during powered versus unpowered walking. Although we did not measure muscle activity for more proximal muscles (e.g. quadriceps, hamstrings), our previous results indicate that changes in those muscles due to powered ankle assistance are not significant (Gordon and Ferris, 2007).

Another possibility is that adaptation to the powered ankle exoskeletons involved compensations at other joints that incur a significant metabolic cost. We found no substantial changes in knee or hip joint kinematics due to powered assistance at the ankle at any point during practice. Furthermore, electromyographic analyses of walking with unilateral powered exoskeletons indicated no differences in quadriceps or hamstrings muscle activation after two 30 minute practice sessions (Gordon and Ferris, 2007). Thus, we think it is unlikely that muscles at other joints substantially changed their dynamics.

Another potential confounding factor is that negative mechanical work performed by the muscles contributes to the net metabolic cost of walking. If we assume that muscles perform equal amounts of positive and negative mechanical work during walking, and 1 Joule of positive work costs 4 Joules metabolic energy while 1 Joule of negative muscle work costs 0.8 Joules

metabolic energy, then only ~83% (4.0/4.8 = 0.83) of the net metabolic cost of walking is due to muscle positive work. Considering this factor, and assuming the exoskeletons only alter the net metabolic cost of positive muscle work, the net metabolic cost of walking would only decrease by 83% of the contribution of average positive mechanical power delivered by the exoskeletons to the summed average lower-limb positive joint mechanical power over a stride. Thus, when exoskeletons delivered 22% of the summed joint positive mechanical power over a stride, the net metabolic power should have still decreased by ~18%. Our value of 10% is still substantially lower than the 18% calculated by assuming only muscle performs the negative work during walking (a doubtful assumption given the possibility for passive tissues to contribute to negative work).

A limitation of our study was that the exoskeletons added mass to the lower limbs of the subjects, increasing the metabolic cost of walking compared to walking without the exoskeletons. Added distal mass (applied at the feet) increases the net metabolic cost of walking by ~8% per added bilateral kilogram (Browning et al., 2007). We compared the net metabolic power for powered to unpowered exoskeletons walking, rather than for powered to without exoskeletons walking, to prevent any increases in metabolic cost due to added distal mass from affecting our results. The inverse dynamics analysis we carried out to assess lower-limb joint powers also accounted for added exoskeleton mass and inertia and should therefore reflect the additional mechanical work required to swing the legs.

We originally hypothesized that ankle joint work is performed with an 'apparent efficiency' of 0.25 but our results indicated a value of 0.61. Predicting the 'apparent efficiency' to be 0.25 relied on the assumption that all of the positive work done at the ankle joint was performed by active muscle with a 'muscular efficiency' that matches values from isolated muscle experiments. However, the mechanical power observed at a given joint through inverse dynamics analysis may not be performed exclusively by the muscles at that joint. Bi-articular muscles, which act across two joints (e.g. medial and lateral gastrocnemius act across both ankle and knee joints) can transfer power between joints. In addition, compliant tendons in series with muscle can perform positive work by returning stored strain energy. These two factors, bi-articular power transfer and elastic energy storage and return (e.g. in the Achilles tendon) could lead to much higher calculations of 'apparent efficiency' for ankle joint mechanical work. If we assume that only elastic energy storage and return is responsible for the high 'apparent efficiency', then up to 60% of the positive work delivered by the ankle joint during push-off comes from elastic recoil. Recent evidence from ultrasound experiments in humans supports this idea. Both soleus and medial gastrocnemius muscles remain nearly isometric during the push-off phase of stance during walking. We estimate more than 50% of the positive mechanical work at the ankle originates from elastic recoil of the Achilles tendon based on the available published data (Ishikawa et al., 2005; Lichtwark and Wilson, 2006). If ~50-60% of the ankle joint positive mechanical power output is performed by recoiling tendon, then an 18-22% reduction in positive mechanical

power output of the lower-limb joints due to powered exoskeletons would yield a 7-11% decrease in net metabolic power. Our observed 10% reduction in net metabolic power falls within that range.

Implications and Future Work. Biomechanists and physiologists have been debating the metabolic costs of human walking for decades (Alexander, 1991; Cavanagh and Kram, 1985; Elftman, 1939; Kuo et al., 2005; Ruina et al., 2005; Saunders et al., 1953; Taylor, 1994; Williams, 1985). A clear relationship between the mechanics and energetics of locomotion remains elusive principally because of the challenge in integrating results from isolated muscle to explain whole-body energy consumption. Using robotic exoskeletons to perturb joint level dynamics can help integrate measurements from isolated muscle with whole-body experiments. Exoskeletons for more proximal joints (hip and knee) could allow calculations of their 'apparent efficiency' and provide some insight into the relative contribution of muscle work versus tendon storage and return at each of lower-limb joints. Similar techniques could also be used to study joint muscle-tendon function during locomotion under various workloads (e.g. changing walking speeds or surface inclines) to study how muscle-tendon systems meet increasing demand for power.

From an applied science standpoint, our findings have implications for the design of the state-of-the art lower-limb assistive devices of the future (i.e. exoskeletons and prostheses). A primary goal of robotic exoskeletons is to reduce metabolic energy expenditure during human locomotion by replacing biological muscle work with artificial muscle work (Guizzo and Goldstein, 2005).

Our results suggest that metabolic energy savings are likely to be much more modest than expected when using an exoskeleton to supplant joint work, especially at joints with considerable elastic compliance. Powering joints that rely more on power production due to positive muscle work rather than positive work performed by recoiling tendon may lead to larger reductions in metabolic cost (Ferris et al., 2007).

Acknowledgements

The work was supported by NSF BES-0347479 to D.P. Ferris. We would like to thank Catherine Kinnaird, Jineane Shibuya and other members of the Human Neuromechanics Laboratory for assisting with data collection and analysis. Jacob Godak and Anne Manier of the University of Michigan Orthotics and Prosthetics Center constructed the exoskeletons.

Figures and Tables

Figure 2.1 Experimental set-up. (A) Subjects completed three practice sessions over a seven day period. In each session, subjects walked on a motorized treadmill for 10 minutes with exoskeletons unpowered, 30 minutes with exoskeletons powered, and 15 minutes with exoskeletons unpowered. Outlined boxes indicate periods where data was analyzed: unpowered beginning (min 7-9), powered beginning (min 3-5), powered end (min 27-29) and unpowered end (min 12-14). **(B)** During powered walking, bilateral ankle-foot orthoses (i.e. exoskeletons) drove ankle extension with artificial pneumatic muscles controlled using the subjects' own soleus surface electromyography (i.e. under proportional myoelectric control). We collected joint kinematics using reflective markers and motion capture, O_2 and CO_2 flow rates using open-circuit spirometry, and artificial muscle forces using compression force transducers.

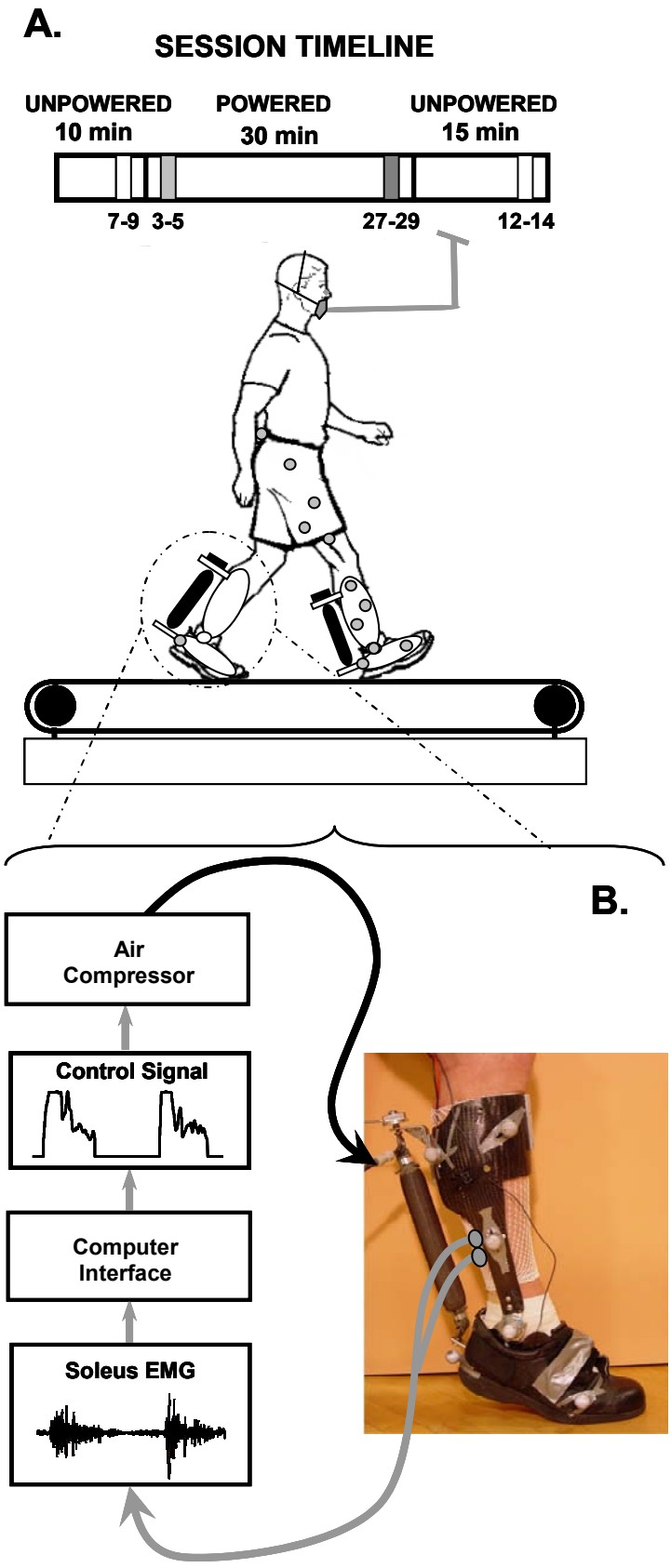
A.
SESSION TIMELINE
UNPOWERED
10 min
POWERED
30 min
UNPOWERED
15 min
7-9
3-5
27-29
12-14
B.
Air
Compressor
Control Signal
Computer
Interface
Soleus EMG

Figure 2.2 Joint kinematics. Thick curves are nine subject mean ankle, knee and hip joint kinematics for unpowered walking from beginning of practice session three (black) and powered walking at the beginning of practice session one (light gray) and end of practice session three (dark gray). Thin curves are + 1 standard deviation and match colors for means. Curves are stride average of left and right legs and plotted from heel-strike (0%) to heel-strike (100%). Stance is ~0-60% of the stride, swing 60-100%. For all joints zero degrees is upright standing posture. Ankle plantarflexion, knee extension and hip extension are positive.

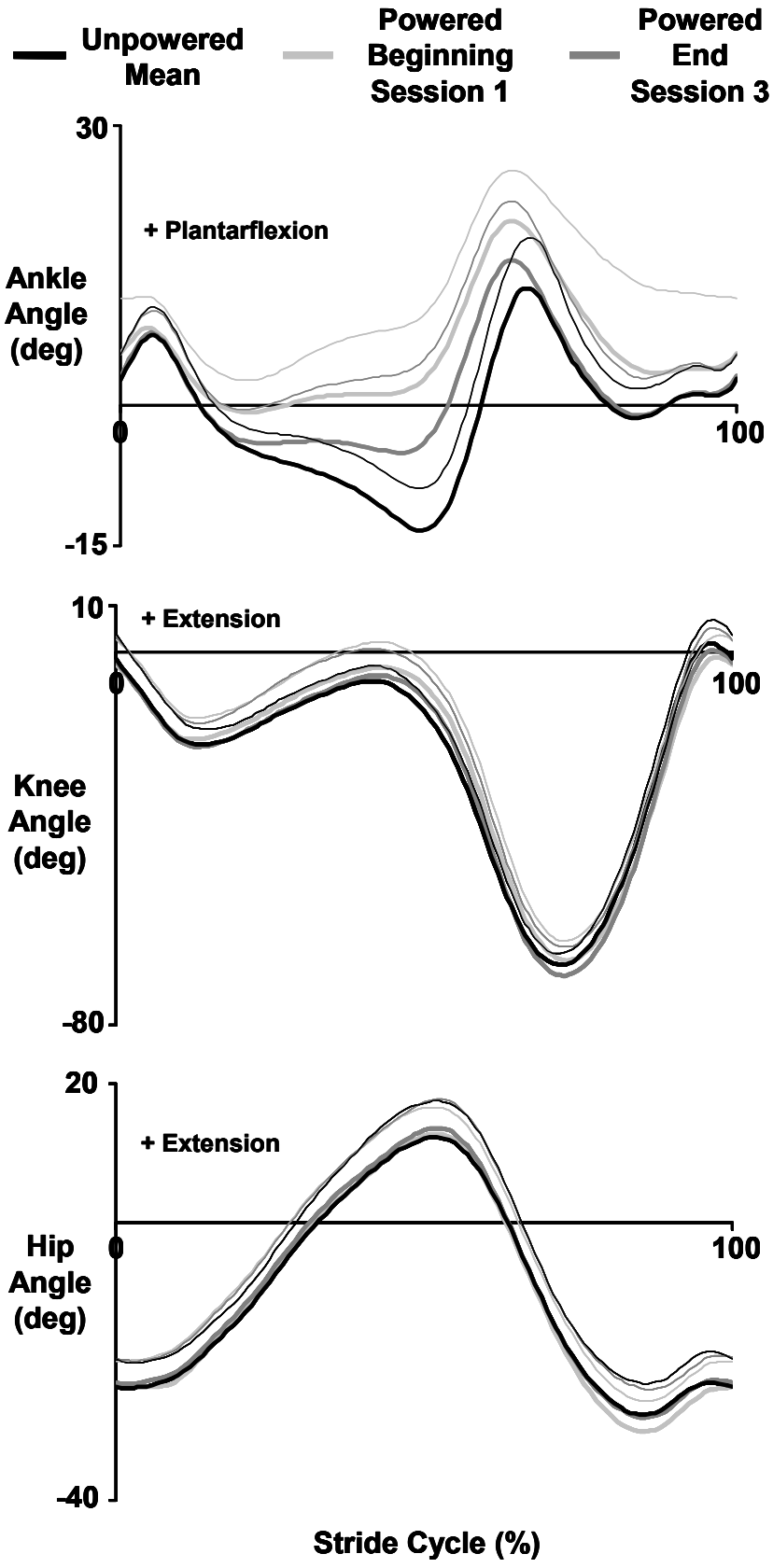
Unpowered Mean
Powered Beginning Session 1
Powered End Session 3
30
+ Plantarflexion
Ankle Angle (deg)
0
100
-15
10
+ Extension
0
100
Knee Angle (deg)
-80
20
+ Extension
Hip Angle (deg)
0
100
-40
Stride Cycle (%)

Figure 2.3 Ankle exoskeleton mechanical power. Top panel **(A)** shows nine subject mean (thick curves) + 1 standard deviation (thin curves) of exoskeleton mechanical power delivered over the stride from heel-strike (0%) to heel-strike (100%) (left and right exoskeletons are averaged for each subject). Curves are three session average for unpowered walking (black) and powered walking at the beginning of practice session one (light gray) and end of practice session three (dark gray). Mechanical power is computed as the product of exoskeleton torque and ankle joint angular velocity and is normalized by subject mass. Positive power indicates energy transferred to the user and negative power indicates energy absorbed from the user. Bottom panel **(B)** shows bars tabulating the nine subject mean exoskeletons average positive and negative mechanical power over a stride for powered walking. Error bars are ± 1 standard error. Practice sessions (1-3) are tabulated left to right with beginning period (minutes 3-5) in light gray and end period (minutes 27-29) in dark gray. All mechanical power values are normalized by subject mass.

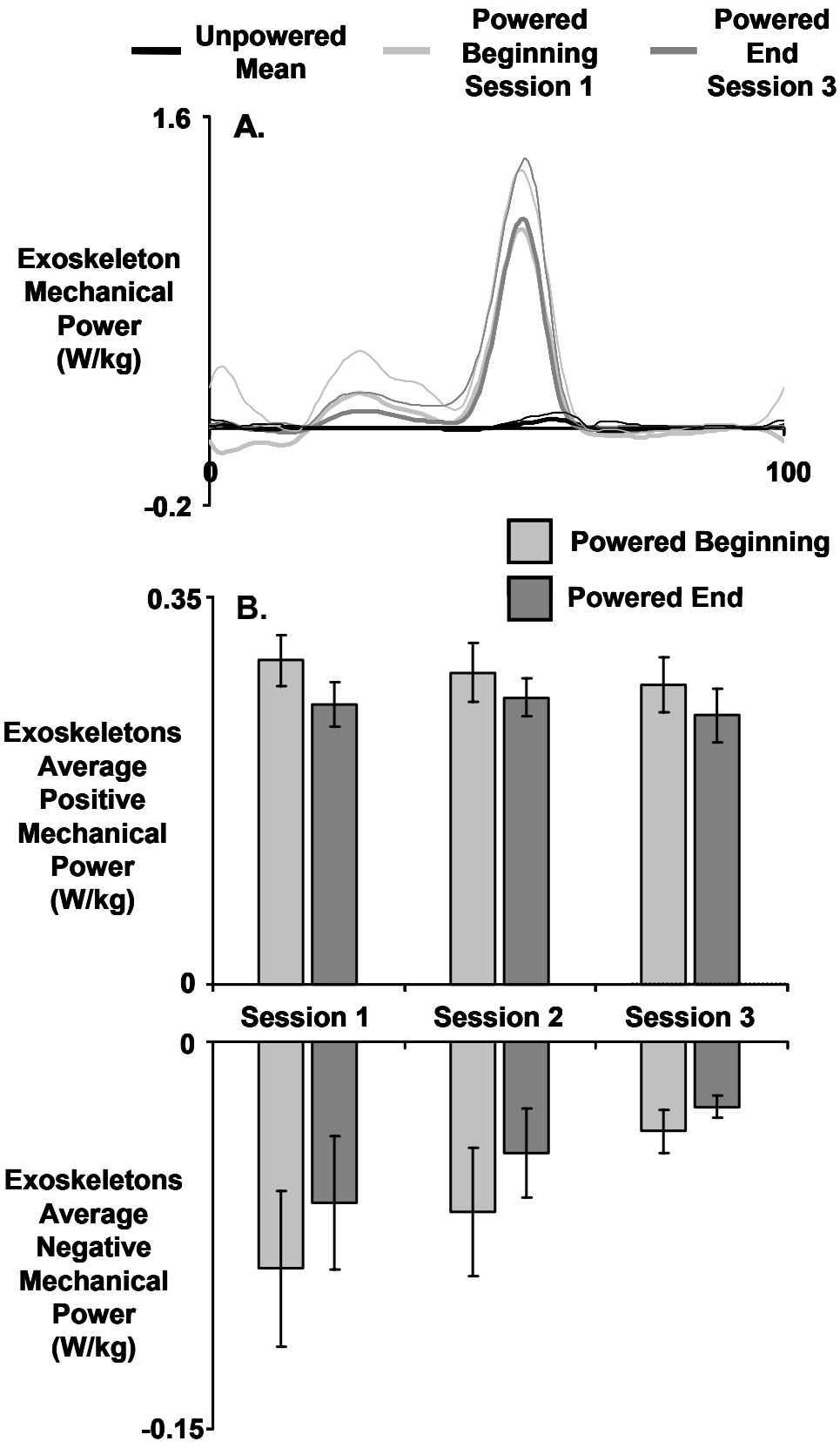
Unpowered Mean
Powered Beginning Session 1
Powered End Session 3
A.
1.6
-0.2
0
100
Exoskeleton Mechanical Power (W/kg)
Powered Beginning
Powered End
B.
0.35
0
-0.15
Session 1
Session 2
Session 3
Exoskeletons Average Positive Mechanical Power (W/kg)
Exoskeletons Average Negative Mechanical Power (W/kg)

Figure 2.4 Exoskeleton performance. Top panel **(A)** shows bars tabulating the nine subject mean change in net metabolic power (powered - unpowered) due to powered assistance from bilateral exoskeletons. Error bars are ± 1 standard error. All metabolic power values are normalized by subject mass. Right axis indicates the change in net metabolic power as a percentage difference from unpowered walking during each session. Bottom panel **(B)** shows bars indicating nine subject mean ± 1 standard error exoskeletons performance index. Performance index indicates the fraction of average exoskeletons positive mechanical power that results in a reduction in net metabolic power, assuming that artificial muscle work directly replaces biological muscle work. Exoskeletons performance index = 1.0 would suggest that all of the exoskeletons average mechanical power replaces underlying biological muscle work. For both panels, practice sessions (1-3) are tabulated left to right with beginning period (minutes 3-5) in light gray and end period (minutes 27-29) in dark gray.

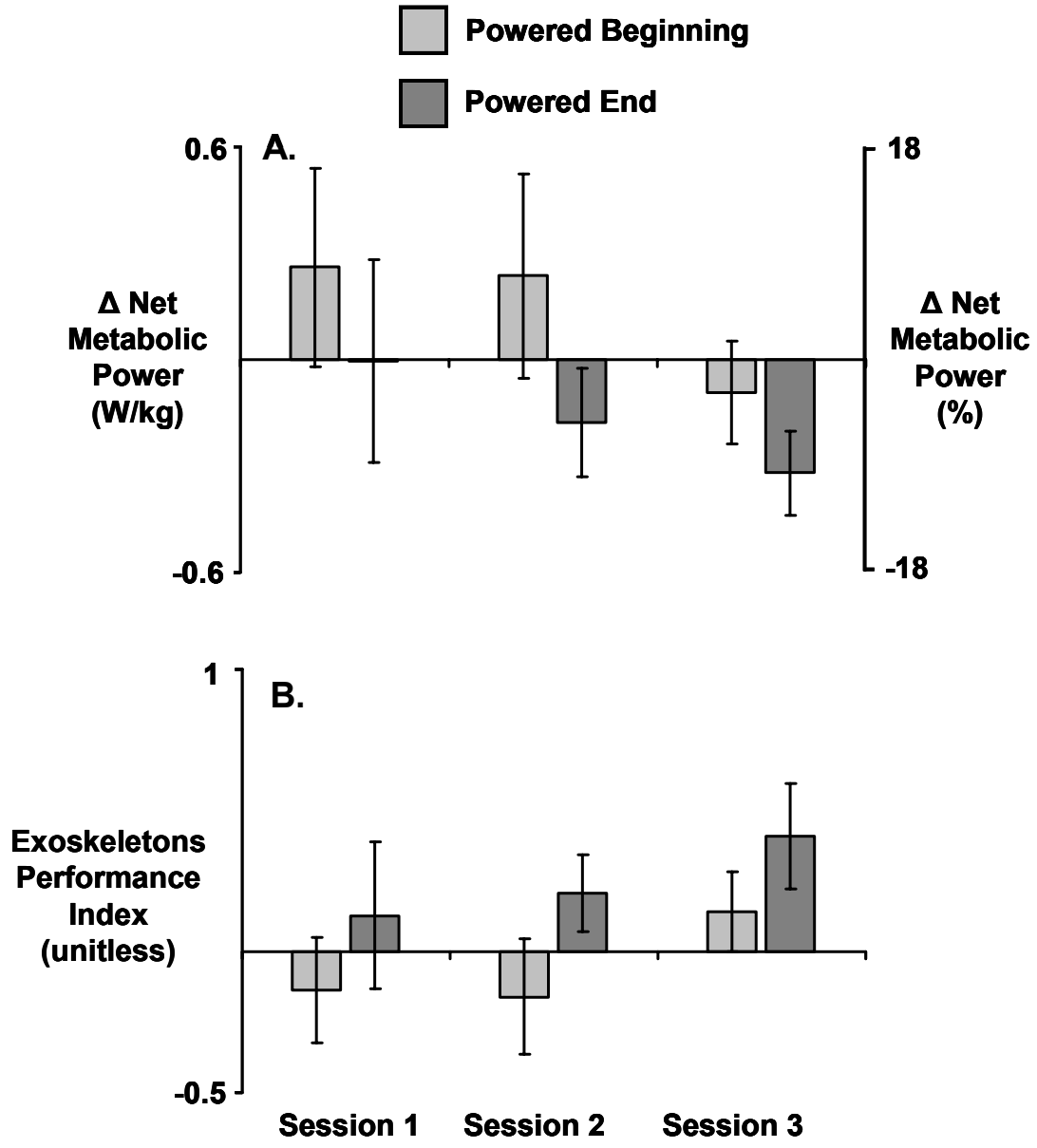
Powered Beginning
Powered End
A.
0.6
-0.6
18
-18
Δ Net Metabolic Power (W/kg)
Δ Net Metabolic Power (%)
B.
1
-0.5
Exoskeletons Performance Index (unitless)
Session 1
Session 2
Session 3

Figure 2.5 Lower-limb joint kinetics. Left panel **(A)** shows nine subject mean (thick black) + 1 standard deviation (thin black) mechanical power delivered by each of the lower limb joints over the stride from heel-strike (0%) to heel-strike (100%) Left and right legs are averaged for each subject. Curves are for unpowered walking overground at 1.25 m/s. The mean exoskeleton mechanical power from the end of practice session three (thick dark gray) + 1 standard deviation (thin dark gray) is overlaid on the bottom subplot for the ankle joint mechanical power. Mechanical power is computed as the product of exoskeleton torque and ankle joint angular velocity and is normalized by subject mass. Positive power indicates energy transferred to the user and negative power indicates energy absorbed from the user. Right panel **(B)** shows bars tabulating the nine subject mean positive mechanical power delivered by the sum of the ankle, knee and hip joints (black) and ankle joint (white) during unpowered walking and the exoskeletons (gray) during powered walking. Error bars are ± 1 standard error. All mechanical power values are normalized by subject mass. Brackets indicate the percent contribution of bars from right to left. For example, the exoskeletons average positive mechanical power was 63% of the ankle joint average positive mechanical power over the stride.

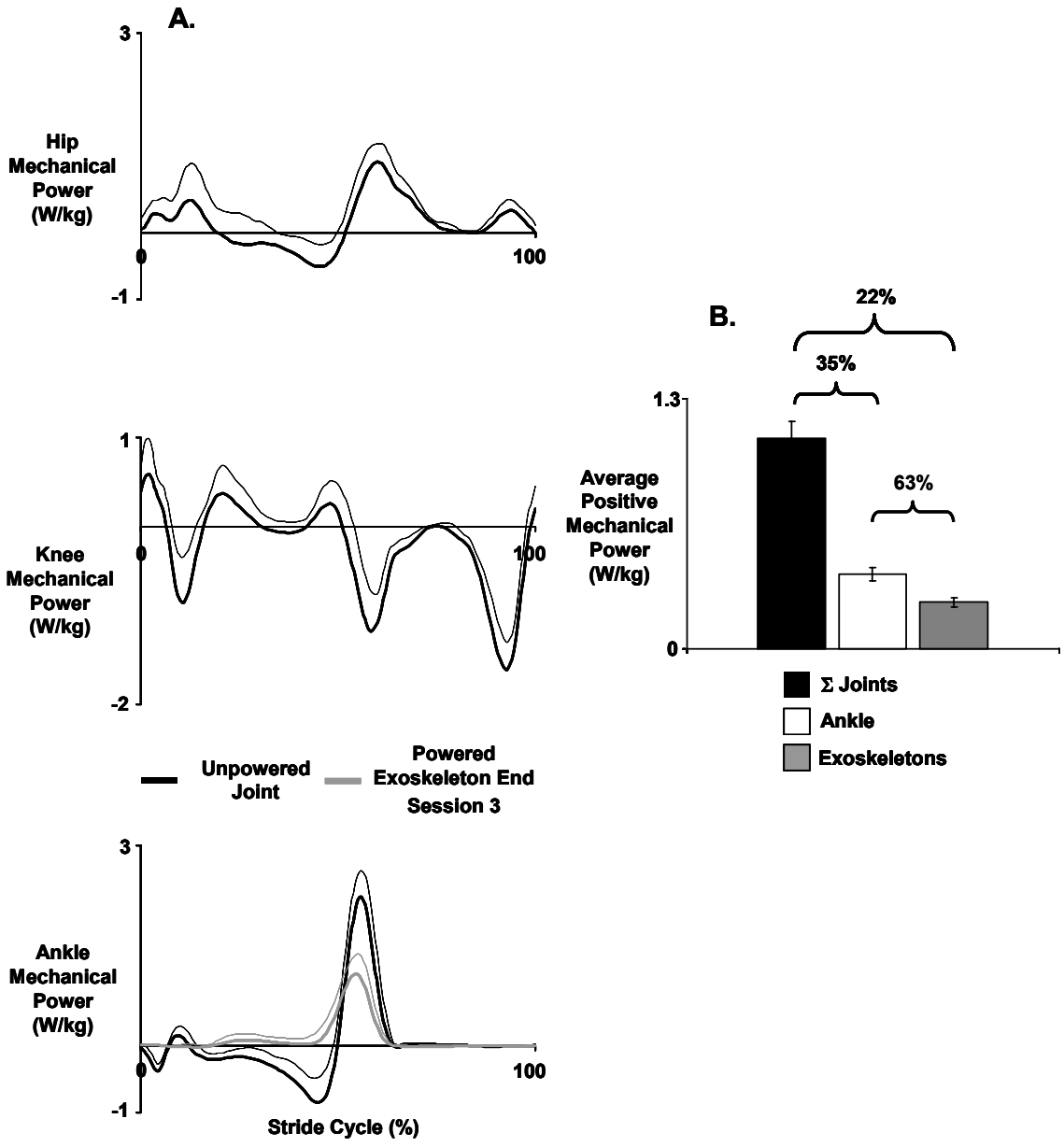
A.
3
Hip
Mechanical
Power
(W/kg)
0
100
-1
1
Knee
Mechanical
Power
(W/kg)
0
100
-2
Unpowered
Joint
Powered
Exoskeleton End
Session 3
3
Ankle
Mechanical
Power
(W/kg)
0
100
-1
Stride Cycle (%)
B.
22%
35%
1.3
Average
Positive
Mechanical
Power
(W/kg)
63%
0
Σ Joints
Ankle
Exoskeletons

Figure 2.6 Soleus electromyography. Top panel **(A)** shows nine subject mean (thick curves) + 1 standard deviation (thin curves) of soleus normalized linear enveloped (high-pass cutoff frequency = 20 Hz and low-pass cutoff frequency = 10 Hz) muscle activity over the stride from heel-strike (0%) to heel-strike (100%) Left and right legs are averaged for each subject. Stance phase is ~0-60% and swing ~60-100% of the stride. Thick curves are three session average for unpowered walking (black) and powered walking at the beginning of practice session one (light gray) and end of practice session three (dark gray). Thin curves are + 1 standard deviation and follow same color scheme as means. Curves are normalized to the peak value during unpowered walking at the beginning of each session. Bottom panel **(B)** shows bars tabulating the nine subject mean of stance phase root mean square average soleus muscle activation. Error bars are ± 1 standard error. Practice sessions (1-3) are tabulated left to right with unpowered walking periods (minutes 7-9 and minutes 12-14 at beginning and end respectively) in white and powered beginning periods (minutes 3-5) in light gray and powered end periods (minutes 27-29) in dark gray. Percentages listed above bars for powered walking indicate difference from unpowered beginning in each session. Asterisks indicate a statistically significant difference between powered and unpowered walking (ANOVA, $p < 0.05$).

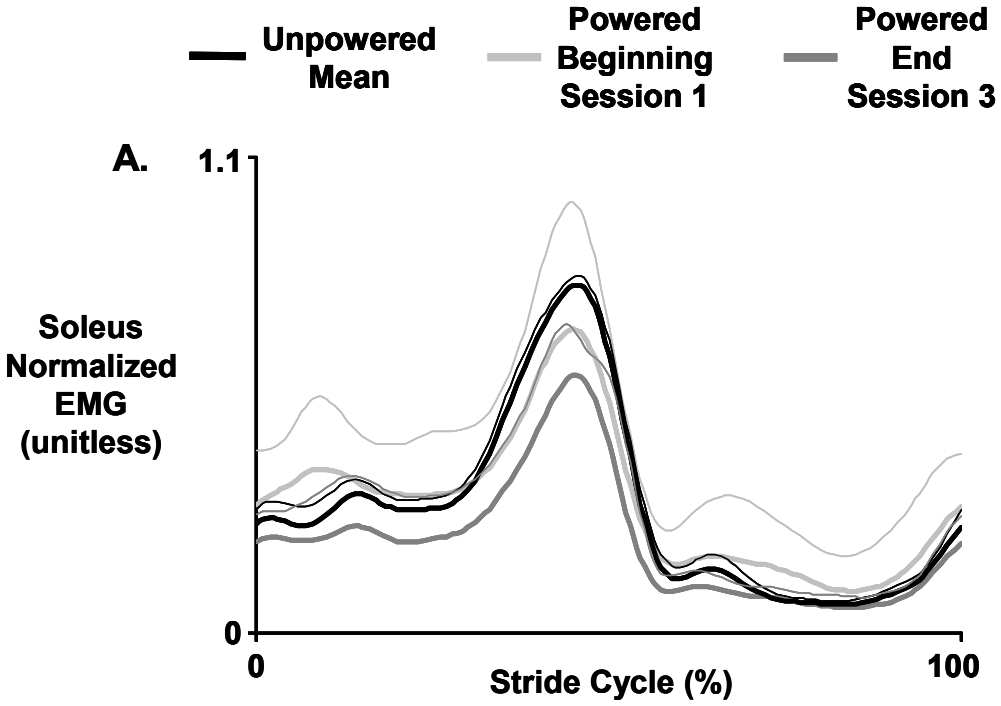
Unpowered Mean
Powered Beginning Session 1
Powered End Session 3
A.
1.1
Soleus Normalized EMG (unitless)
0
0
Stride Cycle (%)
100

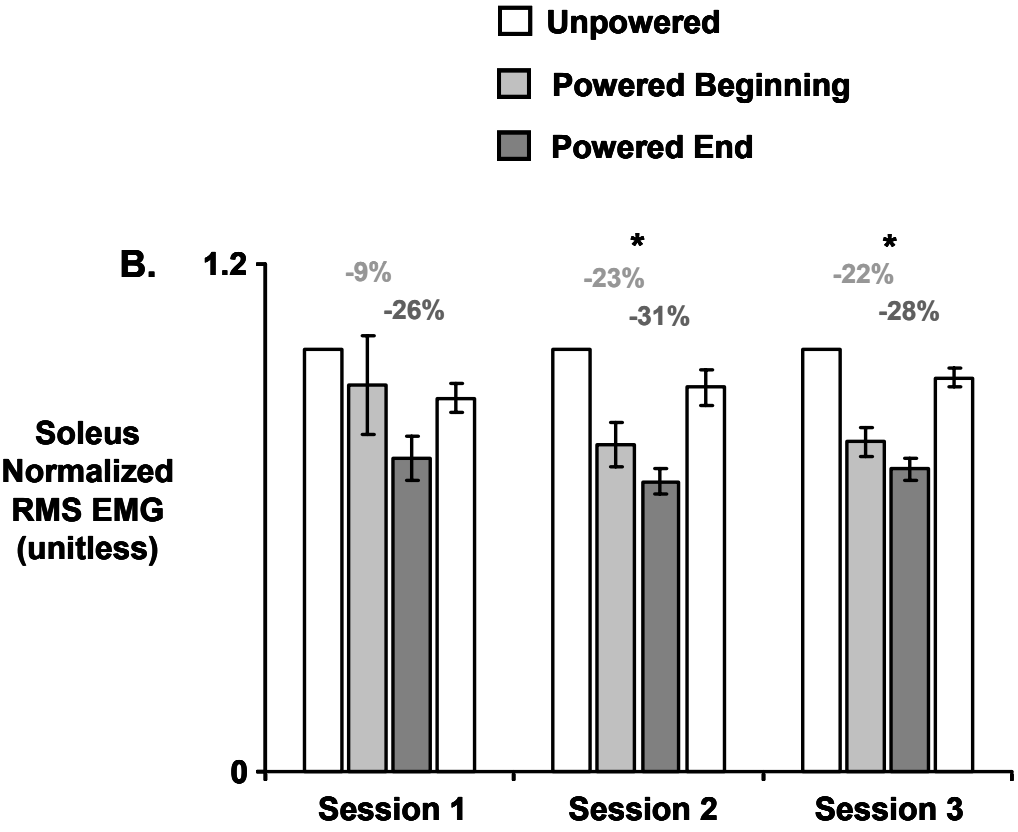
Unpowered
Powered Beginning
Powered End
B.
1.2
-9%
-26%
*
-23%
-31%
*
-22%
-28%
Soleus Normalized RMS EMG (unitless)
0
Session 1
Session 2
Session 3

Figure 2.7 Tibialis anterior electromyography. Top panel **(A)** shows nine subject mean (thick curves) + 1 standard deviation (thin curves) of tibialis anterior normalized linear enveloped (high-pass cutoff frequency = 20 Hz and low-pass cutoff frequency = 10 Hz) muscle activity over the stride from heel-strike (0%) to heel-strike (100%). Left and right legs are averaged for each subject. Stance phase is ~0-60% and swing ~60-100% of the stride. Thick curves are three session average for unpowered walking (black) and powered walking at the beginning of practice session one (light gray) and end of practice session three (dark gray). Thin curves are + 1 standard deviation and follow same color scheme as means. Curves are normalized to the peak value during unpowered walking at the beginning of each session. Bottom panel **(B)** shows bars tabulating the nine subject mean of stance phase root mean square average tibialis anterior muscle activation. Error bars are ± 1 standard error. Practice sessions (1-3) are tabulated left to right with unpowered walking periods (minutes 7-9 and minutes 12-14 at beginning and end respectively) in white and powered beginning periods (minutes 3-5) in light gray and powered end periods (minutes 27-29) in dark gray. Percentages listed above bars for powered walking indicate difference from unpowered beginning in each session. Asterisks indicate a statistically significant difference between powered and unpowered walking (ANOVA, $p < 0.05$).

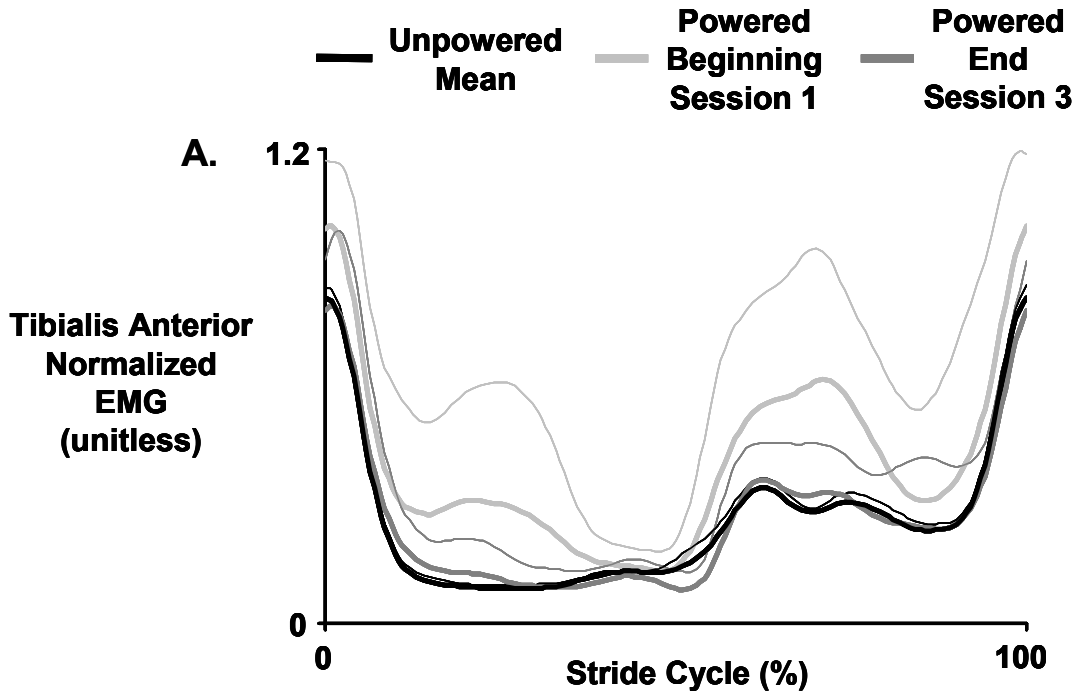
Unpowered Mean
Powered Beginning Session 1
Powered End Session 3
A.
1.2
Tibialis Anterior Normalized EMG (unitless)
0
0
Stride Cycle (%)
100

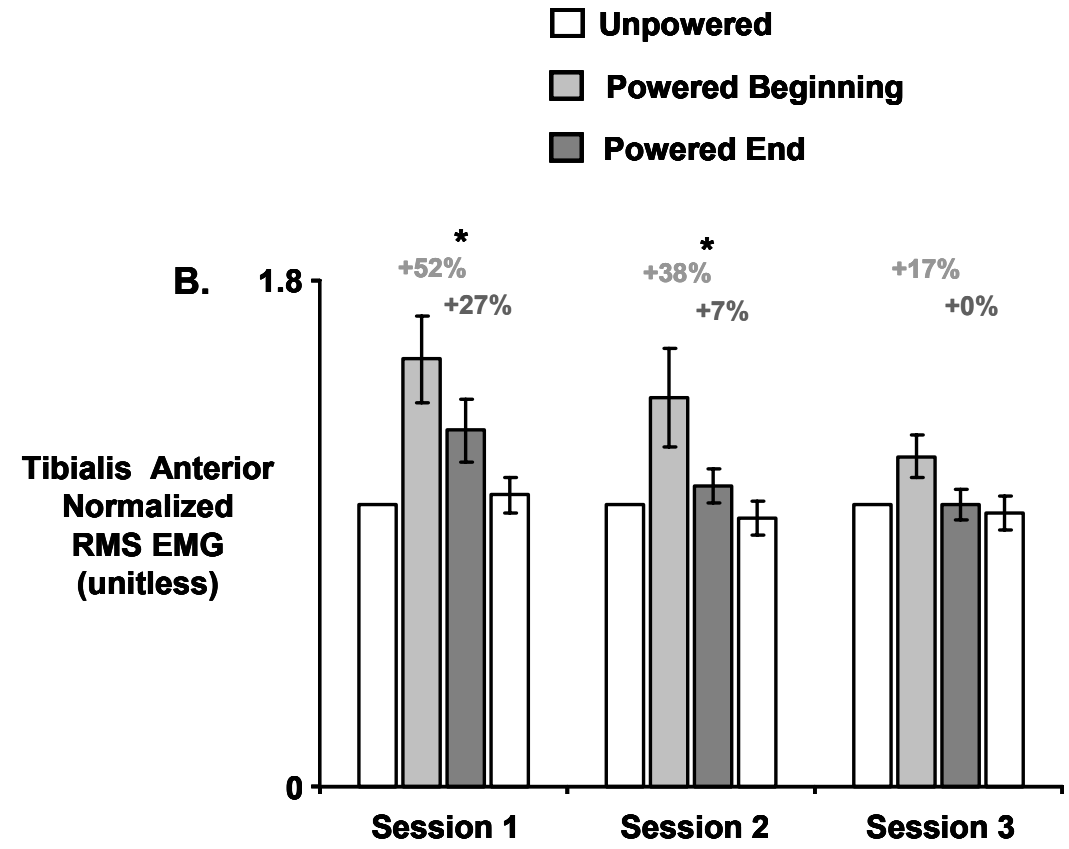
Unpowered
Powered Beginning
Powered End
B.
1.8
*
+52%
+27%
*
+38%
+7%
+17%
+0%
Tibialis Anterior Normalized RMS EMG (unitless)
0
Session 1
Session 2
Session 3

Table 2.1 Net metabolic cost. Table lists values for net metabolic power during unpowered and powered walking during each session. Sessions are listed in rows (Session 1 top to Session 3 bottom). Results of repeated measures ANOVA (n=9 subjects) comparing unpowered and powered walking amplitudes are summarized in the rightmost column.

	METRIC	Unpowered				Powered				STATISTICS
		Beginning		End		Beginning		End		
		Mean	SE	**Mean**	SE	**Mean**	SE	**Mean**	SE	**Condition p-value; THSD**
Session 1	**Net Metabolic Power (W/kg)**	**3.58**	0.10	**3.52**	0.10	**3.84**	0.30	**3.57**	0.31	p=0.33
Session 2	**Net Metabolic Power (W/kg)**	**3.40**	0.10	**3.39**	0.08	**3.64**	0.33	**3.23**	0.18	p=0.81
Session 3	**Net Metabolic Power (W/kg)**	**3.31**	0.11	**3.25**	0.10	**3.22**	0.20	**2.99**	0.17	p=0.03* Powered<Unpowered

n=9, See Materials and Methods for calculations.
THSD=Tukey Honestly Significant Difference Test Results; **SE**=Standard Error
Condition: Unpowered, Powered
p<0.05 indicates statistical significance.
*** indicates statistical power >0.65**

Table 2.2 Ankle joint muscle electromyography. Table lists values for normalized stance phase root mean square average muscle activation amplitudes for the triceps surae (soleus, medial and lateral gastrocnemius) and tibialis anterior for unpowered and powered walking during each session. Sessions are listed in rows (Session 1 top to Session 3 bottom). Results of repeated measures ANOVA (n=9 subjects) comparing unpowered and powered walking amplitudes are summarized in the rightmost column.

	METRIC	Unpowered				Powered				STATISTICS
		Beginning		End		Beginning		End		
		Mean	SE	Mean	SE	Mean	SE	Mean	SE	Condition p-value; THSD
Session 1	Sol RMS (unitless)	**1.00**	0.00	**0.88**	0.03	**0.91**	0.12	**0.74**	0.05	p=0.05
	TA RMS (unitless)	**1.00**	0.00	**1.04**	0.06	**1.52**	0.15	**1.27**	0.11	p=0.001** Powered>Unpowered
	MG RMS (unitless)	**1.00**	0.00	**0.96**	0.04	**1.02**	0.06	**0.92**	0.05	p=0.85
	LG RMS (unitless)	**1.00**	0.00	**0.97**	0.02	**1.06**	0.13	**0.90**	0.06	p=0.93
Session 2	Sol RMS (unitless)	**1.00**	0.00	**0.91**	0.04	**0.77**	0.05	**0.69**	0.03	p<0.0001** Powered<Unpowered
	TA RMS (unitless)	**1.00**	0.00	**0.96**	0.06	**1.38**	0.18	**1.07**	0.06	p=0.02* Powered>Unpowered
	MG RMS (unitless)	**1.00**	0.00	**0.93**	0.06	**0.93**	0.04	**0.94**	0.06	p=0.45
	LG RMS (unitless)	**1.00**	0.00	**0.95**	0.03	**1.00**	0.10	**0.82**	0.06	p=0.21
Session 3	Sol RMS (unitless)	**1.00**	0.00	**0.93**	0.03	**0.78**	0.04	**0.72**	0.03	p<0.0001** Powered<Unpowered
	TA RMS (unitless)	**1.00**	0.00	**0.97**	0.06	**1.17**	0.08	**1.00**	0.06	p=0.05
	MG RMS (unitless)	**1.00**	0.00	**0.98**	0.03	**0.98**	0.05	**0.96**	0.06	p=0.52
	LG RMS (unitless)	**1.00**	0.00	**1.04**	0.03	**0.97**	0.09	**0.90**	0.06	p=0.09

n=9, See Materials and Methods for calculations.

Sol=Soleus, **TA**=tibialis anterior, **MG**=medial gastrocnemius, **LG**=lateral gastrocnemius.

Values are root mean square (RMS) average from stance phase only normalized to Unpowered Beginning condition.
THSD=Tukey Honestly Significant Difference Test Results; **SE**=Standard Error

Condition: Unpowered, Powered

p<0.05 indicates statistical significance. * indicates statistical power >0.65; ** indicates statistical power >0.80.

References

Alexander, R. M. (1991). Energy-saving mechanisms in walking and running. *Journal of Experimental Biology* **160**, 55-69.

Alexander, R. M. (1995). Simple models of human movement. *Applied Mechanics Reviews* **48**, 461-470.

Asmussen, E. and Bonde-Petersen, F. (1974). Apparent efficiency and storage of elastic energy in human muscles during exercise. *Acta Physiol Scand* **92**, 537-45.

Bertram, J. E. and Ruina, A. (2001). Multiple walking speed-frequency relations are predicted by constrained optimization. *J Theor Biol* **209**, 445-53.

Blaxter, K. (1989). Energy Metabolism in Animals and Man. Cambridge: Cambridge University Press.

Brockway, J. M. (1987). Derivation of formulae used to calculate energy expenditure in man. *Hum Nutr Clin Nutr* **41**, 463-71.

Brooks, G. A., Fahey, T. D. and White, T. G. (1996). Exercise physiology: human bioenergetics and its applications. Mountain View, Calif.: Mayfield.

Browning, R. C., Modica, J. R., Kram, R. and Goswami, A. (2007). The effects of adding mass to the legs on the energetics and biomechanics of walking. *Med Sci Sports Exerc* **39**, 515-25.

Cavagna, G. A. and Margaria, R. (1966). Mechanics of walking. *Journal of Applied Physiology* **21**, 271-278.

Cavagna, G. A., Thys, H. and Zamboni, A. (1976). The sources of external work in level walking and running. *Journal of Physiology (London)* **262**, 639-657.

Cavagna, G. A., Willems, P. A., Legramandi, M. A. and Heglund, N. C. (2002). Pendular energy transduction within the step in human walking. *J Exp Biol* **205**, 3413-22.

Cavanagh, P. R. and Kram, R. (1985). Mechanical and muscular factors affecting the efficiency of human movement. *Med Sci Sports Exerc* **17**, 326-31.

Donelan, J. M., Kram, R. and Kuo, A. D. (2001). Mechanical and metabolic determinants of the preferred step width in human walking. *Proceedings of the Royal Society of London Series B-Biological Sciences* **268**, 1985-92.

Donelan, J. M., Kram, R. and Kuo, A. D. (2002a). Mechanical work for step-to-step transitions is a major determinant of the metabolic cost of human walking. *Journal of Experimental Biology* **205**, 3717-27.

Donelan, J. M., Kram, R. and Kuo, A. D. (2002b). Simultaneous positive and negative external mechanical work in human walking. *J Biomech* **35**, 117-24.

Elftman, H. (1939). The function of muscles in locomotion. *American Journal of Physiology* **125**, 357-366.

Eng, J. J. and Winter, D. A. (1995). Kinetic analysis of the lower limbs during walking: what information can be gained from a three-dimensional model? *J Biomech* **28**, 753-758.

Fenn, W. O. (1924). The relation between the work performed and the energy liberated in muscular contraction. *Journal of Physiology, London* **58**, 373-395.

Ferris, D. P., Czerniecki, J. M. and Hannaford, B. (2005). An ankle-foot orthosis powered by artificial pneumatic muscles. *J Appl Biomech* **21**, 189-197.

Ferris, D. P., Gordon, K. E., Sawicki, G. S. and Peethambaran, A. (2006). An improved powered ankle-foot orthosis using proportional myoelectric control. *Gait and Posture* **23**, 425-8.

Ferris, D. P., Sawicki, G. S. and Daley, M. A. (2007). A physiologist's perspective on robotic exoskeleton's for human locomotion. *International Journal of Humanoid Robotics* **in press**.

Fukunaga, T., Kubo, K., Kawakami, Y., Fukashiro, S., Kanehisa, H. and Maganaris, C. N. (2001). In vivo behaviour of human muscle tendon during walking. *Proceedings of the Royal Society of London: Biological Sciences* **268**, 229-33.

Gaesser, G. A. and Brooks, G. A. (1975). Muscular efficiency during steady-rate exercise: effects of speed and work rate. *Journal of Applied Physiology* **38**, 1132-1139.

Gordon, K. E. and Ferris, D. P. (2007). Learning to walk with a robotic ankle exoskeleton. *J Biomech* **in press**.

Gordon, K. E., Sawicki, G. S. and Ferris, D. P. (2006). Mechanical performance of artificial pneumatic muscles to power an ankle-foot orthosis. *J Biomech* **39**, 1832-41.

Gottschall, J. S. and Kram, R. (2003). Energy cost and muscular activity required for propulsion during walking. *J Appl Physiol* **94**, 1766-72.

Grabowski, A., Farley, C. T. and Kram, R. (2005). Independent metabolic costs of supporting body weight and accelerating body mass during walking. *J Appl Physiol* **98**, 579-83.

Griffin, T. M., Roberts, T. J. and Kram, R. (2003). Metabolic cost of generating muscular force in human walking: insights from load-carrying and speed experiments. *Journal of Applied Physiology* **95**, 172-83.

Guizzo, E. and Goldstein, H. (2005). The rise of the body bots. *IEEE Spectrum* **42**, 50-56.

Hill, A. V. (1938). The heat of shortening and the dynamic constants of muscle. *Proceedings of the Royal Society of London: Biological Sciences* **B126**, 136-195.

Ishikawa, M., Komi, P. V., Grey, M. J., Lepola, V. and Bruggemann, G. P. (2005). Muscle-tendon interaction and elastic energy usage in human walking. *J Appl Physiol* **99**, 603-8.

Kuo, A. D., Donelan, J. M. and Ruina, A. (2005). Energetic consequences of walking like an inverted pendulum: step-to-step transitions. *Exerc Sport Sci Rev* **33**, 88-97.

Lichtwark, G. A. and Wilson, A. M. (2006). Interactions between the human gastrocnemius muscle and the Achilles tendon during incline, level and decline locomotion. *Journal of Experimental Biology* **209**, 4379-88.

Mochon, S. and McMahon, T. A. (1980). Ballistic walking. *J. Biomech.* **13**, 49-57.

Norris, J. A., Granata, K. P., Mitros, M. R., Byrne, E. M. and Marsh, A. P. (2007). Effect of augmented plantarflexion power on preferred walking speed and economy in young and older adults. *Gait Posture* **25**, 620-7.

Poole, D. C., Gaesser, G. A., Hogan, M. C., Knight, D. R. and Wagner, P. D. (1992). Pulmonary and leg VO2 during submaximal exercise: implications for muscular efficiency. *Journal of Applied Physiology* **72**, 805-10.

Ruina, A., Bertram, J. E. and Srinivasan, M. (2005). A collisional model of the energetic cost of support work qualitatively explains leg sequencing in walking and galloping, pseudo-elastic leg behavior in running and the walk-to-run transition. *J Theor Biol* **237**, 170-92.

Saunders, J. B., Inman, V. T. and Eberhart, H. D. (1953). The major determinants in normal and pathological gait. *Journal of Bone and Joint Surgery* **35**, 543-558.

Shadmehr, R. and Holcomb, H. H. (1997). Neural correlates of motor memory consolidation. *Science* **277**, 821-825.

Taylor, C. R. (1994). Relating mechanics and energetics during exercise. *Advances in Veterinary Science and Comparative Medicine* **38A**, 181-215.

Williams, K. R. (1985). The relationship between mechanical and physiological energy estimates. *Med Sci Sports Exerc* **17**, 317-25.

Winter, D. A. (1990). Biomechanics and Motor Control of Human Movement. New York: John Wiley & Sons.

Winter, D. A. (1991). The biomechanics and motor control of human gait: normal, elderly and pathological. Waterloo, Ontario: Waterloo Biomechanics.

Zatsiorsky, V. and Seluyanov, V. (1983). The mass and inertial characteristics of the main segments of the human body. In *Biomechanics VIII-B*, (ed. H. a. K. Matsui, K.), pp. 1152-1159. Champaign, IL: Human Kinetics.

Chapter III

Metabolic cost of ankle joint work during level walking with increasing step length

Summary

We examined the metabolic cost of ankle joint mechanical work during human walking at different step lengths. Nine healthy subjects walked at a constant step frequency on a motorized treadmill at speeds corresponding to 80% (1.00 m/s), 100% (1.25 m/s), 120% (1.50 m/s), and 140% (1.75 m/s) of their 1.25 m/s preferred step length (L*). In each condition subjects donned robotic ankle exoskeletons on both legs. The exoskeletons were powered by artificial pneumatic muscles controlled using soleus electromyography (i.e. proportional myoelectric control). We measured subjects' metabolic energy expenditure and exoskeleton mechanics during both unpowered and powered walking to test the hypothesis that ankle plantar flexion requires more metabolic energy at longer step lengths. As step length increased from 0.8 to 1.4 times the preferred step length, exoskeletons delivered ~25% more average positive mechanical power (+0.20 ± 0.02 W/kg to +0.25 ± 0.02 W/kg, respectively; ANOVA, $p = 0.01$). The exoskeletons reduced metabolic energy expenditure more at longer step lengths (-0.21 ± 0.06 W/kg at 0.8L* and -0.70 ± 0.12 W/kg at 1.4L*; ANOVA, $p = 0.002$).

For every 1 J of exoskeleton positive mechanical work subjects saved 0.72 J of metabolic energy ('apparent efficiency' = 1.39) at 0.8L* and 2.6 J of metabolic energy ('apparent efficiency' = 0.38) at 1.4L*. Because the efficiency of isolated muscle positive mechanical work is ~0.25, these results suggest that walking with longer steps increases ankle extensor muscle work relative to Achilles tendon work. However, Achilles tendon recoil still likely contributes up to 35% of ankle joint positive work even at the longest step lengths. Across the range of step lengths we studied, the human ankle joint performed 34%-40% of the total lower-limb positive mechanical work but accounted for only 7%-26% of the total metabolic cost of walking.

Keywords: Locomotion, walking, step length, metabolic cost, exoskeletons, ankle, human, inverse dynamics, joint power, efficiency

Introduction

To walk at faster speeds, humans increase their step length and step frequency, requiring more metabolic energy (Atzler and Herbst, 1927; Bastien et al., 2005; Bertram, 2005; Bertram and Ruina, 2001; Griffin et al., 2003; Margaria, 1938; Ralston, 1958). As walking speed increases, humans optimize their gait by selecting the step length-step frequency combination that minimizes metabolic energy cost per distance traveled (Bertram, 2005; Bertram and Ruina, 2001; Kuo, 2001; Ralston, 1958; Zarrugh et al., 1974).

Kuo used a simple mathematical model of bipedal locomotion to provide insight into how the mechanics and energetics of walking impact the observed

speed-step length relationship in humans (Kuo, 2001). He demonstrated that at any given walking speed, humans must manage a trade-off between the elevated energy cost to use an increased step length and the elevated energy cost to use an increased step frequency. The step length-step frequency combinations that minimized the combined energy costs nearly reproduced the empirically observed speed-step length relationship for human walking (Kuo, 2001).

In Kuo's simple model, single limb support consisted of an energy conservative inverted pendulum cycling kinetic and gravitational potential energy. At the end of stance, the center of mass accelerated downward along a pendular arc prescribed by the trailing leg. As a consequence, mechanical work must be performed to redirect the velocity of the center of mass along the upward pendular arc prescribed by the leading leg (i.e. the new stance leg). Thus, while the net mechanical work over a complete walking stride was zero, equal amounts of negative and positive mechanical work were performed on the center of mass within each stride to transition from stance leg to stance leg. Kuo's simple model also predicted that the magnitude of step-to-step mechanical work increases with step length to the fourth power (Donelan et al., 2002a; Kuo, 2002). Thus, metabolic cost should increase substantially when walking at longer step lengths but the same step frequency.

Experiments on the step-to-step transition in humans support the predictions from Kuo's simple model and confirm that the majority of the mechanical work during walking is performed to move from one stance leg to the next. Donelan et al. used force platforms under each limb (i.e. individual limbs

method) to demonstrate that during double support, the leading leg performs negative work to redirect the center of mass while the trailing leg performs positive work to restore lost energy (Donelan et al., 2002b). The trailing leg positive mechanical work during double support comprises ~60%-70% of the total positive work over a stride and, as predicted, increases with step length to the fourth power (Donelan et al., 2002a). Furthermore, the trailing leg impulse begins just prior to the leading leg heel-strike (i.e. a pre-emptive push-off occurs), reducing the leading leg collision and the magnitude of positive work required to redirect the center of mass velocity (Donelan et al., 2002a; Kuo, 2002; Ruina et al., 2005). Swinging the legs likely accounts for a large portion of the remaining 30-40% of the metabolic energy expenditure of walking (Doke et al., 2005; Doke and Kuo, 2007).

Center of mass level mechanical analyses provide limited insight into how the step-to-step transition mechanical work is generated by the ankle, knee and hip joints (Kuo et al., 2005). Force platform and motion capture data can be combined to estimate the mechanical power generated by muscle-tendons at each of the lower-limb joints at every instant over the walking stride (i.e. inverse dynamics) (Winter, 1990). As walking speed increases, the amplitude of the moments and powers at each of the lower-limb joints increases (Craik and Oatis, 1995; Winter, 1991). Few studies, however, report mechanical joint work during walking and no published study has documented joint work for various walking speeds. Eng et al. reported the relative distribution of lower-limb joint mechanical work over a full walking stride at 1.6 m/s (Eng and Winter, 1995). When

considering just the mechanical energy in the sagittal plane, the ankle (~42%) and hip (~48%) deliver the majority of the total lower-limb joint positive work. The ankle plantar flexors, however, generate the single largest power burst during the trailing limb push-off phase of the step-to-step transition (Eng and Winter, 1995; Gitter et al., 1991; Meinders et al., 1998). Gitter et al. showed that for walking at 1.5 m/s the ankle performed 63% and the hip performed 21% of the stance phase (0-60% of the stride) positive joint mechanical work (Gitter et al., 1991). Meinders et al. focused directly on the push-off phase (44%-62% of the stride) and found that the ankle delivered 78% of the lower-limb positive mechanical work (Meinders et al., 1998). These studies demonstrate that the ankle plantar flexors are a major power source during walking.

Studies using ultrasound to directly examine *in vivo* muscle-tendon behavior in humans demonstrate that the Achilles tendon stores energy throughout stance and then recoils rapidly contributing significantly to ankle joint power output at push-off during walking (Fukunaga et al., 2001; Ishikawa et al., 2005; Ishikawa et al., 2006; Lichtwark et al., 2007; Lichtwark and Wilson, 2006; Lichtwark and Wilson, 2007). To date, no ultrasound study has examined the effects of increasing walking speed on Achilles muscle-tendon mechanics. Indirect evidence, however, suggests that the contribution of the Achilles tendon to ankle joint positive power may be speed dependent (Hansen et al., 2004; Hof et al., 2002).

In our previous work we used bilateral robotic lower-limb exoskeletons to study the metabolic cost of ankle joint mechanical work during level walking at

1.25 m/s (Sawicki and Ferris, 2007). We assumed that exoskeleton artificial pneumatic plantar flexors would directly replace biological ankle extensor muscle work during powered walking. Based on a 0.25 'muscular efficiency' of positive work (Fenn, 1924; Hill, 1939), we hypothesized that for every 1 Joule of biological muscle work we replaced with robotic ankle exoskeletons subjects would save 4 Joules of metabolic energy. Contrary to our hypothesis, we found that for every 1 Joule of ankle joint positive mechanical energy exoskeletons delivered subjects saved only 1.6 J of metabolic energy. This yielded an 'apparent efficiency' of ankle joint positive mechanical work of 0.61. These results were indicative of the Achilles tendon performing up to 60% of the ankle joint positive work. As a result, even though the ankle joint performs ~35% of the total lower-limb joint positive work during walking, that work only requires about 17%-20% of the total metabolic cost of walking.

The purpose of the present study was to examine the role of the ankle joint in contributing to metabolic cost at longer step lengths. We used bilateral pneumatically-powered ankle exoskeletons to alter ankle joint mechanics during push-off. Our goal was to answer two questions: (1) How does the metabolic cost of ankle joint positive work change with increasing walking step length? (2) Does the 'apparent efficiency' of ankle joint positive mechanical work depend on walking step length? We hypothesized that the 'apparent efficiency' of ankle joint positive mechanical work would decrease at longer step lengths. We based this hypothesis on the premise that muscle fibers would contribute more of the ankle joint mechanical work at longer step lengths because of reduced contributions

from the tendon. An inherent assumption of this study was that the exoskeleton mechanical work would replace biological muscle mechanical work rather than augment it. As such, we expected triceps surae muscle activation to be less during walking with the powered exoskeletons compared to walking without exoskeleton power at all step lengths. To test these predictions we compared subjects' net metabolic power and electromyography amplitudes with ankle exoskeletons powered versus unpowered during level, steady-speed walking at various step lengths while holding step frequency constant (Donelan et al., 2002a; Donelan et al., 2002b). We computed the 'apparent efficiency' of ankle joint positve work using simultaneous measurements of the mechanics and energetics of powered walking to gain insight into how underlying ankle extensor muscle-tendon function changes during human walking with increased step length. Our novel joint level approach is an important step in establishing a connection between isolated muscle and whole-body mechanics and energetics during human locomotion. Ultimately, we hope to understand how mechanical and metabolic energy expenditure is partitioned across the lower-limb joints during human walking.

Materials and methods

Subjects: We recruited nine (5 males, 4 females) healthy subjects (body mass = 80.3 ± 14.7 kg; height = 179 ± 3 cm; leg length = 92 ± 2 cm) to participate in the study. Each subject had at least 90 minutes (three or more thirty minute practice sessions) of previous practice walking with powered exoskeletons and exhibited no gait abnormalities. In accordance with the Declaration of Helsinki,

subjects read and signed a consent form approved by the University of Michigan Institutional Review Board for Human Subject research before testing.

Exoskeletons: We custom built lightweight (mass = 1.18 ± 0.11 kg each (mean ± s.d.)) bilateral, ankle-foot exoskeletons (i.e. orthoses) for each subject (**Figure 3.1**). The exoskeletons allowed free rotation about the ankle flexion/extension axis. We used a metal hinge joint to connect a carbon fiber shank to a polypropylene foot section. We used two stainless steel brackets to attach a single artificial pneumatic muscle (length = 45.6 ± 2.2 cm; moment arm = 10.6 ± 0.9 cm) along the posterior shank of each exoskeleton. We used a biomimetic controller to command the exoskeletons plantar flexor torque assistance with timing and amplitude derived from the user's own soleus electromyography (i.e. proportional myoelectric control) (Gordon and Ferris, 2007). Specific details on the design and performance of the exoskeletons are documented elsewhere (Ferris et al., 2005; Ferris et al., 2006; Gordon et al., 2006; Sawicki et al., 2005).

Protocol. Experienced (> 90 minutes walking with powered exoskeletons) subjects walked on a motorized treadmill with bilateral ankle exoskeletons unpowered then powered at four different step lengths (**0.8 x**, **1.0 x, 1.2 x** and **1.4 x** preferred step length (**L***) for unpowered walking at 1.25 m/s) (Donelan et al., 2002a; Donelan et al., 2002b). Our previous work demonstrated no further reductions in net metabolic power after 90 minutes of powered walking (Sawicki and Ferris, 2007). We determined subjects' preferred step period (seconds) using a stopwatch to record the mean time of three 100 step intervals during

unpowered treadmill walking at 1.25 m/s. We took the reciprocal of the mean step period to get the preferred step frequency (steps/s) at 1.25 m/s. Then we divided the treadmill belt speed (m/s) by the step frequency (steps/s) to get the preferred step length (m/step) at 1.25 m/s (**1.0 L***). We used a metronome to enforce subjects' preferred step frequency for all step lengths. We adjusted the treadmill belt speed to constrain subjects' step lengths. The **0.8 L***, **1.0 L***, **1.2 L*** and **1.4 L***, step length conditions corresponded to ~1.00, 1.25, 1.50 and 1.75 m/s treadmill belt speeds respectively. An advantage of adjusting walking speed using this protocol is that it produces an increasing external workload on the center of mass that has a known proportional relationship to the step length (~ step length^4) and limits the effects of frequency dependent (i.e. leg swing) costs on the mechanics and energetics of walking (Donelan et al., 2002a; Donelan et al., 2002b).

Step length conditions were presented in random order but for each step length we followed the same walking timeframe (**Figure 3.1**). First subjects walked for 7 minutes with exoskeletons unpowered (**Unpowered**). Then subjects rested for 3 minutes. Finally, subjects walked for 7 minutes with exoskeletons powered (**Powered**). If the peak force output of the artificial muscles (and exoskeleton torque) is similar in each step length condition then observed differences in average exoskeleton mechanical power output across conditions would be attributed to changes in ankle joint kinematics (range of motion, ankle joint angular velocity) rather than changes in artificial muscles force output. Thus, we tuned the proportional myoelectric controller during the unpowered walking

bout for each step length separately. We set the gain and threshold on soleus surface electromyography so the control signal saturated for at least five consecutive steps. We then doubled the gain in order to encourage reduction in soleus muscle recruitment (Gordon and Ferris, 2007).

Data Collection and Analysis. We recorded subjects' (1) ankle, knee and hip joint kinematics (2) whole-body gait kinematics (3) ankle flexor and extensor surface electromyography and (4) exoskeleton artificial muscles forces. For kinematic, electromyographic and artificial muscle force data we acquired ten second trials (i.e. ~7-9 walking strides) at the beginning of minutes 4, 5, and 6 during each of the eight (unpowered mode and powered mode for each of four step lengths) 7 minute trials. We collected O_2 and CO_2 flow rates during a single 7 minute quiet standing trial of metabolic data for each subject before walking trials commenced. Metabolic data was collected continuously during each of the 7 minute step length conditions.

In addition, on a separate day of testing, we recorded (1) metabolic data while subjects completed each of the step length conditions on the treadmill without (**Without**) wearing powered exoskeletons and (2) simultaneous joint kinematics and ground reaction force data for overground walking with unpowered exoskeletons (7 trials for each step length condition).

Kinematics. During treadmill walking we used an 8-camera video system (frame rate 120 Hz, Motion Analysis Corporation, Santa Rosa, CA, USA) to record the positions of twenty nine reflective markers on the subjects' pelvis and lower-limbs. Raw marker data was smoothed with custom software (Visual 3D,

C-Motion, Rockville, MD) using a 4th-order Butterworth low-pass filter (cutoff frequency 6 Hz). We defined neutral standing posture to be zero degrees for all joints and used the smoothed marker data to calculate ankle knee and hip joint angles (and angular velocities for both legs). We used footswitches (sampling rate = 1200 Hz, B & L Engineering, Tustin, CA, USA) to monitor heel-strike and toe-off events and then calculated the step period (time from heel-strike one leg to heel-strike of the other leg) and double support period (time from heel-strike of one leg to toe-off of the other). The lateral and fore-aft distances between calcaneus markers at heel strike events were obtained to calculate step width and step length respectively. Left and right joint kinematics from heel-strike (0%) to heel-strike (100%) were averaged to get the stride cycle average joint kinematics profiles.

Electromyography. We recorded soleus (Sol), tibialis anterior (TA), medial gastrocnemius (MG) and lateral gastrocnemius (LG) surface electromyography (EMG) for each leg (sampling rate 1200 Hz, Konigsberg Instruments, Inc., Pasadena, CA, USA). EMG amplifier bandwidth was 1000 Hz. We centered bipolar electrodes (inter-electrode distance = 3.5 cm) over the muscle belly and along its long axis in a position to minimize cross-talk. To minimize movement artifact we taped electrodes to the skin when necessary. We high-pass filtered (4th order Butterworth, cutoff frequency 20 Hz), rectified and low-pass filtered (4th order Butterworth, cutoff frequency 10 Hz) each signal (i.e. linear envelope). We averaged data from right and left legs to get stride cycle average profiles of the linear enveloped EMG (from heel-strike to heel-strike for each leg). Curves were

normalized using the peak value (average of left and right) for each muscle during the unpowered walking bout at the steepest incline (**Unpowered 1.4 L***).

To quantify changes in EMG activation levels, stance phase root-mean square (RMS) average EMG amplitudes were computed from the high-pass filtered, rectified EMG data of each leg. We averaged RMS EMG values from each leg and normalized using the average RMS value from the **Unpowered 1.4 L*** trial.

Joint Mechanics. To establish baseline joint mechanical power output we collected seven overground walking trials at each step length with unpowered exoskeletons. To ensure that trials were within $\pm$ 0.05 m/s of the target speed, we used infrared timers triggered at beginning and end of the walkway. We recorded ground reaction forces under each foot (left then right) with two force platforms (1200Hz, Advanced Mechanical Technology Inc., Watertown, MA, USA). Combining force platform data with motion capture data we calculated ankle, knee, and hip mechanical power over the stride for each leg using inverse dynamics (Visual3D software, C-Motion, Rockville, MD, USA). We used standard regression equations to estimate subjects' anthropometry (Zatsiorsky and Seluyanov, 1983) and adjusted foot and shank parameters to account for added exoskeleton mass and inertia. Joint powers for the right and left legs (from heel-strike to heel-strike for each leg) were averaged and divided by subject mass to get the stride cycle average exoskeleton mechanical power.

To quantify the average rate of joint positive and negative mechanical work over a stride we integrated only the positive (or negative) portions of both

the left and right mechanical power curves (from right heel strike to left heel strike to capture simultaneous trailing and leading limb joint powers), summed them, and divided the total by the average step period. The same procedure was used for the ankle, knee and hip.

Exoskeleton Mechanics. With the ankle joint in the neutral position during upright standing posture we measured artificial muscle moment arm (moment arm = 10.6 ± 0.9 cm). We recorded the forces produced by the artificial pneumatic muscles during powered walking with single-axis compression load transducers (1200Hz, Omega Engineering, Stamford, CT, USA). Smoothed artificial muscle force data (low-pass filtered, 4^{th} order Butterworth, cutoff frequency 6 Hz) was scaled by the artificial moment arm length for each leg to obtain exoskeleton torque. The mechanical power delivered by the exoskeletons was computed as the product of the exoskeleton torque and ankle joint angular velocity (from motion capture). We averaged exoskeleton power for the right and left legs (from heel-strike to heel-strike for each leg) then divided by subject mass to get the stride cycle average exoskeletons mechanical power.

We computed the average rate of exoskeleton positive and negative mechanical work in order to relate exoskeleton mechanical power and changes in subjects' net metabolic power. We partitioned the positive and negative portions of both the left and right exoskeleton mechanical power curves (from left heel strike to left heel strike). Then we integrated positive (or negative) mechanical power from each leg, summed over legs, and divided the total by the

average stride period to get average positive (or negative) mechanical power delivered by the exoskeletons over a stride.

Metabolic Cost. We used an open-circuit spirometry system (Physiodyne Instruments, Quogue, NY) to record O_2 and CO_2 flow rates (Blaxter, 1989; Brooks et al., 1996). Seven minute trials were chosen to allow subjects to reach steady-state metabolic energy expenditure. We closely monitored the respiratory exchange ratio (RER) to ensure that subjects relied on aerobic metabolism (RER < 1) (Brooks et al., 1996). When a full 7 minute trial could not be completed, we stopped and re-collected the data after the standard 3 minute period of rest. We used the standard equations documented by Brockway (Brockway, 1987) to calculate gross metabolic power (Watts) from averaged O_2 and CO_2 rates for minutes 4-6 of each trial. Then we subtracted the averaged data from minutes 4-6 of the quiet standing trial to obtain the net metabolic power (Griffin et al., 2003; Poole et al., 1992) and divided net metabolic power values by subject mass to obtain mass specific net metabolic power (W/kg). The net metabolic power from the unpowered trial for each step length was used to compute a percentage difference between unpowered and powered walking.

Exoskeleton Performance Index. By combining measures of mechanical and metabolic power we computed the exoskeleton performance index. First, we subtracted the net metabolic power during unpowered walking from the net metabolic power during powered walking for each step length to get the metabolic power savings due to the exoskeletons assistance. Muscles perform positive mechanical work with a ‘muscular efficiency’ of 0.25 (Fenn, 1924; Hill,

1938) and we assumed that changes in net metabolic power would reflect the cost of the underlying biological muscle positive work replaced by the powered exoskeletons. Therefore, we multiplied changes in net metabolic power by 0.25 to yield the expected amount of positive mechanical power delivered by exoskeletons for a given change in net metabolic power. Then we divided the measured by the expected average positive mechanical power delivered by the exoskeletons to yield the exoskeleton performance index (Equation 1). A performance index of 1.0 would suggest that exoskeletons assistance completely replaced underlying biological muscle positive mechanical work.

$$\text{Exoskeletons Performance Index} = \frac{\Delta \text{ Net Metabolic Power} * 0.25}{\text{Average Exoskeletons Positive Mechanical Power}} \quad (1)$$

In addition, we computed an equivalent 'apparent efficiency' (Asmussen and Bonde-Petersen, 1974) by taking the reciprocal of four times the performance index (i.e. performance index = 1.0 is equivalent to 'apparent efficiency' = 0.25) (Equation 2).

$$\text{Ankle Joint Apparent Efficiency} = \frac{1}{4 * \text{Exoskeletons Performance Index}} = \frac{\text{Average Exoskeletons Positive Mechanical Power}}{\Delta \text{ Net Metabolic Power}} \quad (2)$$

Statistical Analyses. We used JMP IN statistical software (SAS Institute, Inc. Cary, NC, USA) to perform a number of repeated measures analysis of variance tests (ANOVAs) We set significance level at $p < 0.05$ for all tests. For

tests that yielded significance used post-hoc Tukey Honestly Significant Difference (THSD) tests to determine specific differences between means we and computed statistical power

In the first two analyses we assessed the effect of step length (**0.8 L*, 1.0 L*, 1.2 L*, 1.4 L***) on net metabolic power, exoskeleton mechanics, stance phase RMS EMG and gait kinematics metrics (two-way ANOVA (subject, gradient)) for powered and unpowered data grouped together (except powered data only for exoskeletons mechanics and without, unpowered and powered data grouped for net metabolic power).

In the other four ANOVA analyses (one for 0.8 L*, 1.0 L*, 1.2 L* and 1.4 L*) we assessed the effect of exoskeleton mode (**Without, Unpowered, Powered**), on net metabolic power (**Without, Unpowered, Powered**), stance phase RMS EMG and gait kinematics (**Unpowered, Powered**) metrics (two-way ANOVA (subject, mode).

Results

Joint Kinematics. During unpowered walking, as step length increased subjects walked with increased ankle dorsiflexion, knee flexion and hip flexion early in stance phase. Push-off phase kinematics were similar across step lengths for the knee, but the ankle and hip joints were more extended for unpowered walking at longer step lengths (**Figure 3.2**).

The knee and hip joint angles over the stride were nearly identical during powered versus unpowered walking during all step length conditions. Ankle joint

kinematics, however, were altered by exoskeleton mechanical assistance during powered walking for all step length conditions (**Figure 3.2**).

Ankle joint angle was similar at heel strike but more plantar flexed throughout early stance during powered versus unpowered walking for all step lengths. In addition, at push-off, the ankle joint angle peak was larger and occurred earlier during stance during powered versus unpowered walking. For example, during **Unpowered 1.4 L*** the ankle joint angle peaked at 62% of the stride cycle and reached ~+16 degrees. During **Powered 1.4 L*** the ankle joint angle peaked slightly earlier in the stride cycle and reached ~+18 degrees (**Figure 3.2**). For all step lengths, swing phase ankle joint angle was similar during powered and unpowered walking.

Exoskeleton Mechanics. The exoskeletons produced small amounts of torque about the ankle during unpowered walking and delivered near zero mechanical power to the user over the stride (**Figure 3.3**).

During powered walking, exoskeletons produced similar peak torque (~0.40-0.42 N-m/kg) at all step lengths. For walking at preferred step length (**1.0 L*)** peak exoskeleton torque was ~32% of the peak ankle joint moment.

During powered walking, as step length increased, the peak ankle joint angular velocity increased sharply and occurred earlier in the stride. Peak ankle joint angular velocity was ~154 deg/s (at 58% of the stride) during **Powered 0.8 L*** and increased to ~218 deg/s (at 53% of the stride) during **Powered 1.4 L*** (**Figure 3.3**).

As a result of increases in ankle joint angular velocity, the peak exoskeleton mechanical power at push-off increased with step length from ~0.8 W/kg during **Powered 0.8 L*** to ~1.2 W/kg during **Powered 1.4 L*** (**Figure 3.3**). The exoskeleton peak mechanical power was 49% of the overground peak ankle joint mechanical power for walking at the shortest step lengths (0.8 L*) and decreased to 31% of the overground peak ankle joint mechanical power for walking at the longest step lengths (1.4 L*).

As step length increased during powered walking, ankle exoskeletons delivered increasing absolute amounts of positive mechanical power over the stride (ANOVA, $p = 0.01$, THSD, 1.4 L* > 0.8 L*; 1.2 L* > 0.8L*) (**Figure 3.5 B**). Exoskeletons average positive mechanical power was 0.20 ± 0.02 W/kg (mean ± s.e.) during **Powered 0.8 L*** and increased by ~25% to 0.25 ± 0.02 W/kg during **Powered 1.4 L***. When powered, exoskeletons absorbed very little mechanical energy. Exoskeletons average negative mechanical power (-0.03 W/kg) over the stride was not different for powered walking at different step lengths (ANOVA, $p = 0.27$) (**Figure 3.5 B**).

Metabolic Cost. Subjects' net metabolic power increased with increasing step length (ANOVA, $p < 0.0001$, THSD, 1.4 L* > 1.2 L*, 1.0 L*, 0.8 L*; 1.2 L* > 1.0 L*, 0.8 L*; 1.0 L* > 0.8 L*). In addition, net metabolic power was significantly lower during powered versus unpowered walking for step lengths equal to or longer than preferred 1.0 L* (1.0 L* ANOVA, $p = 0.001$, THSD, Powered < Unpowered; 1.2 L* ANOVA, $p = 0.001$, THSD, Powered < Unpowered; 1.4 L* ANOVA, $p = 0.003$, THSD, Powered < Unpowered) (**Figure 3.4**). Net metabolic

power was 2.86 ± 0.07 W/kg during **Unpowered 0.8 L*** and increased to 6.89 ± 0.32 W/kg during **Unpowered 1.4 L***. In comparison, net metabolic power was only 2.65 ± 0.12 W/kg during **Powered 0.8 L*** and increased to 6.19 ± 0.29 W/kg during **Powered 1.4 L***.

The net metabolic power was significantly higher (by ~8%-15%) during walking with unpowered exoskeletons compared with walking without exoskeletons. There was a significant difference between conditions for all step lengths except the longest 1.4 L* (0.8 L* ANOVA, $p = 0.008$, THSD, Unpowered > Without; 1.0 L* ANOVA, $p = 0.001$, THSD, Unpowered > Without; 0.8 L* ANOVA, $p = 0.001$, THSD, Unpowered > Without). The net metabolic power during powered exoskeleton walking (6.19 ± 0.29 W/kg) was lower than for walking without wearing exoskeletons (7.18 ± 0.50 W/kg) for the longest step length condition (1.4 L* ANOVA, $p = 0.003$, THSD, Powered < Without).

The absolute reduction in net metabolic power in powered versus unpowered walking increased steadily with increasing step length (ANOVA, $p = 0.002$, THSD, 1.4 L* < 0.8 L*; 1.2 L* < 0.8 L*) (**Figure 3.5 A**). At the shortest step lengths ground (0.8 x L*), net metabolic power was 0.21 ± 0.06 W/kg less during powered versus unpowered walking. At 1.4 L* the reduction in net metabolic power due to mechanical assistance was 0.70 ± 0.12 W/kg (~233% more than for shortest steps). Although reductions in net metabolic power during powered walking were larger for walking with longer steps, relative changes in net metabolic power were similar between step lengths (8%-12% reduction comparing powered to unpowered) (**Figure 3.4**).

Joint Mechanics. As step length increased during overground walking with unpowered exoskeletons the ankle, knee and hip joints combined to produced more average positive mechanical power over the stride. Average ankle negative mechanical power was similar across step lengths, but the knee and hip produced more average negative mechanical power over the stride as step length increased (**Figure 3.6**).

During overground walking, the hip and ankle produced most of the positive mechanical power at all step lengths. The hip average positive mechanical power over the stride was 0.39 ± 0.04 W/kg at **Unpowered 0.8 L***, 0.47 ± 0.05 W/kg at **Unpowered 1.0 L***, 0.51 ± 0.04 W/kg at **Unpowered 1.2 L***, and 0.60 ± 0.04 W/kg at **Unpowered 1.4 L***. The ankle average positive mechanical power over the stride was 0.28 ± 0.03 W/kg at **Unpowered 0.8 L***, 0.38 ± 0.03 W/kg at **Unpowered 1.0 x L***, 0.52 ± 0.03 W/kg at **Unpowered 1.2 L***, and 0.63 ± 0.04 W/kg at **Unpowered 1.4 L***.

The ankle joint contributed more of the total joint (ankle + knee + hip) average positive mechanical power over the stride as step length increased (34% at 0.8 L* and 39% at 1.4 L*) (**Figure 3.7**). However, the relative contribution of the exoskeletons positive mechanical power to ankle joint positive mechanical power decreased sharply with increasing step length from 70% at the shortest steps (1.2 L*) to 40% at the longest steps (1.4 L*) (**Figure 3.6 and 3.7**). As a result, the exoskeletons delivered less of the average total joint positive mechanical power over the stride during **Powered 1.4 L*** (16%) when compared to **Powered 0.8 L*** (24%) (**Figure 3.7**).

Exoskeleton Performance Index. Exoskeletons performance index increased with increasing step length (ANOVA, $p = 0.01$, THSD, 1.4 L* > 0.8 L*) **(Figure 3.5 C**). Performance index increased 261% from 0.18 ± 0.12 (ankle joint 'apparent efficiency' = 1.39) during **Powered 0.8 L*** to 0.65 ± 0.10 (ankle joint 'apparent efficiency' = 0.38) during **Powered 1.4 L***. For **Powered 1.0 L*** and **Powered 1.2 L*** the performance index was 0.41 ± 0.06 (ankle joint 'apparent efficiency' = 0.61) and 0.56 ± 0.10 (ankle joint 'apparent efficiency' = 0.45) respectively.

Electromyography. Subjects increased activation of the triceps surae muscle group (i.e. soleus, medial and lateral gastrocnemius) as step length increased. Soleus stance phase root mean square (RMS) electromyography (EMG) was ~42% higher during unpowered and ~56% higher during powered walking at 1.4 L* when compared to walking at 0.8 L* (ANOVA, $p < 0.0001$, THSD, 1.4 L* > 1.2 L*, 1.0 L*, 0.8 L*; 1.2 L* > 1.0 L*, 0.8 L*; 1.0 L* > 0.8 L*) (**Figures 3.8, 3.9**). Medial and lateral gastrocnemius stance RMS EMG both increased (by ~47% and 144% respectively) as step length increased from 0.8 L* to 1.4 L* during unpowered walking. For powered walking, medial gastrocnemius stance RMS EMG increased by ~36% and lateral gastrocnemius stance RMS EMG increased ~135% as step length increased from 0.8 L* to 1.4 L* (ANOVA, $p < 0.0001$, THSD, 1.4 L* > 1.2 L*, 1.0 L*, 0.8 L*; 1.2 L* > 0.8 L* for medial gastrocnemius and ANOVA, $p < 0.0001$, THSD, 1.4 L* > 1.2 L*, 1.0 L*, 0.8 L*; 1.2 L* > 1.0 L*; 0.8 L*; 1.0 L* > 0.8 L*) (**Figure 3.9)**.

Subjects altered soleus muscle activation amplitude but not timing during the stance phase of powered walking when compared to unpowered walking in all step length conditions (**Figure 3.8**). For walking with short steps (0.8 L*) soleus stance phase RMS EMG was only ~11% lower during powered versus unpowered walking and the difference was not significant (0.8 L* ANOVA, $p = 0.28$). At steeper surface inclines reductions in soleus stance RMS EMG in the powered versus unpowered mode were larger (~17%-20%) (1.0 L* ANOVA, $p = 0.002$, THSD, Powered < Unpowered; 1.2 L* and 1.4 L* ANOVAs, $p < 0.0001$, THSD, Powered < Unpowered) (**Figure 3.9**).

Reductions in both medial and lateral gastrocnemius stance RMS EMG amplitudes during powered versus unpowered walking were smaller (ranging from ~6%-15%) than in soleus. For medial gastrocnemius, stance phase RMS EMG was reduced in powered versus unpowered walking only at the longest step length conditions (1.2 L* ANOVA, $p = 0.009$, THSD, Powered < Unpowered; 1.4 L* ANOVA, $p = 0.002$, THSD, Powered < Unpowered). In the longest step length condition, lateral gastrocnemius stance phase RMS EMG was reduced during powered walking (1.4 L* ANOVA, $p = 0.006$, THSD, Powered < Unpowered) (**Figure 3.9**).

Tibialis anterior muscle recruitment increased with increasing step length (ANOVA, $p < 0.0001$, THSD, 1.4 L* > 1.2 L*, 1.0 L*, 0.8 L*; 1.2 L* > 1.0 L*, 0.8 L*; 1.0 L* > 0.8 L*) but was not significantly altered when exoskeletons were powered except during walking at 1.2 L* (ANOVA, $p = 0.003$, THSD, Powered < Unpowered) (**Figure 3.9**).

Gait Kinematics. As expected, step length increased significantly from condition to condition (ANOVA, $p < 0.0001$) and step period was the same for all step length conditions (ANOVA, $p = 0.13$) (**Table 3.1**). In addition, subjects took wider steps (ANOVA, $p < 0.002$) and spent less time in double support (ANOVA, $p< 0.0001$) as step length increased (ANOVA, $p < 0.002$) (**Table 3.1**).

There were no significant differences in step period (ANOVA, $p > 0.47$), step width (ANOVA, $p > 0.37$), or double support period (ANOVA, $p > 0.27$), between powered and unpowered walking at any step length. Step length was shorter by ~1% during powered walking at 1.0 L* (ANOVA, $p = 0.04$; THSD, Powered < Unpowered) (**Table 3.1**).

Discussion

Our results suggest that as step length increases from 80% to 140% of the preferred step length the metabolic cost of ankle joint positive mechanical work increases from ~7% to ~26% of the total metabolic cost of walking. The increased metabolic cost of ankle joint positive work is due to (1) a small increase in the relative contribution of the ankle joint to the total lower-limb joint positive mechanical work (from 34% to 39%) and (2) a large decrease in the 'apparent efficiency' of the ankle joint muscle-tendon system (from 1.39 to 0.38) with increasing step length.

With powered ankle exoskeletons, subjects saved more than three times the absolute net metabolic power in the longest (1.4 L*) compared to the shortest (0.8 L*) step length condition, but relative reductions in metabolic cost were similar across step lengths (8%-12%) (**Figure 3.4**). This was because

exoskeletons performed a smaller and smaller percentage of ankle joint (and total joint) average positive mechanical power at longer step lengths (**Figure 3.7**). Normally the human ankle joint generates more positive mechanical power during push-off as walking speed increases by increasing the magnitudes of both the ankle joint extensor moment and the ankle joint extensor angular velocity (Craik and Oatis, 1995; Winter, 1984). In the present study, although the ankle joint angular velocity increased near push-off with increasing walking step length (and therefore speed), the peak torque generated by the exoskeletons was very similar across step lengths. Increases in exoskeletons average mechanical power were due almost entirely to increases in ankle joint angular velocity. Exoskeletons delivered more average mechanical power over the stride with increasing step length, but they did not keep pace with increases in the biological ankle joint moment.

Mechanical properties of the artificial pneumatic muscles could have limited their work output. The force bandwidth of the artificial pneumatic muscles at ~2.4 Hz (Gordon et al., 2006) was sufficient for this task (walking step frequency was ~1.75 Hz for all step lengths tested). However, the artificial pneumatic muscle force-length properties may have affected work output at longer step lengths. As a result of increases in ankle joint angular velocity near push-off, the artificial muscles spent less time at long relative lengths, limiting their positive mechanical work output during the power stroke (Klute et al., 2002). Thus, exoskeletons contributed less of the total ankle joint positive work at longer step lengths. It was still possible to compare exoskeleton positive power output to changes in

subjects' net metabolic power to get insight into the 'apparent efficiency' and relative metabolic cost of the ankle joint during walking.

The accuracy of our estimates for both the relative metabolic cost (% of total cost of walking) and the 'apparent efficiency' of ankle joint positive work depend on a key assumption. We based our calculations on the expectation that changes in subjects' net metabolic power could be attributed to powered exoskeleton mechanical work *directly* replacing ankle joint muscle-tendon positive mechanical work. There are a number of factors that could have influenced the validity of this assumption.

Subjects could have increased their total average external mechanical power in response to exoskeleton mechanical assistance. A higher average external mechanical power during powered versus unpowered walking would indicate that subjects used exoskeleton energy to *augment* rather than *replace* biological muscle-tendon power output. This would make it difficult to attribute changes in subjects' net metabolic power due to differences in overall gait characteristics versus exoskeleton assistance isolated at the ankle joint. Net metabolic power during walking increases with increasing step length (Donelan et al., 2002a), step period (Bertram and Ruina, 2001), and step width (Donelan et al., 2001). We held step frequency constant (using a metronome) and used treadmill belt speed to vary the step length (**Table 3.1**). Keeping step length and step frequency constant highly constrains the average external mechanical power to be similar for unpowered and powered walking. We also measured step

width and found no differences between unpowered and powered walking during any step length condition (**Table 3.1**).

Even with nearly constant external average mechanical power, subjects still could have altered the distribution of mechanical power across the joints between unpowered and powered walking. For example, during powered walking, increased ankle joint positive mechanical power could have been offset by compensatory muscle-tendon mechanical power at the knee or hip. In this study, subjects were limited to walking on a motorized treadmill during powered conditions because of the tethered pneumatic hoses connecting exoskeleton artificial pneumatic muscles to a pressurized air source. Since our treadmill was not instrumented with force platforms, we could not compare joint powers using inverse dynamics for unpowered and powered walking to rule out redistribution of mechanical power. Despite this limitation, we believe that powered exoskeletons only altered ankle joint mechanics. During powered walking, the exoskeletons delivered 32% of the peak ankle moment and 48% of the peak ankle mechanical power observed during overground unpowered walking trials. In response, subjects significantly decreased muscle activity in their biological ankle extensors suggesting that the total ankle joint moment (and presumably mechanical power) was maintained between unpowered and powered conditions.

Reductions in soleus RMS EMG (up to 20%) were larger than in medial gastrocnemius (up to 13%) and lateral gastrocnemius (up to 15%) (**Figures 3.8, 3.9**). It is possible that reductions in the biarticular gastrocnemius muscles due to powered assistance were smaller than in soleus because of their functional role

in assisting with swing leg initiation (Meinders et al., 1998; Neptune et al., 2001). The larger reductions in soleus are consistent with our previous work using powered exoskeletons (20%-30% reductions) (Gordon and Ferris, 2007; Sawicki and Ferris, 2007). Recent evidence indicates that positive force feedback via type Ib afferents contributes significantly to soleus muscle activity (Grey et al., 2007) and suggests that reductions in soleus muscle activity during powered versus unpowered walking may reflect reduced positive force feedback due to partial unloading of the Achilles tendon.

Subjects could also have responded to added ankle joint mechanical power by increasing dorsiflexor activation. Muscle co-activation is an indicator of simultaneous positive and negative joint work and can significantly increase the metabolic cost of walking (Winter, 1990). To address this possibility we measured ankle joint muscles surface electromyography for both unpowered and powered walking at each step length (**Figures 3.8, 3.9**). Tibialis anterior, the primary ankle joint dorsiflexor, RMS EMG was not elevated during powered walking at any of the step lengths we tested. Although we did not measure EMG to check for co-activation at more proximal joints, our previous work has indicated no differences in the vastii, rectus femoris, and medial hamstrings between powered and unpowered ankle exoskeleton walking (Gordon and Ferris, 2007).

Our joint kinematics results provide additional evidence that subjects did not redistribute joint mechanical power due to mechanical assistance. During powered walking, the ankle joint was slightly more plantar flexed during stance,

but the knee and hip joint kinematics were nearly identical for powered and unpowered walking (**Figure 3.2**).

Finally, we assumed that mechanical work performed by the net ankle moment is an accurate estimate of the underlying mechanical work performed by the ankle extensor muscles and Achilles tendon during walking. Biarticular medial and lateral gastrocnemius can theoretically transfer mechanical energy to and from the ankle joint via the knee (Prilutsky et al., 1996; Wells, 1988). However, during the stance phase of walking the energy transfers between the knee and ankle do not significantly confound the accuracy of muscle work estimates based on net moment work (Prilutsky et al., 1996). For example, during the push-off phase of walking, medial and lateral gastrocnemius perform positive work at both the ankle and knee while soleus performs positive work only at the ankle. But because there is no simultaneous negative work by ankle flexors occurring, the positive mechanical work delivered to the ankle joint by the medial and lateral gastrocnemius and soleus are all accounted for by integrating the net ankle joint mechanical power.

Given the validity of our aforementioned assumptions, our results indicate that the ankle muscle-tendon system performs positive mechanical work during walking with remarkably high ‘apparent efficiency’, even at long step lengths. Actively shortening muscle fibers in isolation perform mechanical work with a ‘muscular efficiency’ of ~0.25 (Fenn, 1924; Hill, 1939). In the current study, as walking step length increased, the ankle joint muscle-tendon system performed positive mechanical work with lower ‘apparent efficiency’ (**Figure 3.5 C**). But

even in the longest step length condition (1.4 L*) the ankle joint was considerably more efficient (~0.39) than muscle in isolation (0.25). These results suggest that the Achilles tendon contributes a major portion of the positive work performed by the ankle joint during walking, at all step lengths. Assuming muscle positive work is performed with efficiency 0.25 and accounts for the whole metabolic cost of ankle joint work, we can compute an *upper limit* on the fraction of ankle joint positive work performed by muscles (i.e. ankle muscle work fraction = 0.25/ankle joint 'apparent efficiency'). For walking at 0.8 L* (~1.00 m/s), we estimate that muscles perform at most 18% (i.e. 0.25/1.39 x 100) of the total joint work. The Achilles tendon, therefore, must perform the remaining 82% of the ankle joint positive work. Similarly, for walking at 1.4 L* (~1.75 m/s), muscles perform at most 65% and the Achilles tendon at least 35% of the total ankle joint muscle-tendon positive work.

Our suggestion that Achilles tendon elastic energy storage and return is significant during walking is consistent with recent *in vivo* ultrasound data from humans (Fukunaga et al., 2001; Ishikawa et al., 2005; Ishikawa et al., 2006; Lichtwark and Wilson, 2006). Ishikawa et al. showed that during walking at 1.4 m/s, the soleus and medial gastrocnemius act nearly isometrically to support a 'catapult action' in the Achilles tendon (Ishikawa et al., 2005). Negative work is stored in the Achilles tendon unit over the first 70% and then released rapidly over the final 30% of the stance phase. The reported mechanical power curves for the muscle-tendon unit, and the tendon only, suggest that the vast majority (>80%) of the positive work performed by the muscle-tendon during push-off is

delivered by recoiling Achilles tendon (Ishikawa et al., 2005). Our data from similar walking speeds (1.0 L* and 1.2 L* are ~1.25 and ~1.5 m/s) suggest that the Achilles tendon performs *at least* 44%-59% of the total ankle joint muscle-tendon work. *In vivo* measurement ultrasound experiments have not examined whether ankle muscle-tendon dynamics are altered with increasing walking step length or speed. Hof et al. used indirect methods (force platform and kinematics) to demonstrate that as walking speed (Hof et al., 2002) and step length (Hof et al., 1983) increases soleus and gastrocnemius muscles perform a larger fraction of the ankle joint muscle-tendon work. We estimate from Hof's data that muscles perform ~50% of the ankle joint positive work at ~1.13 m/s and ~90% at ~1.96 m/s (Hof et al., 1983). These increases are consistent with our calculations that the maximum ankle joint muscle work fraction increases from ~18% to ~65% as step length increases from 0.8L* (~1.0 m/s) to 1.4L* (~1.75 m/s). Studies using forward dynamics computer simulations of walking also indicate that Achilles tendon supplies a significant amount of energy during walking and that its relative contribution is lower at higher speeds (Neptune et al., 2004; Sasaki and Neptune, 2006). Sasaki et al. showed that as simulated walking speed increases from 1.6 m/s to 2.4 m/s the fraction of mechanical work performed by soleus muscle fibers increases from ~50% to 65% of the total muscle-tendon mechanical work (Sasaki and Neptune, 2006).

Our results suggest that the relative metabolic cost of ankle joint mechanical work increases with step length during walking. The ankle joint provides a significant fraction of the total positive joint work that increases slightly

with step length (from 34% to 39%) (**Figure 3.7**). In addition, ankle plantar flexor muscles perform a larger fraction of the total ankle joint positive work at longer step lengths, driving down the 'apparent efficiency' of ankle joint positive work (from 1.39 to 0.38) (**Figure 3.5 C**). As step length increases, the ankle joint performs a larger fraction of the total lower-limb joint mechanical work with lower 'apparent efficiency'. Therefore, the fraction of the total metabolic cost of walking due to ankle joint positive mechanical work increases at longer step lengths.

As step length increases from 80% to 140% of preferred, we estimate that the ankle joint consumes 17%-19% more of the total net metabolic energy during walking. For example, at 0.8 L* the percentage of the summed joint positive mechanical work performed by the ankle joint is 34%. The 'apparent efficiency' of summed joint (ankle + knee +hip) positive mechanical work at 0.8 L* is 0.29 (i.e. lower-limb joints average positive mechanical power (0.83 W/kg) / net metabolic power (2.86 W/kg) = 0.29). The 'apparent efficiency' of ankle joint *only* positive mechanical work is 1.39. Thus, the percentage of the total metabolic cost due to ankle joint positive work is 34%*0.29/1.39 = 7%. Similar calculations can be carried out for the other step length conditions. The percentage of joint work from the ankle is 36%, 40% and 39% for the 1.0L*-1.4L* step length conditions. Over the same range of step lengths, the 'apparent efficiency' of summed joint work is 0.31, 0.29 and 0.23 and the ankle joint 'apparent efficiency' is 0.61, 0.45 and 0.38. The ankle joint consumes 18%, 26%, and 24% of the total metabolic energy for walking as step length increases from preferred to 140% preferred.

The metabolic cost of walking may be dominated by positive muscle work at the proximal joints (i.e. hip and knee). Our results suggest that humans can save a significant amount of metabolic energy at the distal ankle joint by using Achilles tendon elastic energy to partially power push-off. As a result, in the worst case (i.e. 1.2 L*) the ankle joint consumes 26% of the total net metabolic energy but produces 40% of the total positive mechanical work during walking. So where is the remaining 74% of the energy spent? Keeping along the lines of lower-limb joint work, we feel that the hip joint might consume a large portion of unaccounted metabolic energy. The hip supplies positive mechanical power on par with the ankle (~30%-40% of the total joint positive work). But the morphology (i.e. large muscle fibers and short or no tendons) of the human hip may significantly reduce its 'apparent efficiency' to perform positive mechanical work. It is likely that most of the positive work supplied by the hip joint is performed almost exclusively by active muscle shortening rather than passive tendon recoil. At the preferred step length, if the combined knee/hip positive mechanical work (64% of the total) accounts for the remaining 82% of the metabolic cost of walking then we estimate the knee/hip 'apparent efficiency' is ~0.24.

Implications and Future Work. From a basic science perspective, our long-term goal is to establish a joint-level relationship between the mechanics and energetics of human locomotion. We hope to be able to approximately explain the metabolic cost of human walking as the sum of the metabolic costs of performing positive work at each of the lower-limb joints (ankle + knee + hip).

With measurements of average positive mechanical power and the ‘apparent efficiency’ of positive mechanical work for each joint this should be possible. Therefore, future studies should examine the ‘apparent efficiency’ of the hip and knee joints during walking under various walking conditions.

The importance of elastic energy storage and return in the Achilles tendon during walking sheds light on an alternative way to view ankle exoskeleton mechanical assistance. Even if ankle joint extensors perform little muscular work during human walking, they must still act like struts, producing the forces necessary to support body weight and series tendon elastic energy storage and return (Griffin et al., 2003). This may be a useful perspective to take when trying to understand changes in net metabolic power due to powering lower-limb joints where elastic energy cycling is important (i.e. the ankle). For example, regardless of the work that exoskeleton artificial muscles perform, the torque that they develop about the ankle reduces the forces required from biological ankle extensors. Although we did not use ankle joint moment data to estimate reductions in muscle forces, it should be possible to calculate an ‘apparent economy’ of ankle joint force production to gain insight into the relative metabolic costs of generating muscle force versus performing muscle work during human walking.

Considerable effort has been placed on developing assistive devices (i.e. exoskeletons and prostheses) designed to reduce the metabolic cost of walking (Guizzo and Goldstein, 2005). From an applied science perspective, our results suggest that metabolic energy savings are likely to be much more modest than

expected when using an exoskeleton to supplant joint work at distal, compliant joints. Instead, powering joints where muscles perform most of the work rather than tendon stretch and recoil (i.e. powering the less efficient joints) may lead to larger reductions in metabolic cost (Ferris et al., 2007). Furthermore, passive devices designed to reduce isometric muscle forces during periods of tendon stretch and recoil could also be useful at relatively elastic joints (i.e. ankle).

Acknowledgements

The work was supported by NSF BES-0347479 to D.P. Ferris. We would like to thank Catherine Kinnaird, Jineane Shibuya and other members of the Human Neuromechanics Laboratory for assisting with data collection and analysis. Jacob Godak and Anne Manier of the University of Michigan Orthotics and Prosthetics Center built the exoskeletons.

Figures and Tables

Figure 3.1 Experimental set-up. (A) Subjects walked on a motorized treadmill for 7 minutes with exoskeletons unpowered, then rested for 3 minutes, then walked for 7 minutes with exoskeletons powered, while a metronome enforced their preferred step frequency (from unpowered walking at 1.25 m/s). Treadmill belt speed was set to achieve step length conditions of 0.8, 1.0, 1.2 and 1.4 x the preferred step length (L*) at 1.25 m/s. Conditions were presented in randomized order. Outlined boxes indicate periods where data was analyzed (minutes 4-6) in both unpowered and powered conditions. **(B)** During powered walking, bilateral ankle-foot orthosis (i.e. exoskeleton) artificial pneumatic muscles were controlled in real-time with users' own soleus muscle activity. We collected joint kinematics using motion capture and reflective markers, O_2 and CO_2 flow rates with a metabolic cart, and artificial muscle forces with series load transducers.

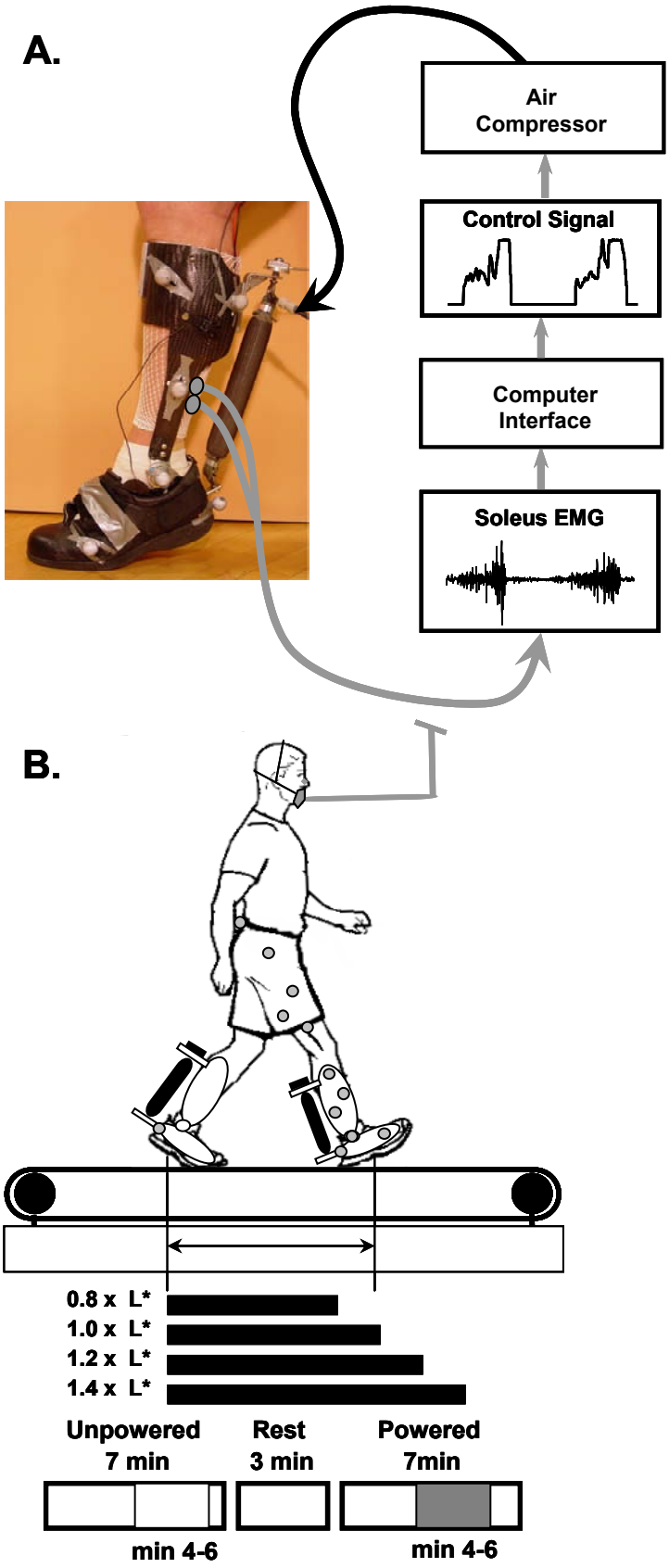
A.
Air Compressor
Control Signal
Computer Interface
Soleus EMG
B.
0.8 x L*
1.0 x L*
1.2 x L*
1.4 x L*
Unpowered 7 min
Rest 3 min
Powered 7min
min 4-6
min 4-6

Figure 3.2 Joint kinematics. Thick curves are nine subject mean ankle (left column), knee (middle column) and hip (right column) joint angles over the stride from heel strike (0%) to heel strike (100%). Data is average of left and right legs. Each row is walking data for a single step length (0.8 x preferred step length (L*) at top to 1.4 L* at bottom). In each subplot, curves are for unpowered (black), and powered walking (gray) and thin lines are + 1 standard deviation. Stance is ~0%-60% of the stride, swing 60%-100%. Ankle joint extension (plantar flexion), knee joint extension and hip joint extension are all positive. For all joints zero degrees is upright standing posture.

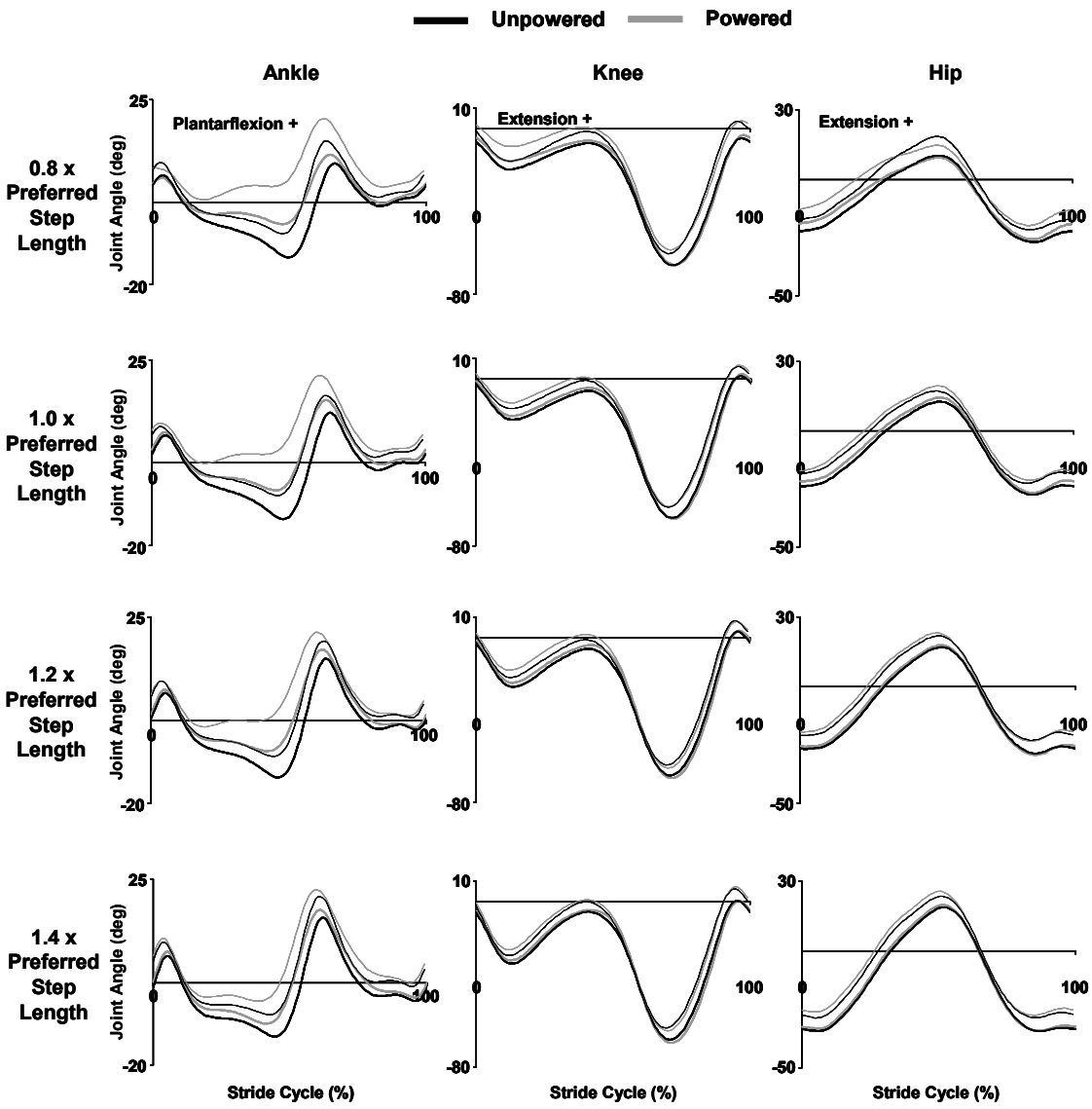
Unpowered
Powered
Ankle
Knee
Hip
Plantarflexion +
Extension +
Extension +
0.8 x Preferred Step Length
1.0 x Preferred Step Length
1.2 x Preferred Step Length
1.4 x Preferred Step Length
Joint Angle (deg)
25
-20
10
-80
30
-50
0
100
Stride Cycle (%)

Figure 3.3 Ankle exoskeleton mechanics. Thick curves are nine subject mean ankle joint angular velocity (left column), exoskeleton torque (middle column) and exoskeleton mechanical power (right column) over the stride from heel strike (0%) to heel strike (100%). Data is average of left and right legs. Each row is walking data at a single step length (0.8 x preferred step length (L*) at top to 1.4 L* at bottom). In each subplot, curves are for unpowered (black), and powered walking (gray) and thin lines are + 1 standard deviation. Stance is ~0%-60% of the stride, swing 60%-100%. Ankle joint angular velocity is positive for ankle extension (i.e. plantar flexion). Exoskeleton torque that acts to extend the ankle is positive. Torque is product of artificial muscle load and moment arm length and normalized by subject mass. Positive exoskeleton mechanical power indicates transfer of energy from exoskeletons to the user's ankle joint. Power is the product of exoskeleton torque and ankle joint angular velocity.

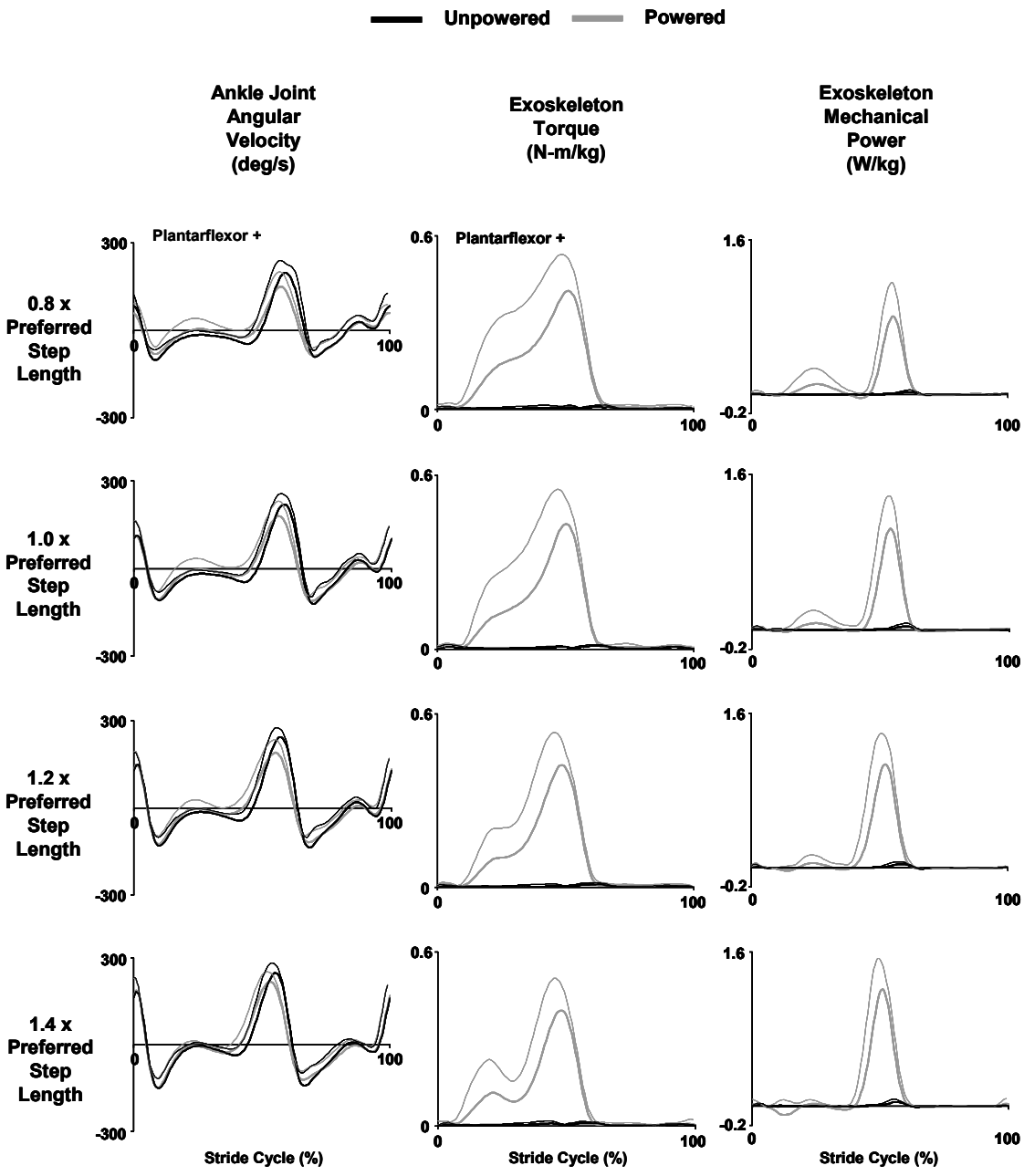
Unpowered
Powered
Ankle Joint Angular Velocity (deg/s)
Exoskeleton Torque (N-m/kg)
Exoskeleton Mechanical Power (W/kg)
Plantarflexor +
Plantarflexor +
0.8 x Preferred Step Length
1.0 x Preferred Step Length
1.2 x Preferred Step Length
1.4 x Preferred Step Length
300
0
-300
100
0.6
1.6
-0.2
Stride Cycle (%)
Stride Cycle (%)
Stride Cycle (%)

Figure 3.4 Net metabolic power. Bars indicate the nine subject mean net metabolic power (W/kg) during unpowered (white) and powered (gray) walking. Error bars are ± 1 standard error. Step lengths (0.8 x preferred step length (L*) to 1.4 L*) are tabulated left to right. Values listed above bars indicate percentage difference in powered versus unpowered walking for each condition. Asterisks indicate a statistically significant difference between powered and unpowered walking (ANOVA, $p < 0.05$).

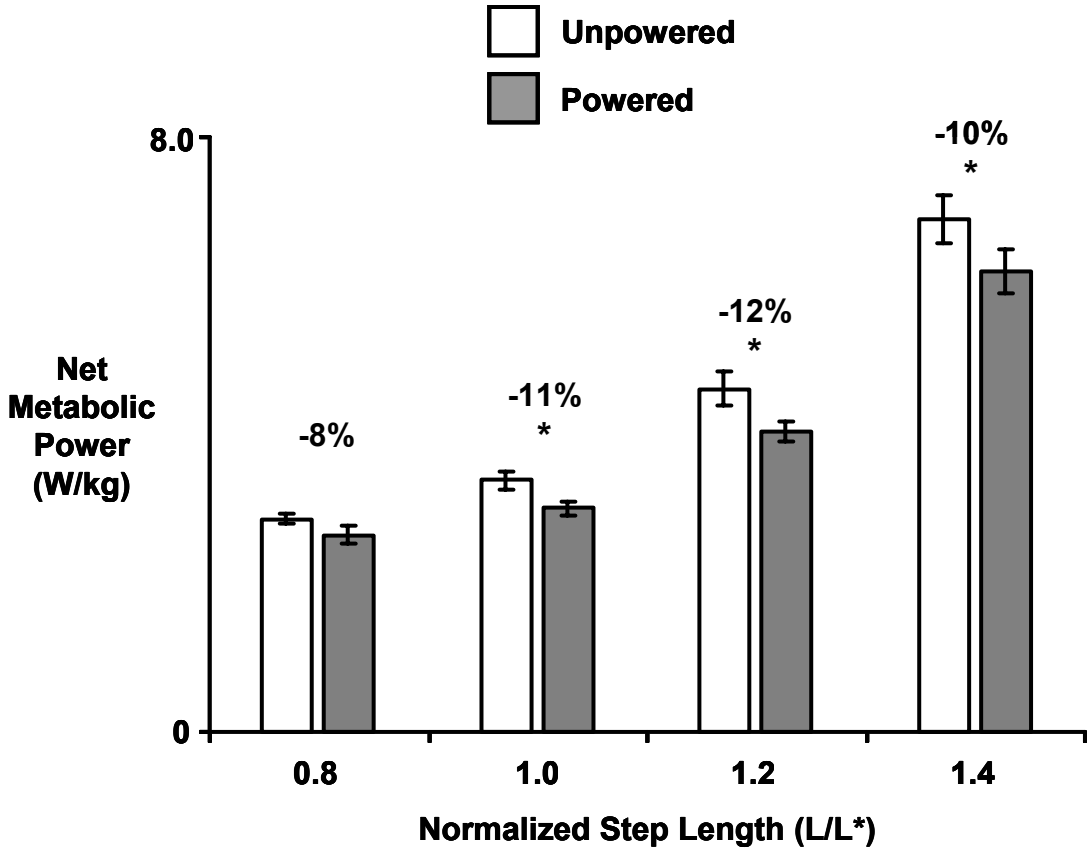
Unpowered
Powered
8.0
0
Net Metabolic Power (W/kg)
-8%
-11%
*
-12%
*
-10%
*
0.8
1.0
1.2
1.4
Normalized Step Length (L/L*)

Figure 3.5 Exoskeleton performance. Bars indicate nine subject mean **(A)** change in net metabolic power (powered - unpowered) due to powered assistance from bilateral ankle exoskeletons **(B)** exoskeleton average positive (dark gray), negative (white) and net (light gray) mechanical power over a stride for powered walking and **(C)** exoskeleton performance index. Performance index indicates the fraction of average exoskeleton positive mechanical power that results in a reduction in net metabolic power, assuming that artificial muscle work directly replaces biological muscle work. Exoskeleton performance index = 1.0 would suggest that all of the exoskeleton average mechanical power replaces underlying biological muscle work. For all panels, step lengths increase from left (0.8 x preferred step length (L*)) to right (1.4 L*). All metabolic power values are normalized by subject mass. Error bars are ± 1 standard error.

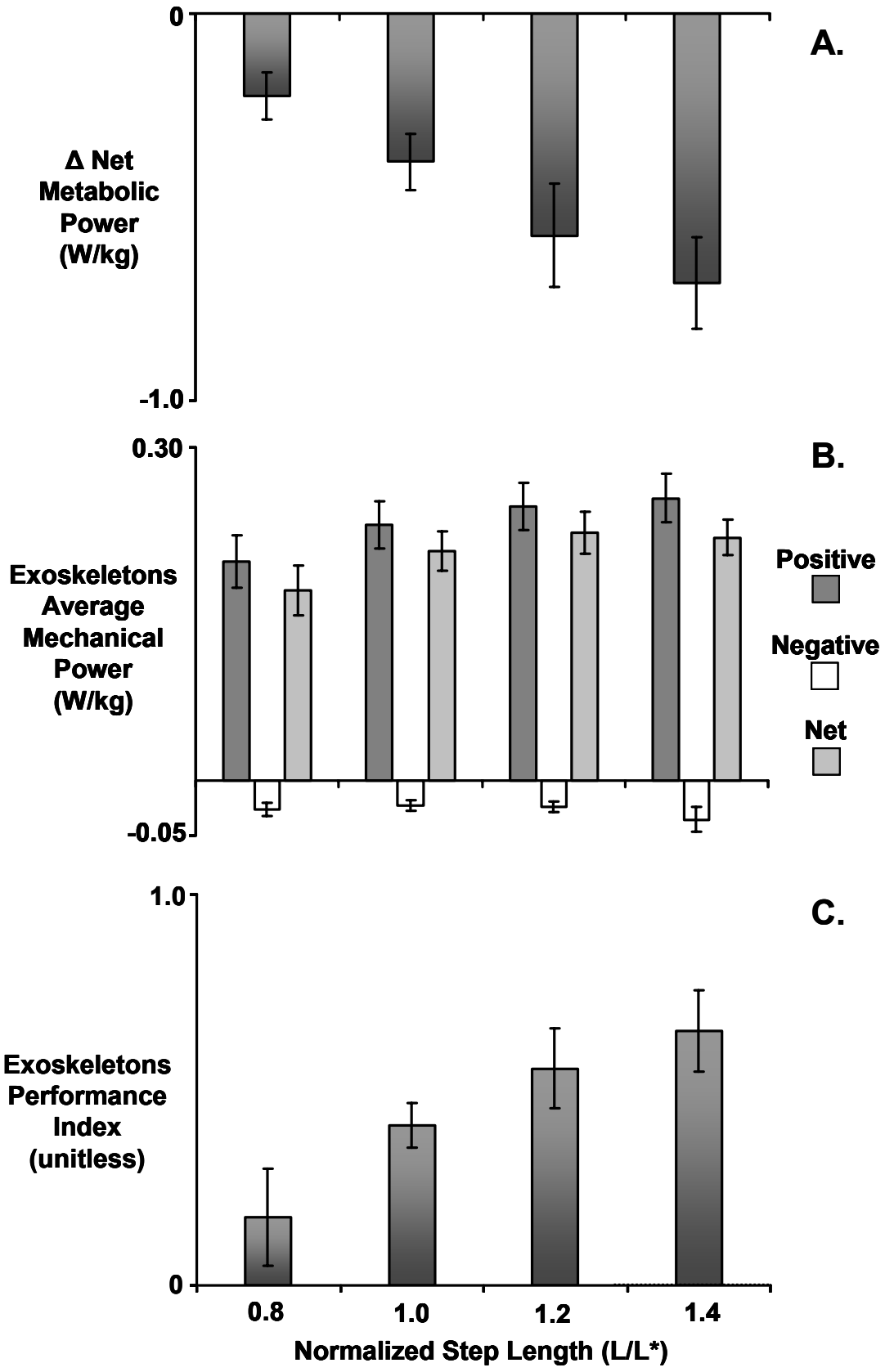
A.
0
-1.0
Δ Net Metabolic Power (W/kg)
B.
0.30
-0.05
Exoskeletons Average Mechanical Power (W/kg)
Positive
Negative
Net
C.
1.0
0
Exoskeletons Performance Index (unitless)
0.8
1.0
1.2
1.4
Normalized Step Length (L/L*)

Figure 3.6 Lower-limb joint mechanics. Each row shows nine subject mean (thick black) + 1 standard deviation (thin black) mechanical power delivered by each of the lower-limb joints over the stride from heel-strike (0%) to heel-strike (100%) for a given step length condition. Curves are for unpowered walking overground at speeds corresponding to step lengths increasing from 0.8 x preferred step length (L*) (top row) to 1.4 x L* (bottom row). Left and right legs are averaged for each subject. Stance is ~0%-60% of the stride, swing 60%-100%. In addition, the mean exoskeleton mechanical power from powered treadmill walking in each condition (gray) + 1 standard deviation (thin gray) is overlaid on subplots for the ankle joint mechanical power. Mechanical power is computed as the product of exoskeleton torque and ankle joint angular velocity and is normalized by subject mass. Positive exoskeleton power indicates energy transferred to the user and negative exoskeleton power indicates energy absorbed from the user.

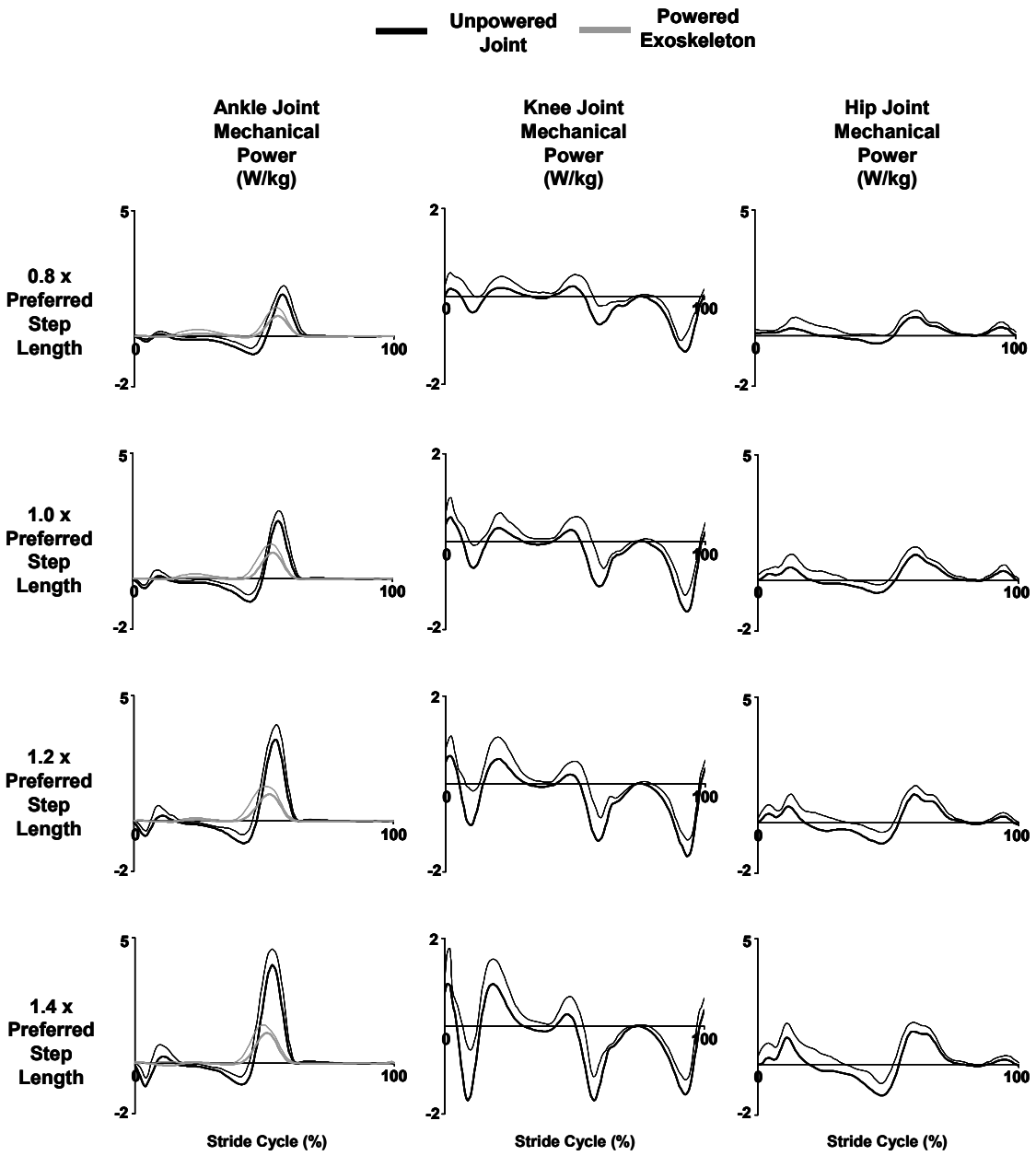
Unpowered Joint
Powered Exoskeleton
Ankle Joint Mechanical Power (W/kg)
Knee Joint Mechanical Power (W/kg)
Hip Joint Mechanical Power (W/kg)
0.8 x Preferred Step Length
1.0 x Preferred Step Length
1.2 x Preferred Step Length
1.4 x Preferred Step Length
5
2
-2
0
100
Stride Cycle (%)

Figure 3.7 Average mechanical power. Bars are the nine subject mean positive mechanical power delivered by the sum of the ankle, knee and hip joints (black) and ankle joint only (white) during unpowered overground walking. Gray bars are exoskeletons positive mechanical power during powered walking on the treadmill. Error bars are ± 1 standard error. All mechanical power values are normalized by subject mass. Step lengths increase from left (0.8 x preferred step length (L*) to right (1.4 L*). Brackets indicate the percent contribution of bars from right to left. For example, in 0.8 L* condition, the exoskeletons average positive mechanical power was 70% of the ankle joint average positive mechanical power, ankle joint positive mechanical power was 34% of the ankle + knee + hip positive mechanical power and the exoskeletons average positive mechanical power was 24% of the ankle + knee + hip positive average positive mechanical power over the stride.

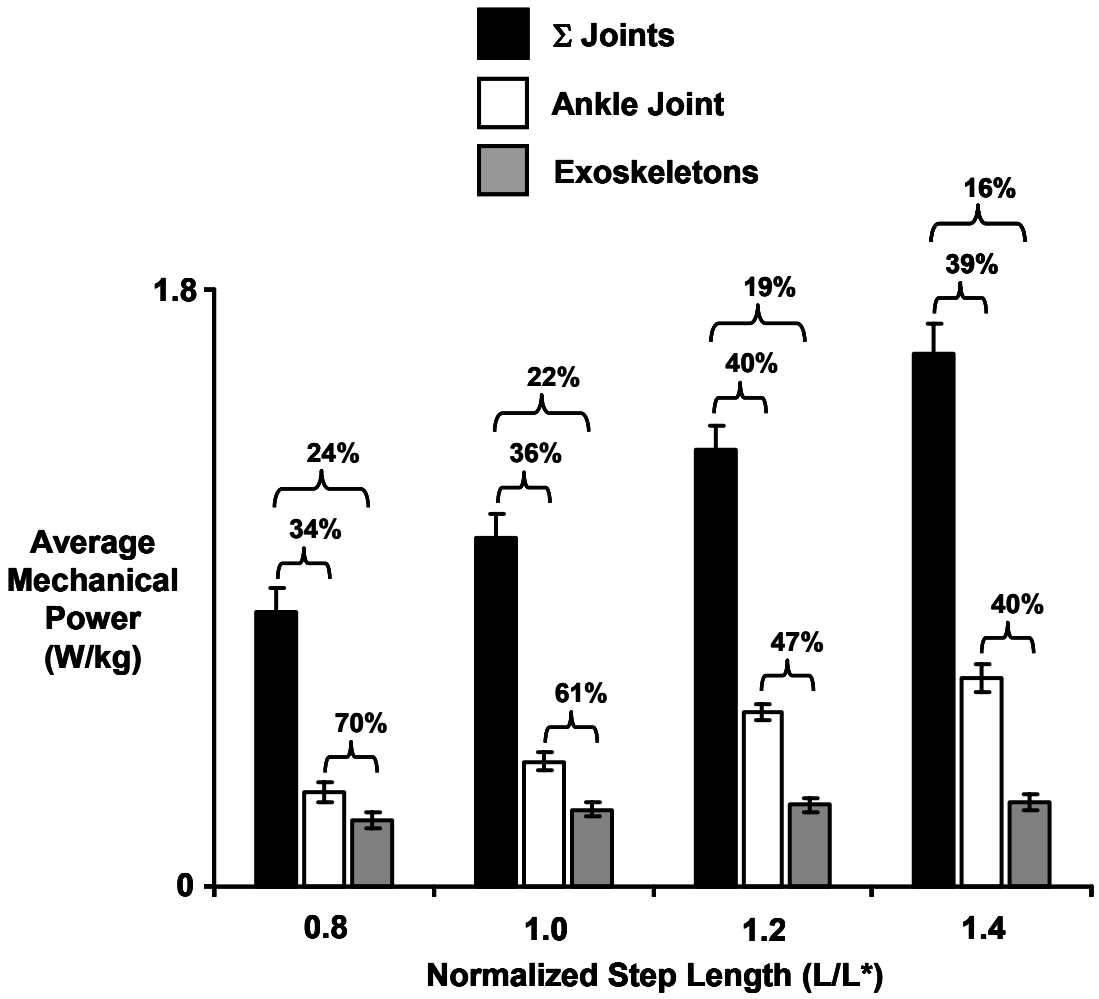
Σ Joints
Ankle Joint
Exoskeletons
1.8
0
Average Mechanical Power (W/kg)
24%
34%
70%
22%
36%
61%
19%
40%
47%
16%
39%
40%
0.8
1.0
1.2
1.4
Normalized Step Length (L/L*)

Figure 3.8 Soleus electromyography. Nine subject mean (thick curves) + 1 standard deviation (thin curves) of soleus normalized linear enveloped (high-pass cutoff frequency = 20 Hz and low-pass cutoff frequency = 10 Hz) muscle activity over the stride from heel-strike (0%) to heel-strike (100%). Thick curves are unpowered walking (black) and powered walking (gray) and normalized to the peak value during unpowered walking for the 1.4 L* condition. Step length increases from top (0.8 L*) to bottom (1.4 L*). Left and right legs are averaged for each subject. Stance phase is ~0%-60% and swing ~60%-100% of the stride.

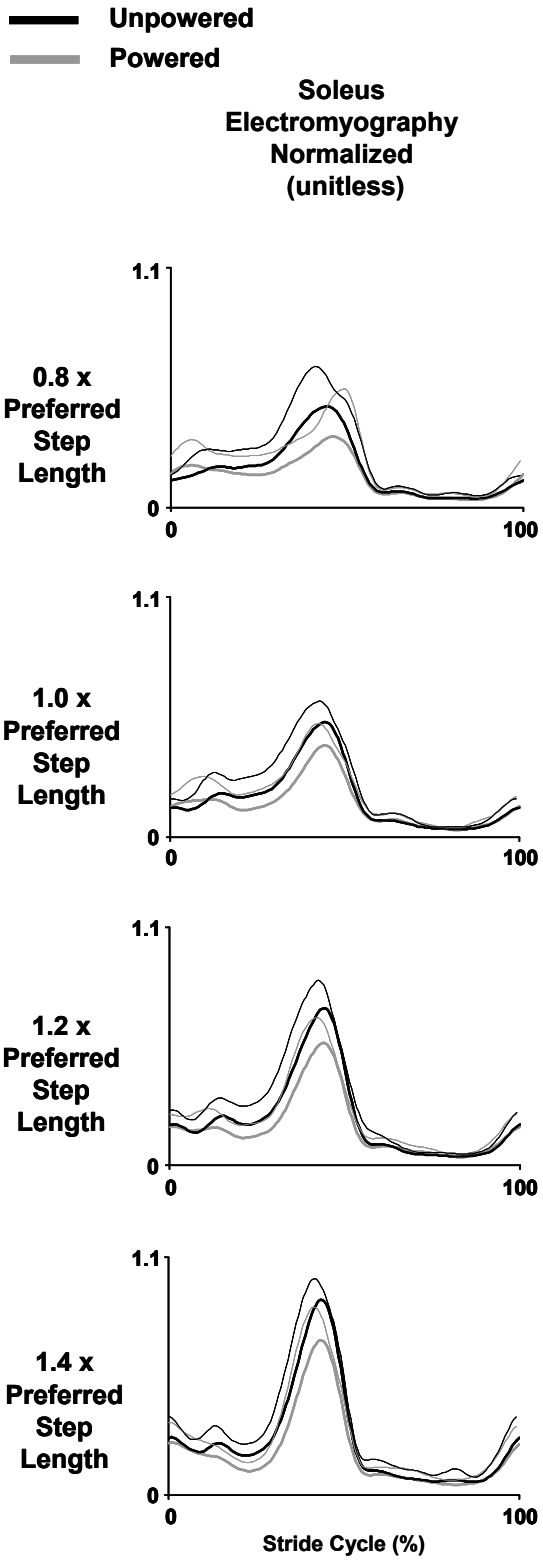
Unpowered
Powered
Soleus
Electromyography
Normalized
(unitless)
1.1
0.8 x Preferred Step Length
0
0
100
1.1
1.0 x Preferred Step Length
0
0
100
1.1
1.2 x Preferred Step Length
0
0
100
1.1
1.4 x Preferred Step Length
0
0
100
Stride Cycle (%)

Figure 3.9 Ankle muscle root mean square electromyography . Subplots are soleus (top), medial gastrocnemius, lateral gastrocnemius, and tibialis anterior (bottom). In each subplot, bars are nine subject mean stance phase root mean square average muscle activation. Error bars are ± 1 standard error. Step lengths increase from left (0.8 x preferred step length (L*)) to right (1.4 L*) with unpowered walking (minutes 4-6) in white and powered walking (minutes 4-6) in gray. Percentages listed above bars indicate percentage difference in powered compared to unpowered condition. Asterisks indicate a statistically significant difference between powered and unpowered walking (ANOVA, $p < 0.05$).

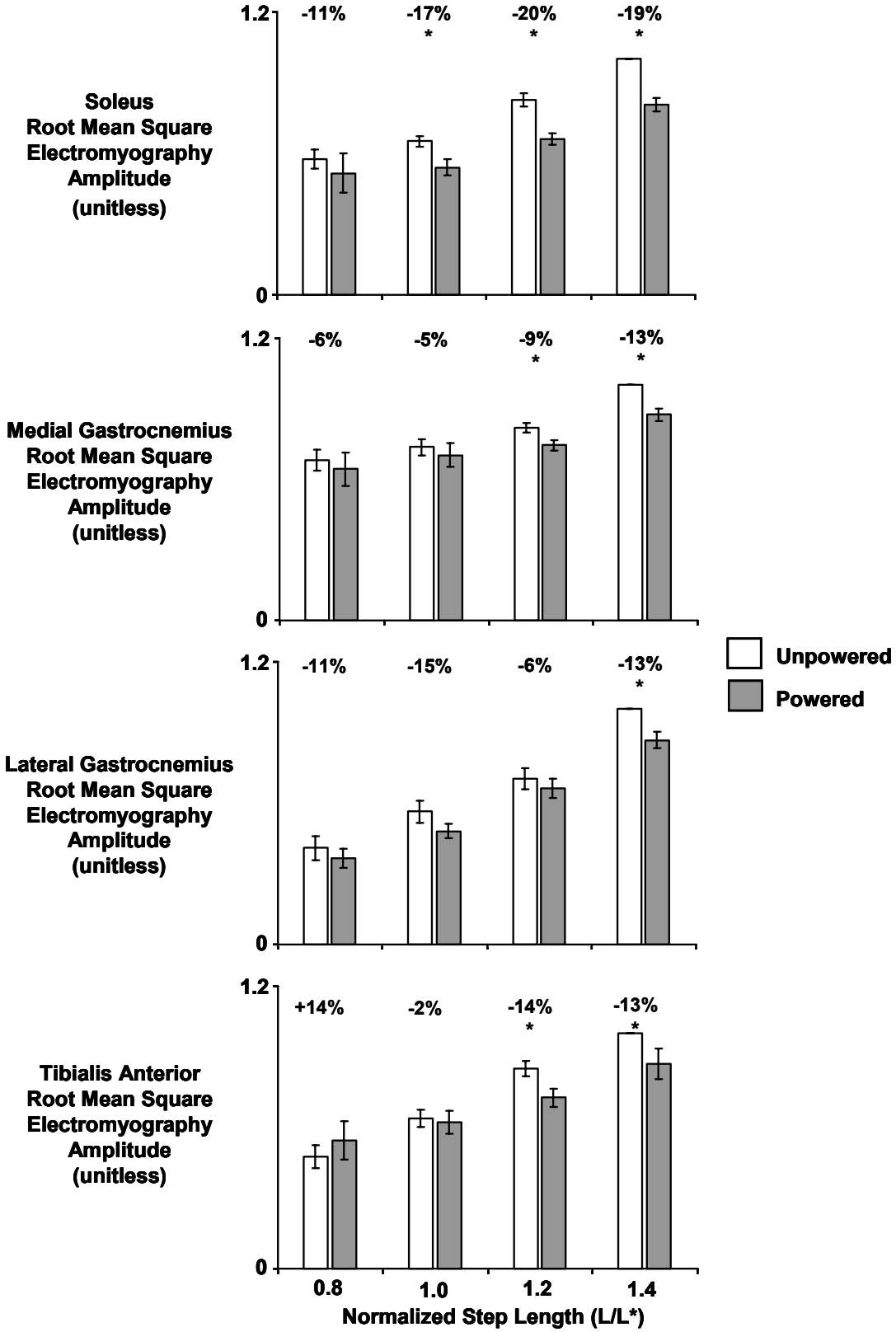
Soleus
Root Mean Square
Electromyography
Amplitude
(unitless)
1.2
0
-11%
-17%
*
-20%
*
-19%
*
Medial Gastrocnemius
Root Mean Square
Electromyography
Amplitude
(unitless)
1.2
0
-6%
-5%
-9%
*
-13%
*
Lateral Gastrocnemius
Root Mean Square
Electromyography
Amplitude
(unitless)
1.2
0
-11%
-15%
-6%
-13%
*
Tibialis Anterior
Root Mean Square
Electromyography
Amplitude
(unitless)
1.2
0
+14%
-2%
-14%
*
-13%
*
0.8
1.0
1.2
1.4
Normalized Step Length (L/L*)
Unpowered
Powered

Table 3.1 Gait kinematics . Table lists mean ± standard error for step length, step width, step period and double support period during unpowered and powered walking at 1.25 m/s at each step length. Step lengths are listed in columns (0.8 L* left to 1.4 L* right). Results of repeated measures ANOVA (n = 9 subjects) comparing pooled unpowered and powered walking data between step lengths are summarized in the rightmost column.

METRIC	0.8 x Preferred Step Length				1.0 x Preferred Step Length				1.2 x Preferred Step Length				1.4 x Preferred Step Length				Step Length p-value; THSD
	Unpowered		Powered		Unpowered		Powered		Unpowered		Powered		Unpowered		Powered		
	Mean	SE	Mean	SE	Mean	SE	Mean	SE	Mean	SE	Mean	SE	Mean	SE	Mean	SE	
Step Length (mm)	**572**	6	**565**	9	**723**	8	**715**	10	**854**	12	**841**	13	**980**	12	**967**	9	p<0.0001** 1.4>1.2,1.0,0.8 1.2>1.0,0.8 1.0>0.8
Step Width (mm)	**123**	8	**127**	12	**111**	10	**111**	12	**107**	6	**113**	10	**123**	11	**125**	9	p=0.002** 1.4>1.2,1.0 1.2<0.8 1.0<0.8
Step Period (ms)	**570**	5	**570**	6	**570**	5	**570**	6	**568**	6	**565**	6	**568**	5	**566**	4	p=0.13
Double Support Period (ms)	**146**	5	**144**	5	**132**	5	**133**	5	**116**	4	**117**	3	**106**	3	**106**	4	p<0.0001** 1.4<1.2,1.0,0.8 1.2<1.0,0.8 1.0<0.8

n=9, See Materials and Methods for calculations.

THSD=Tukey Honestly Significant Difference Test Results; **SE**=Standard Error

Condition: Unpowered, Powered; **Step Length:** 0.8xL*, 1.0xL*, 1.2xL*, 1.4xL*

L* is preferred step length at 1.25 m/s.

p<0.05 indicates statistical significance. * indicates statistical power >0.65; ** indicates statistical power >0.80.

References

Asmussen, E. and Bonde-Petersen, F. (1974). Apparent efficiency and storage of elastic energy in human muscles during exercise. *Acta Physiol Scand* **92**, 537-45.

Atzler, E. and Herbst, R. (1927). Arbeitsphysiologische Studien. III. *Pflugers Arch ges Physiol* **215**, 291-328.

Bastien, G. J., Willems, P. A., Schepens, B. and Heglund, N. C. (2005). Effect of load and speed on the energetic cost of human walking. *Eur J Appl Physiol* **94**, 76-83.

Bertram, J. E. (2005). Constrained optimization in human walking: cost minimization and gait plasticity. *J Exp Biol* **208**, 979-91.

Bertram, J. E. and Ruina, A. (2001). Multiple walking speed-frequency relations are predicted by constrained optimization. *J Theor Biol* **209**, 445-53.

Blaxter, K. (1989). Energy Metabolism in Animals and Man. Cambridge: Cambridge University Press.

Brockway, J. M. (1987). Derivation of formulae used to calculate energy expenditure in man. *Hum Nutr Clin Nutr* **41**, 463-71.

Brooks, G. A., Fahey, T. D. and White, T. G. (1996). Exercise physiology: human bioenergetics and its applications. Mountain View, Calif.: Mayfield.

Craik, R. L. and Oatis, C. A. (1995). Gait Analysis: Theory and Application. St. Louis, MO: Mosby.

Doke, J., Donelan, J. M. and Kuo, A. D. (2005). Mechanics and energetics of swinging the human leg. *Journal of Experimental Biology* **208**, 439-45.

Doke, J. and Kuo, A. D. (2007). Energetic cost of producing cyclic muscle force, rather than work, to swing the human leg. *J Exp Biol* **210**, 2390-8.

Donelan, J. M., Kram, R. and Kuo, A. D. (2001). Mechanical and metabolic determinants of the preferred step width in human walking. *Proceedings of the Royal Society of London Series B-Biological Sciences* **268**, 1985-92.

Donelan, J. M., Kram, R. and Kuo, A. D. (2002a). Mechanical work for step-to-step transitions is a major determinant of the metabolic cost of human walking. *Journal of Experimental Biology* **205**, 3717-27.

Donelan, J. M., Kram, R. and Kuo, A. D. (2002b). Simultaneous positive and negative external mechanical work in human walking. *J Biomech* **35**, 117-24.

Eng, J. J. and Winter, D. A. (1995). Kinetic analysis of the lower limbs during walking: what information can be gained from a three-dimensional model? *J Biomech* **28**, 753-758.

Fenn, W. O. (1924). The relation between the work performed and the energy liberated in muscular contraction. *Journal of Physiology, London* **58**, 373-395.

Ferris, D. P., Czerniecki, J. M. and Hannaford, B. (2005). An ankle-foot orthosis powered by artificial pneumatic muscles. *J Appl Biomech* **21**, 189-197.

Ferris, D. P., Gordon, K. E., Sawicki, G. S. and Peethambaran, A. (2006). An improved powered ankle-foot orthosis using proportional myoelectric control. *Gait and Posture* **23**, 425-8.

Ferris, D. P., Sawicki, G. S. and Daley, M. A. (2007). A physiologist's perspective on robotic exoskeleton's for human locomotion. *International Journal of Humanoid Robotics* **in press**.

Fukunaga, T., Kubo, K., Kawakami, Y., Fukashiro, S., Kanehisa, H. and Maganaris, C. N. (2001). In vivo behaviour of human muscle tendon during walking. *Proceedings of the Royal Society of London: Biological Sciences* **268**, 229-33.

Gitter, A., Czerniecki, J. M. and DeGroot, D. M. (1991). Biomechanical analysis of the influence of prosthetic feet on below-knee amputee walking. *American Journal of Physical Medicine and Rehabilitation* **70**, 142-8.

Gordon, K. E. and Ferris, D. P. (2007). Learning to walk with a robotic ankle exoskeleton. *J Biomech* **in press**.

Gordon, K. E., Sawicki, G. S. and Ferris, D. P. (2006). Mechanical performance of artificial pneumatic muscles to power an ankle-foot orthosis. *J Biomech* **39**, 1832-41.

Grey, M. J., Nielsen, J. B., Mazzaro, N. and Sinkjaer, T. (2007). Positive force feedback in human walking. *J Physiol* **581**, 99-105.

Griffin, T. M., Roberts, T. J. and Kram, R. (2003). Metabolic cost of generating muscular force in human walking: insights from load-carrying and speed experiments. *Journal of Applied Physiology* **95**, 172-83.

Guizzo, E. and Goldstein, H. (2005). The rise of the body bots. *IEEE Spectrum* **42**, 50-56.

Hansen, A. H., Childress, D. S., Miff, S. C., Gard, S. A. and Mesplay, K. P. (2004). The human ankle during walking: implications for design of biomimetic ankle prostheses. *J Biomech* **37**, 1467-74.

Hill, A. V. (1938). The heat of shortening and the dynamic constants of muscle. *Proceedings of the Royal Society of London: Biological Sciences* **B126**, 136-195.

Hill, A. V. (1939). The mechanical efficiency of frog's muscle. *Proceedings of the Royal Society of London: Biological Sciences* **127**, 434-451.

Hof, A. L., Geelen, B. A. and Van den Berg, J. (1983). Calf muscle moment, work and efficiency in level walking; role of series elasticity. *J Biomech* **16**, 523-37.

Hof, A. L., Van Zandwijk, J. P. and Bobbert, M. F. (2002). Mechanics of human triceps surae muscle in walking, running and jumping. *Acta Physiol Scand* **174**, 17-30.

Ishikawa, M., Komi, P. V., Grey, M. J., Lepola, V. and Bruggemann, G. P. (2005). Muscle-tendon interaction and elastic energy usage in human walking. *J Appl Physiol* **99**, 603-8.

Ishikawa, M., Pakaslahti, J. and Komi, P. V. (2006). Medial gastrocnemius muscle behavior during human running and walking. *Gait Posture*.

Klute, G. K., Czerniecki, J. M. and Hannaford, B. (2002). Artificial muscles: Actuators for biorobotic systems. *International Journal of Robotics Research* **21**, 295-309.

Kuo, A. D. (2001). A simple model of bipedal walking predicts the preferred speed-step length relationship. *Journal of Biomechanical Engineering* **123**, 264-9.

Kuo, A. D. (2002). Energetics of actively powered locomotion using the simplest walking model. *Journal of Biomechanical Engineering* **124**, 113-20.

Kuo, A. D., Donelan, J. M. and Ruina, A. (2005). Energetic consequences of walking like an inverted pendulum: step-to-step transitions. *Exerc Sport Sci Rev* **33**, 88-97.

Lichtwark, G. A., Bougoulias, K. and Wilson, A. M. (2007). Muscle fascicle and series elastic element length changes along the length of the human gastrocnemius during walking and running. *J Biomech* **40**, 157-64.

Lichtwark, G. A. and Wilson, A. M. (2006). Interactions between the human gastrocnemius muscle and the Achilles tendon during incline, level and decline locomotion. *Journal of Experimental Biology* **209**, 4379-88.

Lichtwark, G. A. and Wilson, A. M. (2007). Is Achilles tendon compliance optimised for maximum muscle efficiency during locomotion? *J Biomech* **in press**.

Margaria, R. (1938). Sulla fisiologia e specialmente sul consumo energetico della marcia e della corsa a varie velocita ed inclinazioni del terreno. *Atti Accad. Naz. Lincei Memorie, serie VI* **7**, 299-368.

Meinders, M., Gitter, A. and Czerniecki, J. M. (1998). The role of ankle plantar flexor muscle work during walking. *Scandinavian Journal of Rehabilitation Medicine* **30**, 39-46.

Neptune, R. R., Kautz, S. A. and Zajac, F. E. (2001). Contributions of the individual ankle plantar flexors to support, forward progression and swing initiation during walking. *J Biomech* **34**, 1387-98.

Neptune, R. R., Zajac, F. E. and Kautz, S. A. (2004). Muscle mechanical work requirements during normal walking: the energetic cost of raising the body's center-of-mass is significant. *J Biomech* **37**, 817-25.

Poole, D. C., Gaesser, G. A., Hogan, M. C., Knight, D. R. and Wagner, P. D. (1992). Pulmonary and leg VO2 during submaximal exercise: implications for muscular efficiency. *Journal of Applied Physiology* **72**, 805-10.

Prilutsky, B. I., Petrova, L. N. and Raitsin, L. M. (1996). Comparison of mechanical energy expenditure of joint moments and muscle forces during human locomotion. *J Biomech* **29**, 405-15.

Ralston, H. J. (1958). Energy-speed relation and optimal speed during level walking. *Int Z Angew Physiol* **17**, 277-83.

Ruina, A., Bertram, J. E. and Srinivasan, M. (2005). A collisional model of the energetic cost of support work qualitatively explains leg sequencing in walking and galloping, pseudo-elastic leg behavior in running and the walk-to-run transition. *J Theor Biol* **237**, 170-92.

Sasaki, K. and Neptune, R. R. (2006). Muscle mechanical work and elastic energy utilization during walking and running near the preferred gait transition speed. *Gait Posture* **23**, 383-90.

Sawicki, G. S. and Ferris, D. P. (2007). Mechanics and energetics of level walking with powered ankle exoskeletons. *J Exp Biol* **submitted**.

Sawicki, G. S., Gordon, K. E. and Ferris, D. P. (2005). Powered lower limb orthoses: applications in motor adaptation and rehabilitation. In *IEEE International Conference on Rehabilitation Robotics*. Chicago, IL: IEEE.

Wells, R. P. (1988). Mechanical energy costs of human movement: an approach to evaluating the transfer possibilities of two-joint muscles. *J Biomech* **21**, 955-64.

Winter, D. A. (1984). Kinematic and kinetic patterns in human gait: variability and compensating effects. *Human Movement Science* **3**, 51-76.

Winter, D. A. (1990). Biomechanics and Motor Control of Human Movement. New York: John Wiley & Sons.

Winter, D. A. (1991). The biomechanics and motor control of human gait: normal, elderly and pathological. Waterloo, Ontario: Waterloo Biomechanics.

Zarrugh, M. Y., Todd, F. N. and Ralston, H. J. (1974). Optimization of energy expenditure during level walking. *Eur J Appl Physiol Occup Physiol* **33**, 293-306.

Zatsiorsky, V. and Seluyanov, V. (1983). The mass and inertial characteristics of the main segments of the human body. In *Biomechanics VIII-B*, (ed. H. a. K. Matsui, K.), pp. 1152-1159. Champaign, IL: Human Kinetics.

Chapter IV

Mechanics and energetics of incline walking with robotic ankle exoskeletons

Summary

We examined healthy human subjects wearing robotic ankle exoskeletons to study the metabolic cost of ankle joint work during uphill walking. The exoskeletons were powered by artificial pneumatic muscles and controlled by the users' own soleus electromyography. We hypothesized that as the demand for net positive external mechanical work increased with surface gradient, the positive work delivered by ankle exoskeletons would produce greater reductions in users' metabolic cost. Nine human subjects walked at 1.25 m/s on gradients of 0%, 5%, 10% and 15%. We compared O_2 and CO_2 flow rates, exoskeleton mechanics, joint kinematics, and surface electromyography between unpowered and powered exoskeleton conditions. On steeper inclines, ankle exoskeletons delivered more average positive mechanical power (ANOVA, $p<0.0001$; +0.37 ± 0.03 W/kg at 15% grade and +0.23 ± 0.02 W/kg at 0% grade) and reduced subjects' net metabolic power by more (ANOVA, $p<0.0001$; -0.98 ± 0.12 W/kg at 15% grade and -0.45 ± 0.07 W/kg at 0% grade). Soleus muscle activity was reduced by ~16%-25% when wearing powered exoskeletons on all surface

gradients ($p<0.0008$). Subjects walked with increased ankle, knee, and hip extension during powered versus unpowered walking, maintaining a more upright posture as surface gradient increased. The 'apparent efficiency' of ankle joint mechanical work decreased from ~0.53 on level ground to ~0.38 on 15% grade. This suggests a decreased contribution of Achilles tendon recoil and increased contribution of ankle extensor muscle active shortening to ankle joint positive work during walking on steep uphill inclines. Although exoskeletons replaced ~61% more biological ankle work up a 15% grade compared to level walking, relative reductions in net metabolic power were similar across surface gradients (~10%-13%). These results suggest a shift in the relative distribution of mechanical power output to more proximal (knee and hip) joints during inclined walking.

Keywords: Locomotion, walking, incline, metabolic cost, exoskeletons, ankle, human, efficiency

Introduction

Human steady-speed walking on level ground requires zero net mechanical energy per stride but exacts a substantial metabolic cost (Atzler and Herbst, 1927; Cotes and Meade, 1960; Ralston, 1958). Mechanical energy fluctuates within each stride and both positive and negative work is performed on the center of mass in the transition from the pendular arc of one step to the next. To meet the mechanical demands of step-to-step transitions active muscles consume metabolic energy to produce force and perform mechanical work. Up to

~70% of the total metabolic cost of level walking can be attributed to step-to-step transitions (Donelan et al., 2002a; Donelan et al., 2002b; Gottschall and Kram, 2003; Kuo et al., 2005) while swinging the legs likely accounts for the remaining ~30% (Doke et al., 2005; Doke and Kuo, 2007; Gottschall and Kram, 2005).

The demand for both mechanical and metabolic energy is higher for walking uphill than for walking on the level. Metabolic energy consumption is markedly elevated for walking on an inclined surface (Bobbert, 1960; Davies and Barnes, 1972; Dean, 1965; Margaria, 1938; Minetti et al., 1993; Minetti et al., 2002). For example, when humans walk on a +40% surface gradient (~+22° inclination angle) the metabolic cost of transport is ~6-fold higher when compared to level walking (0% surface gradient) (Margaria, 1938). The increased metabolic demand during incline walking has a simple mechanical explanation. Work must be done against gravity to raise the body center of mass during each uphill walking step. Thus, in addition to the mechanical work needed to redirect the center of mass velocity and swing the legs (e.g. as is required on level ground), on an incline, extra positive work must be performed to increase the gravitational potential energy of the body (Margaria, 1938).

Center of mass mechanical analyses combined with measurements of oxygen consumption have given some insight into underlying muscle function during uphill walking on various gradients. For steady-speed walking on the level (0% grade) an equal amount of positive and negative external work is performed on the center of mass (i.e. net work is zero). As surface gradient increases the relative amount of positive versus negative external mechanical work performed

on the center of mass increases from 50% at 0% grade to >95% at 15% grade. Thus, for walking uphill at very steep inclines (>15%) virtually zero negative external work is performed on the center of mass (Minetti et al., 1993) and incline walking is a dominated by a demand for positive external mechanical work. Margaria showed that the efficiency of the positive mechanical work done for vertical displacement of the center of mass asymptotically approaches 0.25 when humans walk on extreme uphill slopes (>20% grade). Similarly, isolated muscle performs positive mechanical work with an efficiency of 0.25-0.30 (Fenn, 1924; Heglund and Cavagna, 1987; Hill, 1938; Hill, 1939; Woledge, 1985). The close agreement between the efficiencies of positive mechanical work for isolated muscle and the whole-body for walking at grades greater than 20% suggests that actively shortening muscle rather than recoiling elastic tendon supplies the majority (if not all) of the positive work to raise the center of mass on steep uphill inclines (Davies and Barnes, 1972; Margaria, 1968).

Whole-body efficiency calculations give a relatively accurate indication of underlying muscle-tendon function for tasks that are dominated by positive or negative external mechanical work (e.g. extreme uphill or downhill walking, cycle ergometry, sledge ergometry) (Abbott et al., 1952; Aura and Komi, 1986; Bigland-Ritchie and Woods, 1976; Margaria, 1968). Walking on inclines between 0% and 15% grade, however, involves a mixture of positive and negative external mechanical work that is performed partly by active muscle and partly by passive tendon stretch and recoil. Minetti et al. estimated that the efficiency of external positive mechanical work (as computed from motion analysis) ranges

from 0.18 for walking at 1.08 m/s to 0.15 for walking at 1.86 m/s and is independent of surface gradient (Minetti et al., 1993). Other studies using estimates of muscle-tendon positive mechanical work from force platform data of the individual limbs report mechanical efficiencies of 0.10 to 0.27 for level walking (Donelan et al., 2002a; Griffin et al., 2003). These values suggest that elastic energy recoil by tendons contributes little to the overall positive mechanical work performed on the center of mass. On the other hand, studies that estimate muscle-tendon work via motion capture to compute summed contributions from external and internal work during walking report efficiencies from 0.35 to 0.55 for level walking (Burdett et al., 1983; Cavagna and Kaneko, 1977; Massaad et al., 2007; Willems et al., 1995). These values suggest that tendon recoil does contribute to the overall positive mechanical work during walking. Thus, the relative contribution of active muscle shortening versus tendon recoil to the positive mechanical work required for both level and incline walking remains unclear. In addition, center of mass level efficiency calculations cannot directly address the relative roles of the lower-limb joints in generating external mechanical work during walking.

Recently, direct *in vivo* measurements animal models have given insight into how muscle-tendon systems across the lower-limb joints meet the increased demand for positive mechanical work during uphill locomotion. During level running in turkeys (Roberts et al., 1997) and level hopping in tammar wallabies (Biewener et al., 2004b) muscles at distal joints remain nearly isometric and produce force (but little work) to support energy saving tendon stretch and recoil.

As turkeys move up an inclined surface, the mechanical behavior of the lateral gastrocnemius shifts from a force producing strut (active isometric) to a work producing motor (active shortening) in order to provide a portion of the mechanical work needed to raise the animal's center of mass (Roberts et al., 1997). More detailed studies in both turkeys (Gabaldon et al., 2004) and guinea fowl (Daley and Biewener, 2003) also demonstrate that distal leg muscles (lateral gastrocnemius, digital flexor and peroneous longus) increase net active shortening and positive mechanical work output during uphill locomotion. On the other hand, when wallabies hop uphill, the lateral gastrocnemius and plantaris muscles retain the benefits of tendon storage and return, producing nearly isometric contractions while performing little mechanical work (Biewener et al., 2004b). In that study, the authors suggested that animals with long compliant tendons specialized for elastic energy cycling at distal joints use their muscles at more proximal joints to meet most of the mechanical work demand on an incline. In line with this suggestion, McGowan et al. recently showed that when wallabies hop uphill, the more proximal biceps femoris (a hip extensor) and vastus lateralis (a knee extensor) showed significant increases in active shortening (McGowan et al., 2007). Blood flow measurements in guinea fowl also indicate that proximal stance phase extensor muscles with short tendons increase their mass-specific energy use significantly more than distal muscles with long compliant tendons (Rubenson et al., 2006).

In humans, less is known about how the joints of the lower limb meet the increased mechanical demands on an uphill gradient. Roberts et al. computed

joint work from inverse dynamics power curves during running on surfaces of increasing uphill gradient (Roberts and Belliveau, 2005). The ankle and knee joints functioned similarly on all inclines, and the hip joint delivered virtually all of the additional positive work required to move uphill (Roberts and Belliveau, 2005). Joint moments (Lay et al., 2006) and joint powers (Lay et al., 2007; McIntosh et al., 2006) computed from inverse dynamics during uphill walking for the ankle knee and hip have been recently documented, but these studies did not quantify joint work. Peak ankle, knee and hip joint extensor moments were 18%, 45%, and 50% higher for walking at 15% grade when compared to walking at 0% grade (Lay et al., 2006). Accompanying power curves suggest that the positive mechanical work produced by the ankle, knee and hip joint all increase with increasing surface gradient, but that the majority of the increase occurs at the hip joint (Lay et al., 2007; McIntosh et al., 2006). Trends in electromyography data also highlight the increasing importance of more proximal joints during incline walking. Muscle activity at all three lower-limb joints increases for walking up steeper slopes, but the largest increases are observed in the duration of thigh, not shank, muscle activity (Lay et al., 2007; Leroux et al., 1999).

An important step in relating mechanics and energetics during locomotion is deciphering the relative contributions of muscle and tendon to joint work. Recent evidence from non-invasive, *in vivo* ultrasound measurements indicates that during level, steady-speed walking the majority of ankle joint positive mechanical work during push-off is delivered by recoiling Achilles tendon (Fukunaga et al., 2001; Ishikawa et al., 2005; Lichtwark and Wilson, 2006).

Lichtwark et al. also showed that the mechanical behavior of the medial gastrocnemius-Achilles tendon complex is not different for walking on inclined versus level surfaces (Lichtwark and Wilson, 2006). Although the nominal medial gastrocnemius fascicle length is longer for uphill versus level walking, Achilles tendon stretch is still developed by fascicles producing force isometrically. As the muscle is deactivated near push-off, it performs a small amount of positive work at relatively slow shortening velocity while the recoiling elastic tissues simultaneously performs the majority of the total muscle-tendon positive work (Lichtwark and Wilson, 2006). Ultrasound studies give important insight into the mechanical behavior of the ankle joint muscle-tendon system, but cannot quantify the metabolic energy required to perform those actions.

Powered exoskeletons can be used to alter the mechanical power output of the lower-limb joints and study the human physiological response. Our recent work with both unilateral (Gordon and Ferris, 2007) and bilateral (Sawicki and Ferris, 2007a; Sawicki and Ferris, 2007b) ankle exoskeletons has established that humans can rapidly adapt an efficient walking pattern with powered ankle assistance during level steady walking. Humans save ~1.6 J of metabolic energy for every 1 J of mechanical energy delivered by bilateral powered ankle exoskeletons assisting push-off during level walking at preferred step length. This yields an ‘apparent efficiency’ for ankle joint positive work of ~0.61, much higher than the. efficiency of isolated muscle (0.25) (Fenn, 1924; Hill, 1938), indicating a substantial contribution of Achilles tendon recoil to ankle mechanical power (Sawicki and Ferris, 2007a). Furthermore, we determined that the ‘apparent

efficiency' of ankle joint positive work decreases sharply with increasing walking step length but remains >0.25, even for very long steps (i.e. ~0.39 at 140% of preferred step length) (Sawicki and Ferris, 2007b). These results indicate that as the demand for external mechanical work increases, the human ankle extensor muscles perform a larger fraction of the total ankle joint muscle-tendon work during walking.

The overall objective of the present study was to examine how the human ankle muscle-tendon system meets the demands of increasing external mechanical workload due to increasing surface incline. We used bilateral pneumatically-powered ankle exoskeletons under soleus proportional myoelectric control to alter joint level mechanics and answer two questions (1) Can powered assistance at the ankle joint reduce the metabolic cost of uphill walking? (2) What is the 'apparent efficiency' of ankle joint mechanical work for uphill walking? We hypothesized that as surface incline increased, exoskeletons would deliver more average positive mechanical power and subjects' net metabolic power would decrease by more than on the level. If biological ankle extensors, rather than recoiling Achilles tendon, perform more ankle work on steeper inclines, then the 'apparent efficiency' of ankle joint work should decrease as surface gradient increases. We also expected reduced muscle activation amplitudes in muscles of the triceps surae group during powered walking on all gradients. We compared subjects' net metabolic power and electromyography amplitudes during walking with exoskeletons powered versus unpowered at steady-speed on inclines of increasing uphill surface gradient. In addition, for powered walking we used

measurements of artificial muscle forces and moment arm lengths to compute the average mechanical power delivered by the exoskeletons over a stride. With simultaneous measurements of the mechanics and energetics of powered walking we computed the 'apparent efficiency' of ankle joint positve work to gain insight into how underlying ankle extensor muscle-tendon function changes during uphill walking in humans.

Materials and methods

Subjects: Nine (5 males, 4 females) healthy subjects (body mass = 80.3 ± 14.7 kg; height = 179 ± 3 cm; leg length = 92 ± 2 cm) gave written, informed consent in accordance with the Declaration of Helsinki. The protocol was approved by the University of Michigan Institutional Review Board for Human Subject research. Subjects exhibited no gait abnormalities and had practiced for at least 90 minutes (three or more thirty minute practice sessions) previously with powered exoskeletons.

Exoskeletons: We built lightweight bilateral, ankle-foot exoskeletons (i.e. orthoses) for each subject (mass of 1.18 ± 0.11 kg each (mean ± s.d.)) (**Figure 4.1**). Details on the design and performance of the exoskeletons are documented elsewhere (Ferris et al., 2005; Ferris et al., 2006; Gordon et al., 2006; Sawicki et al., 2005). Briefly, the exoskeletons consisted of a carbon fiber shank attached to a polypropylene foot section with a metal hinge joint that allowed free rotation about the ankle flexion/extension axis. We used two stainless steel brackets to attach a single artificial pneumatic muscle (length = 45.6 ± 2.2 cm; moment arm = 10.6 ± 0.9 cm) along the posterior shank of each exoskeleton. We controlled

exoskeleton plantar flexor torque assistance with a physiologically inspired controller that incorporated the user's own soleus electromyography to mimic the timing and amplitude of biological muscle activation (i.e. proportional myoelectric control) (Gordon and Ferris, 2007).

Protocol. Experienced (> 90 minutes walking with powered exoskeletons) subjects walked at 1.25 m/s with bilateral powered ankle exoskeletons at four different surface inclines (**0%**, **5%, 10%** and **15%** surface gradient (i.e. **0°, 2.9°, 5.7°,** and **8.5°** inclination angle)) during unpowered and powered exoskeleton walking. Our previous work demonstrated that subjects plateau in net metabolic power after 90 minutes of powered walking practice (Sawicki and Ferris, 2007a). Subjects chose their preferred step length, step width and step frequency. Inclines were presented randomly. For each incline we followed the same walking timeframe (**Figure 4.1**).

First subjects walked for 7 minutes with exoskeletons unpowered (**Unpowered**). Then subjects rested for 3 minutes. Finally, subjects walked for 7 minutes with exoskeletons powered (**Powered**). During the unpowered bout for each surface incline, we tuned the gain and threshold of the proportional myoelectric controller so that the control signal saturated for at least five consecutive steps. We then doubled the gain in order to encourage reduction in soleus muscle recruitment (Gordon and Ferris, 2007). We re-tuned the controller gains for each incline so that the exoskeletons delivered similar peak torque across the powered trials independent of surface gradient. Thus, changes in average exoskeleton mechanical power output would be attributed to changes in

ankle joint kinematics (range of motion, ankle joint angular velocity) rather than artificial muscle force output.

Data Collection and Analysis. We recorded subjects' ankle, knee and hip joint kinematics, whole-body gait kinematics, ankle flexor and extensor surface electromyography, O_2 and CO_2 flow rates, and exoskeleton artificial muscles forces. For kinematic, electromyographic and artificial muscle force data, we collected ten second trials (i.e. ~7-9 walking strides) at the beginning of minutes 4, 5, and 6 during each of the eight (unpowered mode and powered mode for each of four surface gradients) 7 minute trials. Metabolic data were collected continuously during each 7 minute trial. In addition, we collected a single 7 minute quiet standing trial of metabolic data for each subject before walking trials commenced.

Kinematics. We placed twenty nine reflective markers on the subjects' pelvis and lower limbs and used an 8-camera video system (frame rate 120 Hz, Motion Analysis Corporation, Santa Rosa, CA, USA) to record the positions of reflective markers during treadmill walking. We smoothed raw marker data with custom software (Visual 3D, C-Motion, Rockville, MD) by applying a 4^{th}-order Butterworth low-pass filter (cutoff frequency 6 Hz). We used the smoothed marker data, and calculated ankle knee and hip joint angles (neutral standing posture was zero degrees for all joints) and angular velocities for both legs. We used footswitches (1200 Hz, B & L Engineering, Tustin, CA, USA) to mark heel-strike and toe-off events and calculated the step period (time from heel-strike one leg to heel-strike of the other leg) and double support period (time from heel-

strike of one leg to toe-off of the other). To calculate step width and step length we computed lateral and fore-aft distances between calcaneus markers at heel strike events. We averaged left and right joint kinematics from heel-strike (0%) to heel-strike (100%) to get the stride cycle average joint kinematics profiles.

Electromyography. We recorded bilateral lower-limb surface electromyography (EMG) (sampling rate 1200 Hz, Konigsberg Instruments, Inc., Pasadena, CA, USA) using bipolar electrodes (inter-electrode distance = 3.5 cm) of the soleus (Sol), tibialis anterior (TA), medial gastrocnemius (MG) and lateral gastrocnemius (LG) muscles. EMG amplifier bandwidth was 1000 Hz. We centered electrodes over the muscle belly and along its long axis always placing electrodes to minimize cross-talk. To minimized movement artifact we taped electrodes to the skin when necessary. We processed raw EMG by high-pass filtering (4^{th} order Butterworth, cutoff frequency 20 Hz), rectifying and low-pass filtering (4^{th} order Butterworth, cutoff frequency 10 Hz) each signal (i.e. linear envelope). Linear enveloped EMG was averaged for the right and left legs (from heel-strike to heel-strike for each leg) to get stride cycle averages. Finally, we normalized the curves using the peak value (average of left and right) for each muscle during the unpowered walking bout at the steepest incline (**Unpowered 15% grade**).

We computed stance phase root-mean square (RMS) average EMG amplitudes from the high-pass filtered, rectified EMG data of each leg to quantify changes in EMG activation levels. We averaged RMS EMG values from each leg

and normalized using the average RMS value from the **Unpowered 15% grade** trial.

Exoskeleton Mechanics. We recorded the forces produced by the artificial pneumatic muscles during powered walking with single-axis compression load transducers (1200Hz, Omega Engineering, Stamford, CT, USA). With the ankle joint in the neutral position during upright standing posture we measured artificial muscle moment arm (moment arm = 10.6 ± 0.9 cm). We converted smoothed artificial muscle force data (low-pass filtered, 4^{th} order Butterworth, cutoff frequency 6 Hz) to exoskeleton torque using the artificial moment arm length for each leg. We multiplied the exoskeleton torque and ankle joint angular velocity (from motion capture) to determine the mechanical power delivered by the exoskeletons. Exoskeleton power for the right and left legs (from heel-strike to heel-strike for each leg) was averaged then divided by subject mass to get the stride cycle average exoskeleton mechanical power.

To relate exoskeleton mechanical power and changes in subjects' net metabolic power we computed the average rate of exoskeleton positive and negative mechanical work. We partitioned the positive and negative portions of both the left and right exoskeleton mechanical power curves (from left heel strike to left heel strike). Then we integrated positive (or negative) mechanical power from each leg, summed over legs, and divided the total by the average stride period to get average positive (or negative) mechanical power delivered by the exoskeletons over a stride.

Metabolic Cost. We recorded O_2 and CO_2 flow rates using an open-circuit spirometry system (Physiodyne Instruments, Quogue, NY) (Blaxter, 1989; Brooks et al., 1996). We chose 7 minute trials to allow subjects to reach steady-state metabolic energy expenditure and monitored the respiratory exchange ratio (RER) to ensure that subjects relied on aerobic metabolism (RER < 1) (Brooks et al., 1996). If a continuous 7 minute trial could not be completed, we stopped and re-collected the data after the standard 3 minute period of rest. To calculate gross metabolic power we converted averaged O_2 and CO_2 rates for minutes 4-6 of each trial to units of metabolic power (Watts) using the standard equations documented by Brockway (Brockway, 1987). Then we subtracted the averaged data from minutes 4-6 of the quiet standing trial to obtain the net metabolic power (Griffin et al., 2003; Poole et al., 1992). Finally, we divided net metabolic power values by subject mass to obtain mass specific net metabolic power (W/kg). We used the net metabolic power from the unpowered trial at each level of surface incline to compute a percentage difference between unpowered and powered walking.

Exoskeleton Performance Index. We computed the exoskeleton performance index by combining measures of mechanical and metabolic power. First, we subtracted the net metabolic power during unpowered walking from the net metabolic power during powered walking for each level of surface incline to get the metabolic power savings due to the exoskeleton assistance. Muscles perform positive mechanical work with a 'muscular efficiency' of 0.25 (Fenn, 1924; Hill, 1938). We assumed that changes in net metabolic power would reflect

the cost of the underlying biological muscle positive work replaced by the powered exoskeletons. Thus, we multiplied changes in net metabolic power by 0.25 to yield the expected amount of positive mechanical power delivered by the exoskeletons for a given change in net metabolic power. Finally we divided the measured by the expected average positive mechanical power delivered by the exoskeletons to yield the exoskeleton performance index (Equation 1). A performance index of 1.0 would suggest that exoskeleton assistance completely replaced underlying biological muscle positive mechanical work.

$$\text{Exoskeletons Performance Index} = \frac{\Delta \text{ Net Metabolic Power} * 0.25}{\text{Average Exoskeletons Positive Mechanical Power}} \quad (1)$$

In addition, we computed an equivalent 'apparent efficiency' (Asmussen and Bonde-Petersen, 1974) by taking the reciprocal of four times the performance index (i.e. performance index = 1.0 is equivalent to 'apparent efficiency' = 0.25).

$$\text{Ankle Joint Apparent Efficiency} = \frac{1}{4 * \text{Exoskeletons Performance Index}} = \frac{\text{Average Exoskeletons Positive Mechanical Power}}{\Delta \text{ Net Metabolic Power}} \quad (2)$$

'Apparent efficiency' can be compared with the 'muscular efficiency' of isolated muscle positive mechanical work to gain insight into the relative roles of muscle shortening versus tendon recoil to overall joint positive work.

Statistical Analyses. We performed repeated measures analysis of variance tests (ANOVAs) using JMP IN statistical software (SAS Institute, Inc.

Cary, NC, USA). For significant effects ($p < 0.05$) we computed statistical power and used post-hoc Tukey Honestly Significant Difference (THSD) tests to determine specific differences between means.

In the first analysis we assessed the effect of surface gradient (**0%, 5%, 10% and 15% grade**) on net metabolic power, exoskeleton mechanics, stance phase RMS EMG and gait kinematics metrics (two-way ANOVA (subject, gradient)) for powered and unpowered walking data taken together (for exoskeleton mechanics metrics we analyzed powered walking data only).

In the other four ANOVA analyses (one for 0%, 5%, 10% and 15% grade) we assessed the effect of exoskeleton mode (**Unpowered, Powered**) on net metabolic power, stance phase RMS EMG and gait kinematics metrics (two-way ANOVA (subject, mode).

Results

Joint Kinematics. During unpowered walking, as surface gradient increased, subjects walked with increased ankle dorsiflexion, knee flexion and hip flexion early in stance phase. Push-off phase kinematics were similar across surface gradients for all joints during unpowered walking (**Figure 4.2**).

Subjects adopted a more upright posture during powered versus unpowered walking. The ankle, knee and hip joint angles were all more extended early in stance during powered walking. This effect was pronounced at steeper inclines (**Figure 4.2**). For walking on the steepest incline (15% grade), increases in lower-limb joint extension angles at heel strike were ~4 degrees for ankle, ~8

degrees for knee, ~6 degrees for hip during powered versus unpowered exoskeleton walking.

The peak ankle angle during push-off was larger (by ~3 to 5 degrees) and occurred earlier in the stride cycle during powered walking when compared to unpowered walking at all surface gradients. Knee joint peak flexion angle and hip joint peak extension angle during push-off were similar for unpowered and powered walking on all levels of incline (**Figure 4.2**).

Exoskeleton Mechanics. During unpowered walking, the exoskeletons produced small amounts of torque about the ankle and thus delivered virtually zero mechanical power to the user (**Figure 4.3**).

When the exoskeletons were powered, they produced ~0.40-0.48 N-m/kg peak torque (increasing slightly with increasing surface gradient). In addition, as surface incline increased exoskeletons delivered increasing amounts of plantar flexor torque earlier in the stance phase (**Figure 4.3**). For level walking (0% grade), the peak exoskeleton torque during powered walking was ~33% the normal peak ankle joint moment during level walking at 1.25 m/s.

The peak ankle joint angular velocity during push-off increased with increasing surface gradient (+193 deg/s during **Powered 0% grade** and +223 deg/s during **Powered 15% grade**). Increases in exoskeleton torque and ankle joint angular velocity resulted in larger peak exoskeleton mechanical power at steeper inclines (~1.1 W/kg at 0% grade and ~1.3 W/kg at 15% grade) (**Figure 4.3)**. The peak exoskeleton mechanical power was ~55% of peak ankle joint mechanical power during unpowered walking at 1.25 m/s on level ground.

Powered ankle exoskeletons delivered increasing amounts of positive mechanical power over the stride with increasing surface gradient (ANOVA, $p < 0.0001$, THSD, 15% > 10%, 5%, 0%; 10% > 5%, 0% and 5% > 0%) (**Figure 4.5 B**). Exoskeleton average positive mechanical power was 0.23 ± 0.02 W/kg (mean ± s.e.) during **Powered 0% grade** and increased by ~61% to 0.37 ± 0.03 W/kg during **Powered 15% grade**. Powered exoskeletons absorbed very little mechanical energy. Exoskeleton average negative mechanical power (~-0.02 W/kg) over the stride was not different for powered walking on surfaces of different incline (ANOVA, $p = 0.52$) (**Figure 4.5 B**).

Metabolic Cost. Subjects' net metabolic power increased with increasing surface incline (ANOVA, $p < 0.0001$, THSD, 15% > 10%, 5%, 0%; 10% > 5%, 0%; 5% > 0%). In addition, net metabolic power was significantly lower during powered versus unpowered walking at every level of surface incline (0% grade ANOVA, $p = 0.0002$, THSD, Powered < Unpowered; 5% grade ANOVA, $p < 0.0001$, THSD, Powered < Unpowered; 10% grade ANOVA, $p < 0.0001$, THSD, Powered < Unpowered; 15% grade ANOVA, $p < 0.0001$, THSD, Powered < Unpowered) (**Figure 4.4**). Net metabolic power was 3.36 ± 0.13 W/kg during **Unpowered 0% grade** and increased to 9.79 ± 0.23 W/kg during **Unpowered 15% grade**. In comparison, net metabolic power was only 2.91 ± 0.13 W/kg during **Powered 0% grade** and increased to 8.80 ± 0.26 W/kg during **Powered 15% grade**.

Subjects' absolute reduction in net metabolic power in powered versus unpowered walking increased steadily with increasing surface gradient (ANOVA,

$p < 0.0001$, THSD, 15% < 5%, 0%; 10% < 5%, 0%) (**Figure 4.5 A**). On level ground (0% grade), net metabolic power was 0.45 ± 0.07 W/kg less during powered versus unpowered walking. At 15% grade, the reduction in net metabolic power due to mechanical assistance was 0.98 ± 0.12 W/kg (~117% more than on the level). Although reductions in net metabolic power during powered walking were larger on steeper inclines, relative changes in net metabolic power were similar between surface gradients (10%-13% reduction from powered to unpowered mode) (**Figure 4.4**).

Exoskeleton Performance Index. Exoskeleton performance index increased with increasing surface gradient (ANOVA, $p = 0.02$, THSD, 15% > 0%; 10% > 0%) **(Figure 4.5 C**). Performance index increased ~40% from 0.47 ± 0.05 (ankle joint 'apparent efficiency' = 0.53) during **Powered 0% grade** to 0.66 ± 0.06 (ankle joint 'apparent efficiency' = 0.38) during **Powered 15% grade**.

Electromyography. Subjects increased activation of the triceps surae muscle group (i.e. soleus, medial and lateral gastrocnemius) as surface incline increased. Soleus stance phase root mean square (RMS) electromyography (EMG) was ~32% higher during unpowered and ~44% higher during powered walking at 15% grade when compared to walking on the level (i.e. 0% grade) (ANOVA, $p < 0.0001$, THSD, 15% > 10%, 5%, 0%; 10% > 0%; 5% > 0%). Medial and lateral gastrocnemius stance RMS EMG both increased by ~56% as surface gradient increased from 0% to 15% grade during unpowered walking. For powered walking, medial gastrocnemius stance RMS EMG increased by ~58% and lateral gastrocnemius stance RMS EMG increased ~77% as surface incline

increased from 0% to 15% grade (ANOVA, $p < 0.0001$, THSD, 15% > 10%, 5%, 0%; 10% > 5%, 0%; 5% > 0% for both medial and lateral gastrocnemius). (**Figure 4.7)**.

Subjects significantly altered soleus muscle activation amplitude but not timing during the stance phase of powered walking when compared to unpowered walking for all levels of surface incline (**Figure 4.6**). On the level (0% grade) soleus stance phase RMS EMG was ~25% lower during powered versus unpowered walking (0% grade ANOVA, $p = 0.0008$, THSD, Powered < Unpowered). At steeper surface inclines reductions in soleus stance RMS EMG in the powered versus unpowered mode were smaller (~16%-18%) but still significant (5% grade ANOVA, $p = 0.0007$, THSD, Powered < Unpowered; 10% grade ANOVA, $p < 0.0001$, THSD, Powered < Unpowered; 15% grade ANOVA, $p < 0.0001$, THSD, Powered < Unpowered) (**Figure 4.7**).

Similar to the soleus muscle, subjects walked with reduced lateral gastrocnemius RMS EMG amplitudes during powered versus unpowered walking (0% grade ANOVA, $p = 0.002$, THSD, Powered < Unpowered; 5% grade ANOVA, $p = 0.006$, THSD, Powered < Unpowered; 10% grade ANOVA, $p = 0.07$, 15% grade ANOVA, $p = 0.001$, THSD, Powered < Unpowered). For level walking, lateral gastrocnemius activation amplitude was ~24% lower in powered versus unpowered exoskeleton mode and ranged from 8% to 15% for walking at steeper inclines (**Figure 4.7**).

Reductions in medial gastrocnemius stance RMS EMG during powered versus unpowered walking were less significant than in soleus or lateral

gastrocnemius. Medial gastrocnemius stance phase RMS EMG was lower during powered versus unpowered walking during the 5% grade condition only (by ~11%) (5% grade ANOVA, $p = 0.01$, THSD, Powered < Unpowered; 0%, 10% and 15% grade ANOVAs, $p > 0.08$) (**Figure 4.7**).

Tibialis anterior muscle recruitment did not change with increasing surface gradient (ANOVA, $p = 0.52$) and was not significantly altered when exoskeletons were powered at any level of surface incline (ANOVA, $p > 0.05$ for all surface gradients) (**Figure 4.7**).

Gait Kinematics. Step length (ANOVA, $p = 0.02$, THSD, 15% < 5%) and step period (ANOVA, $p = 0.04$, THSD, 15% < 5%) were both shorter for walking at steeper inclines (unpowered and powered data pooled) (**Table 4.1**). Subjects took wider steps as surface gradient increased (ANOVA, $p = 0.004$, THSD, 15% > 0%). Double support period did not change with surface gradient (ANOVA, $p = 0.90$) (**Table 4.1**).

When comparing unpowered and powered walking, step length (ANOVA, $p > 0.30$), step period (ANOVA, $p > 0.75$), step width (ANOVA, $p > 0.20$), and double support period (ANOVA, $p > 0.39$), were not significantly different for any incline level (**Table 4.1**).

Discussion

Our results indicate that the 'apparent efficiency' of ankle joint positive mechanical work decreased from 0.53 to 0.38 as surface gradient increased from 0% to 15% grade. Lower 'apparent efficiency' suggests an increased contribution of actively shortening muscle fibers, rather than passively recoiling Achilles

tendon, to overall ankle joint work. On a 15%-uphill grade, powered ankle exoskeleton artificial muscles replaced 61% more biological ankle muscle-tendon work than on the level. In response, during powered walking on 15% grade, subjects decreased their absolute metabolic cost by more than twice as much as on the level. However, the net metabolic cost of walking was three-fold higher for uphill walking on a 15% versus 0%-level grade. Absolute reductions in net metabolic power due to powered assistance could not outpace the increasing net metabolic power of walking on steeper inclines. Thus, powered assistance at the ankle joint reduced the metabolic cost of walking by 10%-13%, independent of surface gradient.

Our 'apparent efficiency' estimates give insight into the relative contribution of muscle versus tendon to overall joint positive power output (Sawicki and Ferris, 2007a; Sawicki and Ferris, 2007b). In this study, for walking on surface inclines up to 15% grade, the 'apparent efficiency' of ankle joint positive mechanical work was always greater than the 'muscular efficiency' of positive mechanical work for isolated muscle (~0.25) (Fenn, 1924; Woledge, 1985). This suggests a significant contribution from Achilles tendon recoil to total ankle joint positive mechanical power output, even during steep uphill walking. The 'apparent efficiency' of ankle joint positive mechanical work decreased from 0.53 during level walking to 0.38 on a 15% uphill surface gradient (**Figure 4.5**). These values imply that active ankle extensor muscle shortening provides a larger fraction of total ankle joint positive mechanical work on 15% grade than on the level. Based on an 'apparent efficiency' of 0.53 during level walking-0%

grade, we estimate that active muscle shortening accounts for *at most* ~47% of the total positive mechanical power output at the ankle (i.e. 47% = 0.25/0.53 x 100 assuming ankle efficiency is determined by the metabolic cost of ankle muscles positive work *only*). This implies that the Achilles tendon delivers more than half (~53%) of the ankle joint positive mechanical work during level walking. Our estimates of the fraction of ankle joint work delivered by active muscle versus passive Achilles tendon for the other surface gradient conditions yield: for walking at 5% grade 54% muscles and 46% tendon; at 10% grade 68% muscles and 32% tendon; and at 15% grade 66% muscles and 34% tendon. Muscles contribute more of the ankle joint work on steeper inclines. But the Achilles tendon still contributes >30% of the positive ankle joint mechanical power, even for walking on relatively steep uphill inclines.

Recent ultrasound data supports our suggestion that tendon recoil is a major contributor to ankle joint positive mechanical power during human walking on level ground and on uphill inclines. Lichtwark et al. showed that during both level and uphill walking on a 10% surface gradient, the Achilles tendon is stretched significantly while in series muscle fascicles produce force nearly isometrically (Lichtwark and Wilson, 2006). Tendon elastic stretch is followed by a mechanical power burst near push-off that is shared by muscle fascicles (shortening at relatively slow velocity) and recoiling elastic Achilles tendon.

Our ‘apparent efficiency’ estimates depend on the validity of a key assumption: that the observed changes in metabolic cost are due to exoskeleton positive mechanical work directly replacing ankle joint muscle-tendon work.

Subjects could have used exoskeletons to *augment* total lower-limb joint work rather than to *replace* only ankle joint work. In that case we would expect increases in the total lower-limb joints average mechanical power during powered versus unpowered walking trials. During uphill walking, the external mechanical power (and net metabolic cost) increase in proportion to both speed and surface incline (Margaria, 1938). We held the treadmill speed and surface gradient constant between unpowered and powered walking trails to constrain the average external mechanical power to be similar during trials. Walking with longer (Donelan et al., 2002a), wider (Donelan et al., 2001) or more frequent steps (Bertram and Ruina, 2001) increases the mechanical and metabolic energy expenditure of walking. Although subjects took slightly shorter, wider, and higher frequency steps on steeper inclines, there were no significant differences in these gait parameters between powered and unpowered walking conditions on any surface incline (**Table 4.1**). Therefore changes in overall gait parameters did not confound our measured changes in net metabolic power due to powered exoskeleton assistance.

Our electromyography data provide additional evidence that subjects used exoskeleton mechanical assistance to replace ankle joint work. The stance phase RMS EMG amplitudes for all three major ankle extensor muscles were lower during powered versus unpowered walking (**Figures 4.6 and 4.7**). This indicates that exoskeleton artificial muscles directly reduced the load on the underlying biological muscle-tendon units. Reductions in soleus RMS EMG (16%-25%) were more pronounced than for the biarticular medial and lateral

gastrocnemius (5%-24%) (**Figure 4.7**). It could be that positive force feedback from Ib afferents plays a larger role in modifying soleus versus gastrocnemius muscle activity during uphill walking (Grey et al., 2007). In that case, reduced loading on the Achilles tendon due to exoskeleton torque assistance would reduce soleus activity by more than gastrocnemius activity.

Subjects' joint kinematics indicated that exoskeleton assistance altered only the ankle joint mechanics. Highly constraining the external mechanical power between unpowered and powered walking does not rule out subjects' redistributing joint power output across the lower-limb joints. For example, subjects could have offset ankle exoskeleton positive mechanical power, by performing simultaneous positive work at the knee or hip. This did not appear to be the case. The ankle, knee and hip joint angles were all slightly more extended during powered versus unpowered walking trials (**Figure 4.2**). As a result subjects walked with a more upright posture, and slightly increased the effective mechanical advantage of the muscles spanning each of the lower-limb joints (Biewener, 1989; Biewener et al., 2004a). Increased effective mechanical advantage reduces net muscle moments, especially at proximal joints (knee, hip). If compensatory negative work occurred at the knee or hip, we would expect considerable increases in the angular velocity at those joints over the stride. The hip and knee joint angles were slightly shifted (i.e. towards extension) but their slopes were similar over the entire stride, especially near push-off (**Figure 4.2**).

Muscle co-activation at the ankle to stabilize the joint during powered walking could exact a significant metabolic cost and confound our measured

differences in net metabolic power due to exoskeleton assistance. We measured muscle activity in the tibialis anterior (the major ankle flexor) to rule out this possibility. Our results indicate no significant differences in tibialis anterior RMS EMG amplitudes between powered and unpowered walking conditions on any surface incline (**Figure 4.7**). This indicates that co-activation was not a factor at the ankle joint. Our previous work indicates that during powered walking, muscle co-activation is not a factor at the knee or hip (Gordon and Ferris, 2007).

The metabolic cost of swinging the legs is significant during human walking, accounting for up to 30% of the total metabolic cost (Doke et al., 2005; Doke and Kuo, 2007; Gottschall and Kram, 2005) and increases with added mass on the lower limbs (Browning et al., 2007). It is possible that leg swing metabolic cost accounts for a larger percentage of the total metabolic cost of walking as surface incline increases. Exoskeleton mechanical assistance might then have a smaller effect on whole-body metabolism, keeping relative changes in net metabolic power due to mechanical assistance constant. We believe this is unlikely for two reasons. First, Minetti et al. showed that although the external positive work (W_{ext} +) done on the center of mass increases with increasing surface incline, the internal work done to move the limbs relative to the center of mass (W_{int} +) remains relatively constant with increasing surface incline (Minetti et al., 1993) This indicates that leg swing costs likely remain nearly constant. Second, a recent study by Doke et al. demonstrated that the cost of swinging the legs may not depend on performing mechanical work, but instead on producing force in short bursts (Doke and Kuo, 2007). That is, leg swing cost during walking

should depend mainly on step frequency. In this study, subjects increased step frequency by ~2.5% as surface gradient increased from 0% grade (level) to 15% grade. Although this change was statistically significant, it is too small to appreciably affect the relative cost of leg swing to the overall metabolic cost of walking across surface inclines.

Subjects saved more absolute net metabolic power due to mechanical assistance on steeper uphill gradients, but relative reductions in net metabolic power remained a nearly constant 10-13% independent of surface gradient. This is likely a result of decreased effectiveness of the exoskeletons as the grade increased. Increased exoskeleton average mechanical power (+60% from 0% to 15% grade) (**Figure 4.5 B**) contributed a smaller fraction of the total ankle + knee + hip average positive mechanical power on steeper inclines. A limitation of the current study is that we could not compute lower-limb joint inverse dynamics on inclined surfaces. As a result it was not possible to calculate the relative contribution of exoskeleton positive mechanical power to the overall mechanical power of the ankle joint (or summed joints). However, recent studies in humans (Lay et al., 2006; McIntosh et al., 2006; Roberts and Belliveau, 2005) and other animals (Biewener et al., 2004b; McGowan et al., 2007; Rubenson et al., 2006) suggest that as surface incline increases, there is a shift in the relative distribution of lower-limb positive power output from the distal (e.g. ankle) to the proximal (e.g. hip and knee) joints. If the hip and knee joints perform a larger fraction of the total joints (ankle + knee +hip) positive mechanical work then they should also account for the majority of the total metabolic cost of uphill walking.

Thus, ankle exoskeleton positive mechanical power influenced a smaller fraction of the total metabolic cost of walking on steeper inclines and relative changes in metabolic cost remained independent of surface gradient.

In our previous work, during level walking at 1.25 m/s, exoskeletons delivered 63% of the ankle joint positive mechanical work, and the ankle performed 35% of the total lower-limb positive mechanical work (Sawicki and Ferris, 2007a). In that case the 'apparent efficiency' of ankle joint positive mechanical work was 0.61 and subjects' net metabolic power was reduced by 10%. In this study, if we assume that exoskeletons deliver 63% of the ankle joint positive work (likely and overestimate) on a 15% uphill gradient, then the ankle joint would need to contribute ~24% of the summed joint positive work with 'apparent efficiency' 0.38 to get the observed 10% reduction in net metabolic cost. In other words, we estimate that the relative contribution of the knee/hip to summed lower-limb positive mechanical work increases from ~65% to about 76% as surface gradient increases from 0%-level to 15%-uphill.

Finally, it is interesting to note that our ankle joint 'apparent efficiency' values didn't change much from 10% (0.37) to 15% (0.38) uphill walking gradient. It is possible that the muscle-tendon architecture of human ankle joint limits its ability to modulate mechanical work output during tasks that require increased external work (e.g. uphill inclines). The idea that muscle-tendon morphology might constrain mechanical performance is not new, and has been suggested for other animals (e.g. wallabies) that have long tendons at distal joints that are likely specialized for elastic energy storage and return (Biewener et al., 2004b;

McGowan et al., 2007). It would be interesting to test whether ankle joint 'apparent efficiency' goes down further on inclines > 15% uphill gradient, or if a long elastic Achilles tendon does indeed pose a mechanical constraint.

Implications and Future Work. Powered exoskeletons are a novel tool for studying the relationship between the mechanics and energetics of locomotion at the level of the lower-limb joints. Our work demonstrates that ankle joint positive mechanical power is relatively cheap from a metabolic perspective. That is, for steady walking across different speeds (Sawicki and Ferris, 2007a; Sawicki and Ferris, 2007b) and inclines, the ankle joint delivers positive mechanical power with remarkably high 'apparent efficiency'. Future studies could use powered exoskeletons to study the mechanics and energetics of other joints (hip and knee) and other locomotor tasks (i.e. running, hopping or accelerating). In addition, combining this approach with non-invasive *in vivo* techniques (e.g. ultrasound measurements) could help validate our suggestions regarding changes in underlying muscle-tendon mechanical function during walking under different locomotor conditions.

Our findings have important implications for engineering devices designed to reduce the metabolic cost of locomotion. Although it seems counterintuitive, our results suggest that powering the joints that generate the most mechanical power during locomotion may not lead to the largest reductions in metabolic cost. A better approach is to target the joints that utilize the most metabolic energy to perform a given amount of mechanical work (i.e. the least efficient joints). Our findings suggest that powering proximal joints (e.g. hip) where muscles rather

than tendons contribute most of the positive mechanical joint work may lead to the largest reductions in metabolic cost (Ferris et al., 2007). This is especially true for walking uphill where the hip joint performs more of the total work than any other joint and at the lowest efficiency, making it by far the most expensive joint metabolically speaking.

Acknowledgements

We would like to thank Catherine Kinnaird, Jineane Shibuya and other members of the Human Neuromechanics Laboratory for their assistance on data collections and analyses. Jacob Godak and Anne Manier of the University of Michigan Orthotics and Prosthetics Center constructed the exoskeletons. The work was supported by NSF BES-0347479 to D.P. Ferris.

Figures and Tables

Figure 4.1 Experimental set-up. (A) Subjects walked on a motorized treadmill at 1.25 m/s for 7 minutes with exoskeletons unpowered, then rested for 3 minutes, then walked for 7 minutes with exoskeletons powered at surface inclines of 0%, 5% 10% and 15% grade presented in randomized order. Outlined boxes indicate periods where data was analyzed (minutes 4-6) in both unpowered and powered conditions. **(B)** During powered walking, bilateral ankle-foot orthoses (i.e. exoskeletons) were operated under proportional myoelectrical control. Users' soleus muscle activity generated a real-time control signal commanding timing and amplitude of artificial pneumatic muscles forces. We used reflective markers and motion capture to collect joint kinematics, open-circuit spirometery to collect O_2 and CO_2 flow rates, and compression load transducers to record artificial muscle forces.

A.

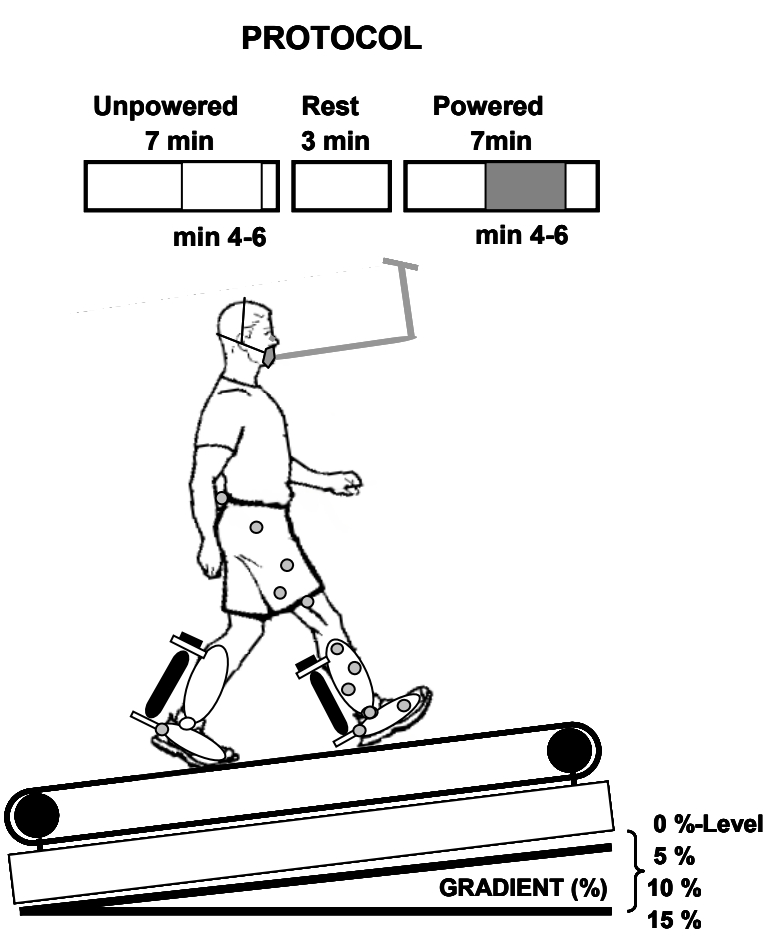
PROTOCOL
Unpowered
7 min
Rest
3 min
Powered
7min
min 4-6
min 4-6
0 %-Level
5 %
GRADIENT (%)
10 %
15 %

B.

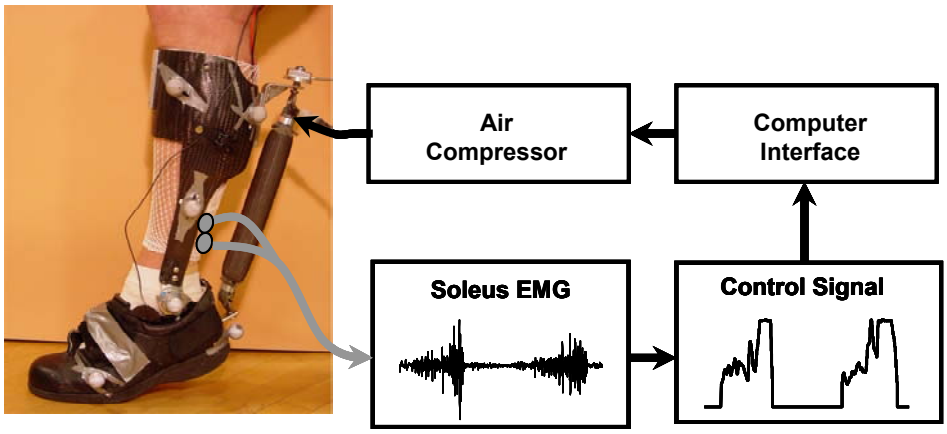
Air
Compressor
Computer
Interface
Soleus EMG
Control Signal

Figure 4.2 Joint kinematics. Thick curves are nine subject mean ankle (left column), knee (middle column) and hip (right column) joint angles over the stride from heel strike (0%) to heel strike (100%). Data is average of left and right legs. Each row is walking data at 1.25 m/s on a single surface gradient (0%-level at top to 15%-uphill at bottom). In each subplot, curves are for unpowered (black), and powered walking (gray) and thin lines are + 1 standard deviation. Stance is ~0%-60% of the stride, swing 60%-100%. For all joints zero degrees is upright standing posture. Ankle joint extension (plantarflexion), knee joint extension and hip joint extension are all positive.

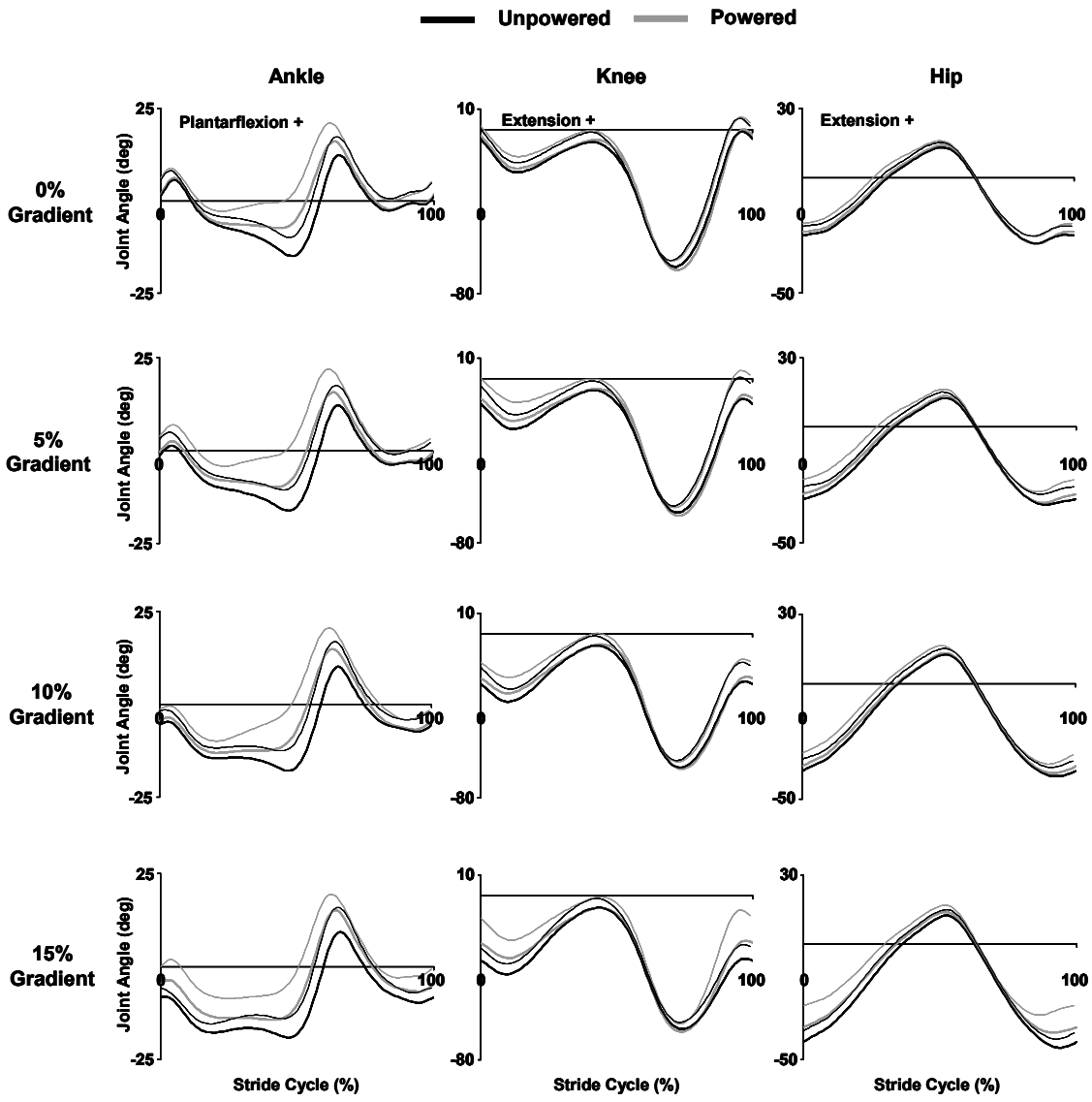
Unpowered
Powered
Ankle
Knee
Hip
0% Gradient
5% Gradient
10% Gradient
15% Gradient
Joint Angle (deg)
Plantarflexion +
Extension +
Extension +
25
-25
10
-80
30
-50
0
100
Stride Cycle (%)

Figure 4.3 Ankle exoskeleton mechanics. Thick curves are nine subject mean ankle joint angular velocity (left column), exoskeleton torque (middle column) and exoskeleton mechanical power (right column) over the stride from heel strike (0%) to heel strike (100%). Data is average of left and right legs. Each row is walking data at 1.25 m/s on a single surface gradient (0%-level at top to 15%-uphill at bottom). In each subplot, curves are for unpowered (black), and powered walking (gray) and thin lines are + 1 standard deviation. Stance is ~0%-60% of the stride, swing 60%-100%. Ankle joint angular velocity is positive for ankle extension (i.e. plantar flexion). Exoskeleton torque that acts to extend the ankle is positive. Torque is product of artificial muscle load and moment arm length and normalized by subject mass. Positive exoskeleton power indicates transfer of energy from the exoskeletons to the user's ankle joints. Power is the product of exoskeleton torque and ankle joint angular velocity.

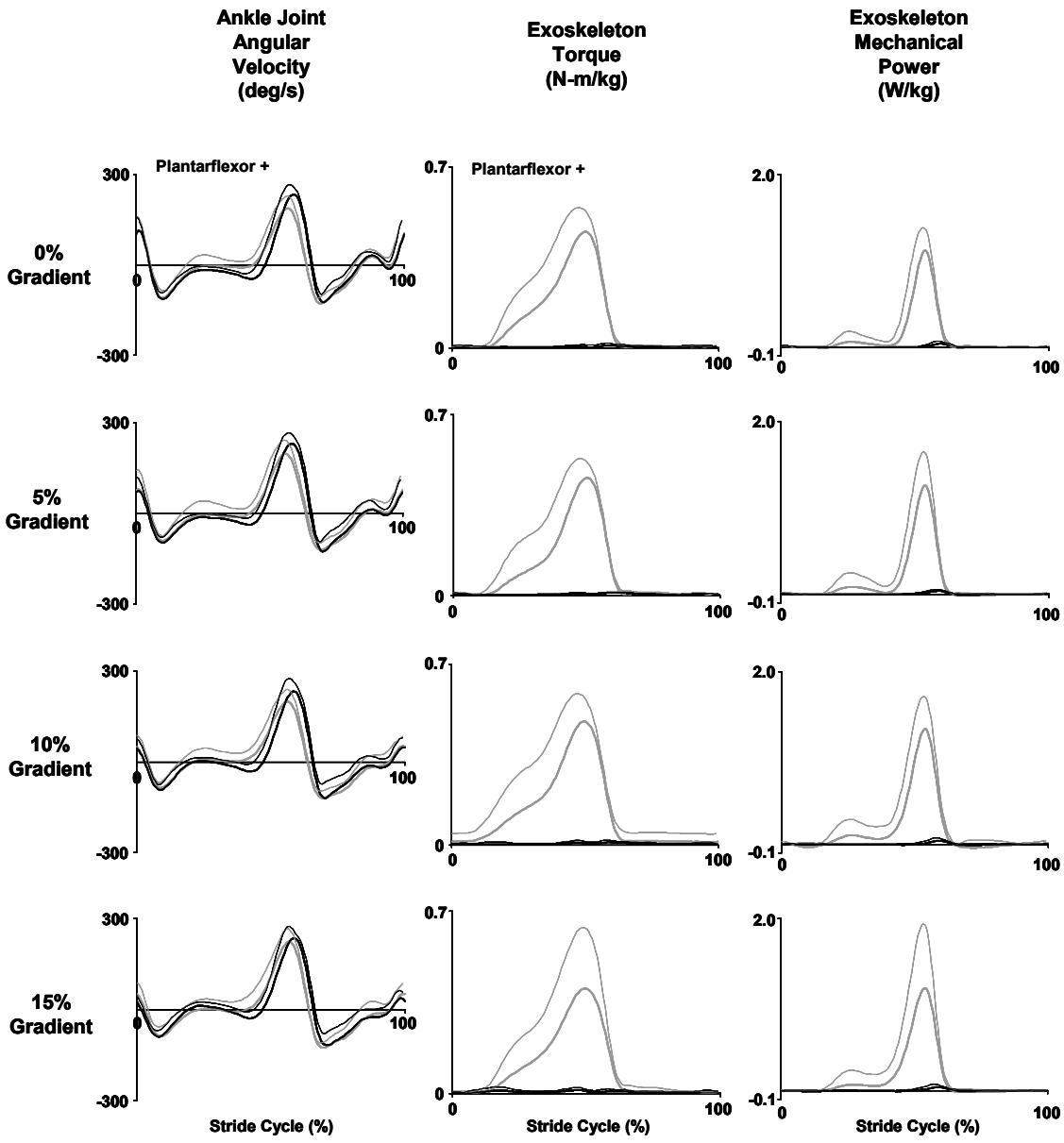
Ankle Joint Angular Velocity (deg/s)
Exoskeleton Torque (N-m/kg)
Exoskeleton Mechanical Power (W/kg)
Plantarflexor +
Plantarflexor +
0% Gradient
5% Gradient
10% Gradient
15% Gradient
300
-300
0
100
0.7
2.0
-0.1
Stride Cycle (%)
Stride Cycle (%)
Stride Cycle (%)

Figure 4.4 Net metabolic power. Bars indicate the nine subject mean net metabolic power (W/kg) during unpowered (white) and powered (gray) walking. Error bars are ± 1 standard error. Surface gradients (0%-level to 15% uphill) are tabulated left to right. Values listed above bars indicate percentage difference in powered versus unpowered walking for each condition. Asterisks indicate a statistically significant difference between powered and unpowered walking (ANOVA, $p < 0.05$).

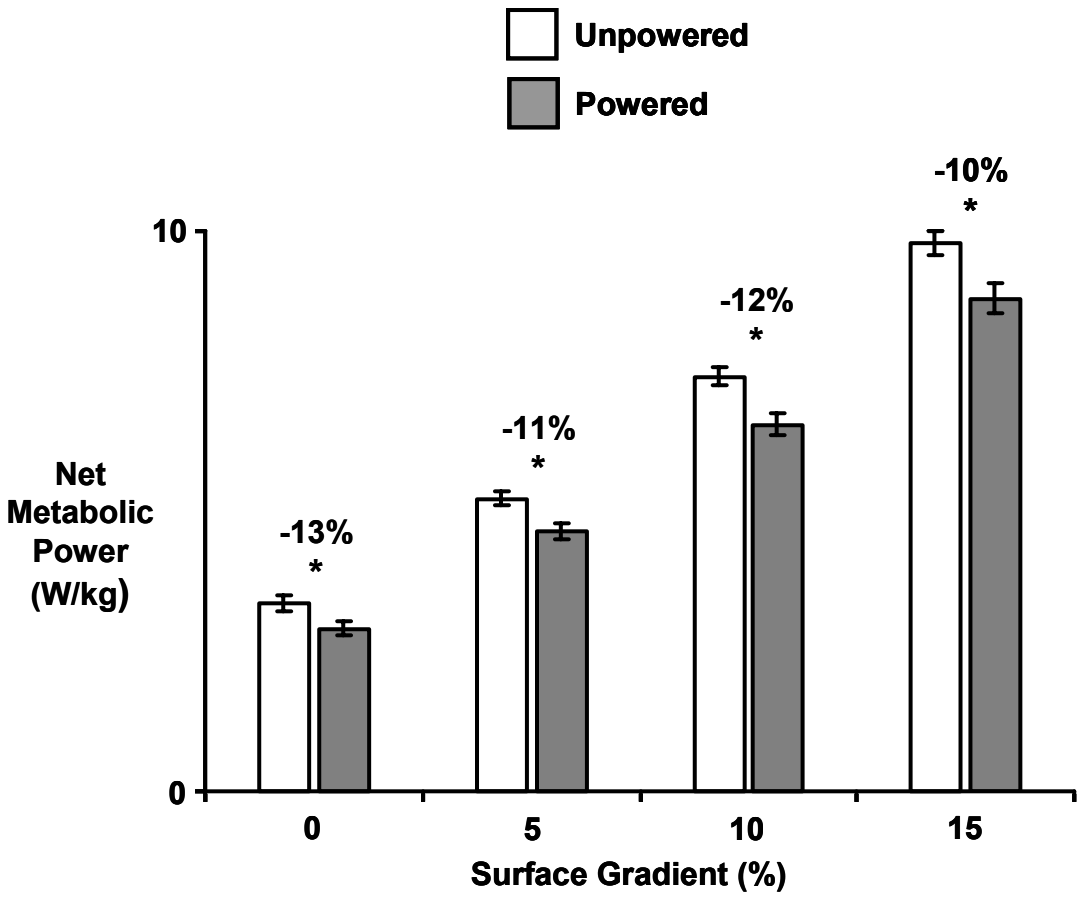
Unpowered
Powered
10
0
Net Metabolic Power (W/kg)
-13%
*
-11%
*
-12%
*
-10%
*
0
5
10
15
Surface Gradient (%)

Figure 4.5 Exoskeleton performance. Bars indicate nine subject mean **(A)** change in net metabolic power (powered - unpowered) due to powered assistance from bilateral ankle exoskeletons **(B)** exoskeleton average positive (dark gray), negative (white) and net (light gray) mechanical power over a stride for powered walking and **(C)** exoskeleton performance index. Performance index indicates the fraction of average exoskeleton positive mechanical power that results in a reduction in net metabolic power, assuming that artificial muscle work directly replaces biological muscle work. Exoskeleton performance index = 1.0 would suggest that all of the exoskeleton average mechanical power replaces underlying biological muscle work. For all panels, surface inclines increase from left (0%-level) to right (15%-uphill). All metabolic power values are normalized by subject mass. Error bars are ± 1 standard error.

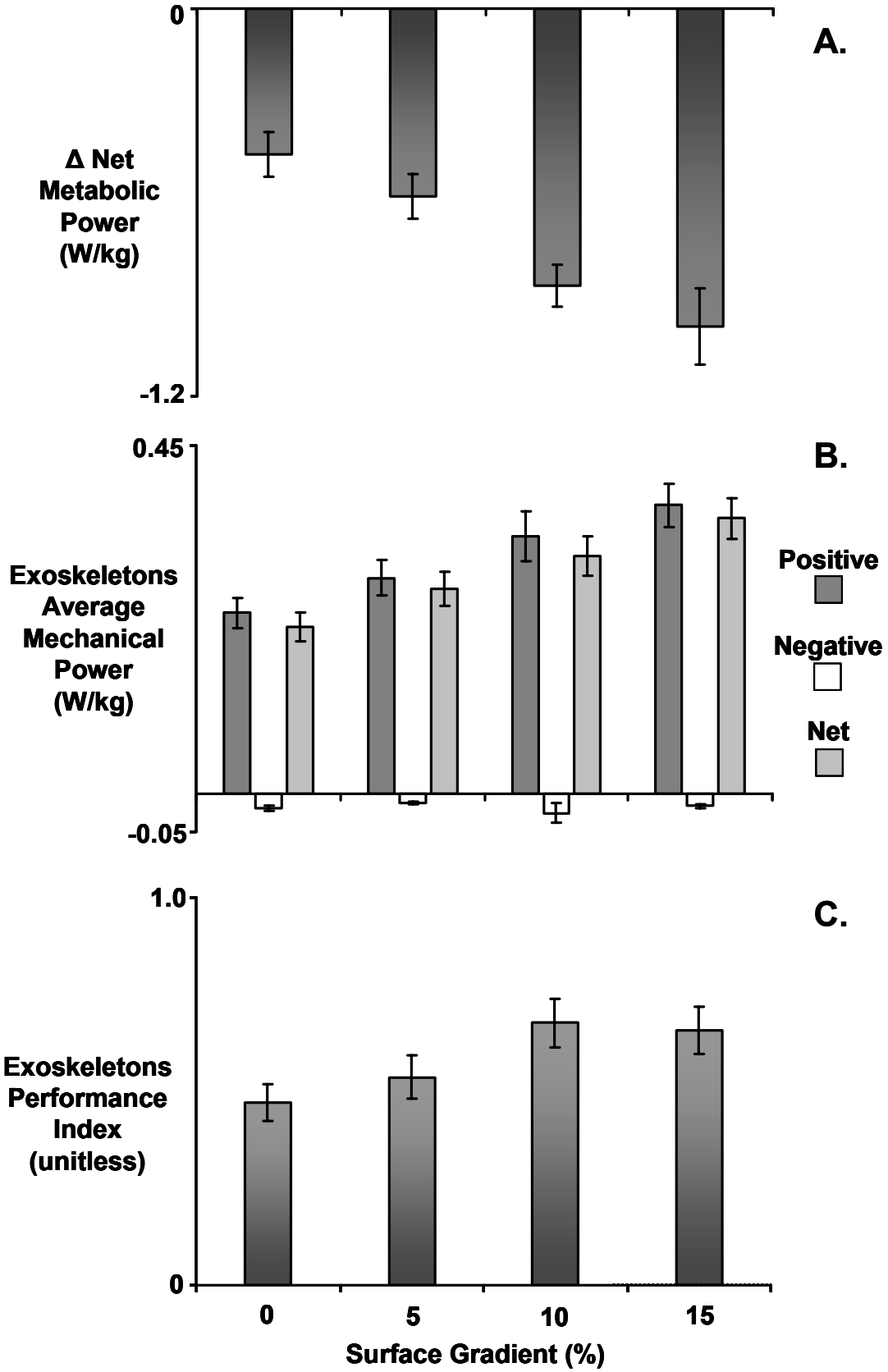
A.
0
Δ Net
Metabolic
Power
(W/kg)
-1.2
B.
0.45
Exoskeletons
Average
Mechanical
Power
(W/kg)
-0.05
Positive
Negative
Net
C.
1.0
Exoskeletons
Performance
Index
(unitless)
0
0
5
10
15
Surface Gradient (%)

Figure 4.6 Soleus electromyography. Nine subject mean (thick curves) + 1 standard deviation (thin curves) of soleus normalized linear enveloped (high-pass cutoff frequency = 20 Hz and low-pass cutoff frequency = 10 Hz) muscle activity over the stride from heel-strike (0%) to heel-strike (100%). Thick curves are unpowered walking (black) and powered walking (gray) and normalized to the peak value during unpowered walking for the 15%-grade condition. Surface inclination increases from top (0% grade-level) to bottom (15% grade-uphill). Left and right legs are averaged for each subject. Stance phase is ~0%-60% and swing ~60%-100% of the stride.

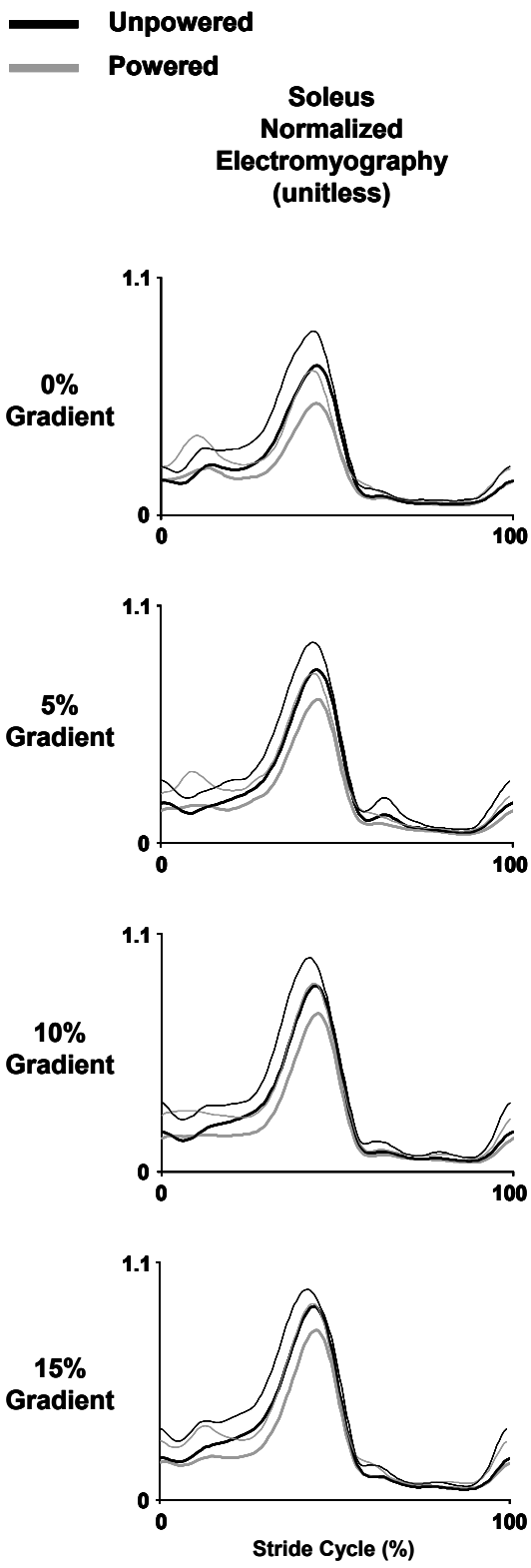
Unpowered
Powered
Soleus
Normalized
Electromyography
(unitless)
1.1
0%
Gradient
0
0
100
1.1
5%
Gradient
0
0
100
1.1
10%
Gradient
0
0
100
1.1
15%
Gradient
0
0
100
Stride Cycle (%)

Figure 4.7 Ankle joint muscle root mean square electromyography. Subplots are soleus (top), medial gastrocnemius, lateral gastrocnemius, and tibialis anterior (bottom). In each subplot, bars are nine subject mean stance phase root mean square average muscle activation. Error bars are ± 1 standard error. Surface gradients increase from left (0%-level) to right (15%-uphill) with unpowered walking (minutes 4-6) in white and powered walking (minutes 4-6) in gray. Values listed above bars indicate percentage difference in powered versus unpowered condition. Asterisks indicate a statistically significant difference between powered and unpowered walking (ANOVA, $p < 0.05$).

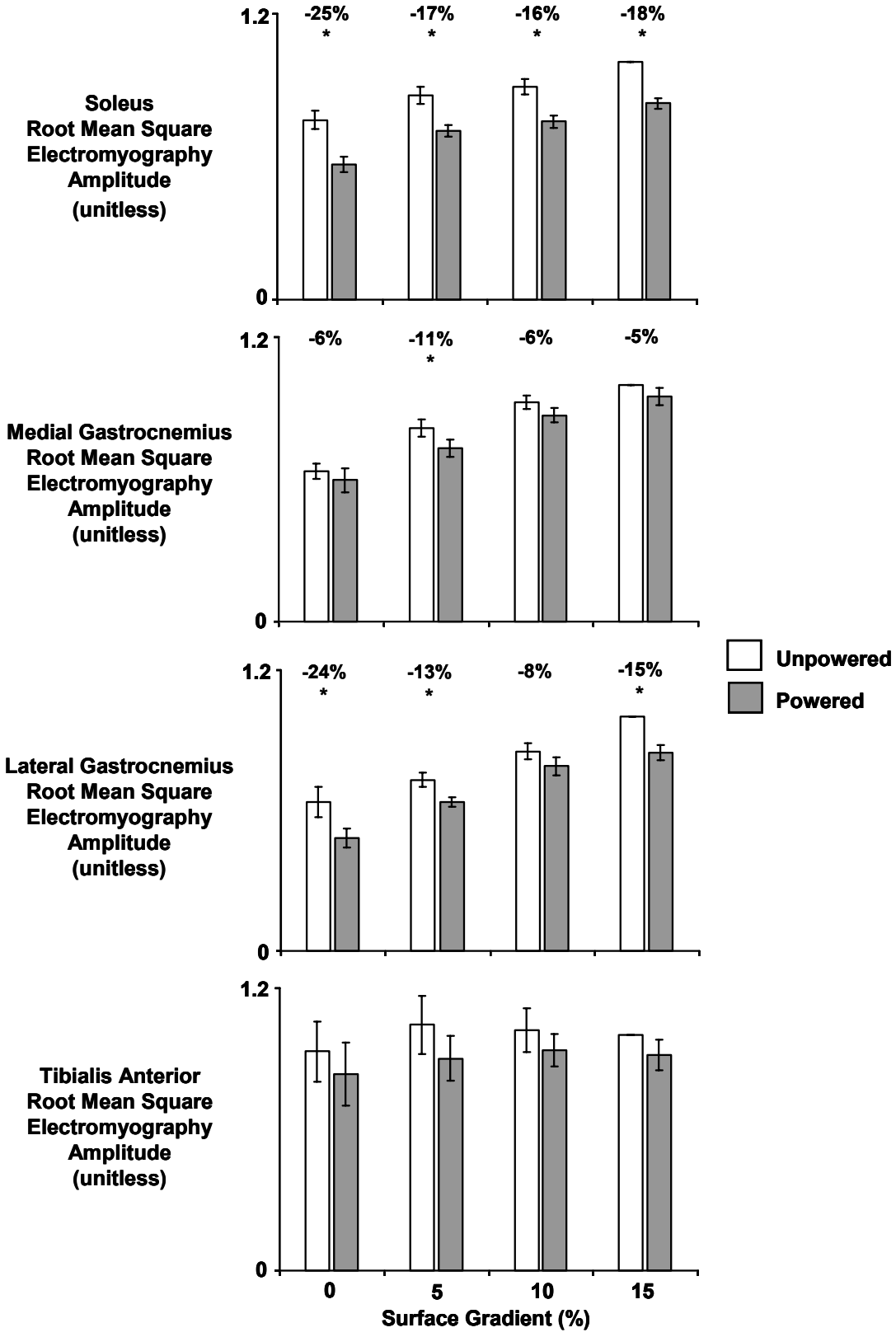
Soleus
Root Mean Square
Electromyography
Amplitude
(unitless)
1.2
0
-25%
*
-17%
*
-16%
*
-18%
*
Medial Gastrocnemius
Root Mean Square
Electromyography
Amplitude
(unitless)
1.2
0
-6%
-11%
*
-6%
-5%
Lateral Gastrocnemius
Root Mean Square
Electromyography
Amplitude
(unitless)
1.2
0
-24%
*
-13%
*
-8%
-15%
*
Tibialis Anterior
Root Mean Square
Electromyography
Amplitude
(unitless)
1.2
0
0
5
10
15
Surface Gradient (%)
Unpowered
Powered

Table 4.1 Gait kinematics. Table lists mean ± standard error for step length, step width, step period and double support period during unpowered and powered walking at 1.25 m/s on each surface gradient. Surface gradients are listed in columns (0%-level to 15%-uphill from left to right). Results of repeated measures ANOVA (n = 9 subjects) comparing pooled unpowered and powered walking data between surface gradients are summarized in the rightmost column.

METRIC	0% Grade				5% Grade				10% Grade				15% Grade				Gradient p-value; THSD
	Unpowered		Powered		Unpowered		Powered		Unpowered		Powered		Unpowered		Powered		
	Mean	SE	Mean	SE	Mean	SE	Mean	SE	Mean	SE	Mean	SE	Mean	SE	Mean	SE	
Step Length (mm)	**729**	4	**722**	8	**734**	7	**731**	13	**723**	11	**718**	16	**712**	13	**709**	16	p=0.02* 15%<5%
Step Width (mm)	**99**	12	**106**	13	**107**	12	**109**	11	**112**	11	**114**	8	**118**	9	**120**	6	p=0.004** 15%>0%
Step Period (ms)	**573**	3	**574**	5	**575**	6	**576**	9	**570**	9	**572**	12	**559**	11	**562**	12	p=0.04* 15%<5%
Double Support Period (ms)	**136**	4	**136**	5	**137**	4	**137**	6	**138**	5	**137**	6	**135**	5	**138**	6	p=0.90

n=9, See Materials and Methods for calculations.

THSD=Tukey Honestly Significant Difference Test Results; **SE**=Standard Error

Condition: Unpowered, Powered; **Gradient:** 0%, 5%, 10%, 15%

p<0.05 indicates statistical significance. * indicates statistical power >0.65; ** indicates statistical power >0.80.

References

Abbott, B. C., Bigland, B. and Ritchie, J. M. (1952). The physiological cost of negative work. *Journal of Physiology (London)* **117**, 380-390.

Asmussen, E. and Bonde-Petersen, F. (1974). Apparent efficiency and storage of elastic energy in human muscles during exercise. *Acta Physiol Scand* **92**, 537-45.

Atzler, E. and Herbst, R. (1927). Arbeitsphysiologische Studien. III. *Pflugers Arch ges Physiol* **215**, 291-328.

Aura, O. and Komi, P. V. (1986). Mechanical Efficiency of Pure Positive and Pure Negative Work with Special Reference to the Work Intensity. *International Journal of Sports Medicine* **7**, 44-49.

Bertram, J. E. and Ruina, A. (2001). Multiple walking speed-frequency relations are predicted by constrained optimization. *J Theor Biol* **209**, 445-53.

Biewener, A. A. (1989). Scaling Body Support in Mammals - Limb Posture and Muscle Mechanics. *Science* **245**, 45-48.

Biewener, A. A., Farley, C. T., Roberts, T. J. and Temaner, M. (2004a). Muscle mechanical advantage of human walking and running: implications for energy cost. *J Appl Physiol* **97**, 2266-74.

Biewener, A. A., McGowan, C., Card, G. M. and Baudinette, R. V. (2004b). Dynamics of leg muscle function in tammar wallabies (M. eugenii) during level versus incline hopping. *J Exp Biol* **207**, 211-23.

Bigland-Ritchie, B. and Woods, J. J. (1976). Integrated electromyogram and oxygen uptake during positive and negative work. *Journal of Physiology (London)* **260**, 267-77.

Blaxter, K. (1989). Energy Metabolism in Animals and Man. Cambridge: Cambridge University Press.

Bobbert, A. C. (1960). Energy expenditure in level and grade walking. *J Appl Physiol* **15**, 1015-1021.

Brockway, J. M. (1987). Derivation of formulae used to calculate energy expenditure in man. *Hum Nutr Clin Nutr* **41**, 463-71.

Brooks, G. A., Fahey, T. D. and White, T. G. (1996). Exercise physiology: human bioenergetics and its applications. Mountain View, Calif.: Mayfield.

Browning, R. C., Modica, J. R., Kram, R. and Goswami, A. (2007). The effects of adding mass to the legs on the energetics and biomechanics of walking. *Med Sci Sports Exerc* **39**, 515-25.

Burdett, R. G., Skrinar, G. S. and Simon, S. R. (1983). Comparison of mechanical work and metabolic energy consumption during normal gait. *J Orthop Res* **1**, 63-72.

Cavagna, G. A. and Kaneko, M. (1977). Mechanical work and efficiency in level walking and running. *Journal of Physiology (London)* **268**, 647-681.

Cotes, J. E. and Meade, F. (1960). The energy expenditure and mechanical energy demand in walking. *Ergonomics* **3**, 97-119.

Daley, M. A. and Biewener, A. A. (2003). Muscle force-length dynamics during level versus incline locomotion: a comparison of in vivo performance of two guinea fowl ankle extensors. *Journal of Experimental Biology* **206**, 2941-2958.

Davies, C. T. M. and Barnes. (1972). Negative (eccentric) work. 2. Physiological responses to walking uphill and downhill on a motor-driven treadmill. *Ergonomics* **15**, 121.

Dean, G. (1965). An analysis of the energy expenditure in level and grade walking. *Ergonomics* **8**, 31-47.

Doke, J., Donelan, J. M. and Kuo, A. D. (2005). Mechanics and energetics of swinging the human leg. *Journal of Experimental Biology* **208**, 439-45.

Doke, J. and Kuo, A. D. (2007). Energetic cost of producing cyclic muscle force, rather than work, to swing the human leg. *J Exp Biol* **210**, 2390-8.

Donelan, J. M., Kram, R. and Kuo, A. D. (2001). Mechanical and metabolic determinants of the preferred step width in human walking. *Proceedings of the Royal Society of London Series B-Biological Sciences* **268**, 1985-92.

Donelan, J. M., Kram, R. and Kuo, A. D. (2002a). Mechanical work for step-to-step transitions is a major determinant of the metabolic cost of human walking. *Journal of Experimental Biology* **205**, 3717-27.

Donelan, J. M., Kram, R. and Kuo, A. D. (2002b). Simultaneous positive and negative external mechanical work in human walking. *J Biomech* **35**, 117-24.

Fenn, W. O. (1924). The relation between the work performed and the energy liberated in muscular contraction. *Journal of Physiology, London* **58**, 373-395.

Ferris, D. P., Czerniecki, J. M. and Hannaford, B. (2005). An ankle-foot orthosis powered by artificial pneumatic muscles. *J Appl Biomech* **21**, 189-197.

Ferris, D. P., Gordon, K. E., Sawicki, G. S. and Peethambaran, A. (2006). An improved powered ankle-foot orthosis using proportional myoelectric control. *Gait and Posture* **23**, 425-8.

Ferris, D. P., Sawicki, G. S. and Daley, M. A. (2007). A physiologist's perspective on robotic exoskeleton's for human locomotion. *International Journal of Humanoid Robotics* **in press**.

Fukunaga, T., Kubo, K., Kawakami, Y., Fukashiro, S., Kanehisa, H. and Maganaris, C. N. (2001). In vivo behaviour of human muscle tendon during walking. *Proceedings of the Royal Society of London: Biological Sciences* **268**, 229-33.

Gabaldon, A. M., Nelson, F. E. and Roberts, T. J. (2004). Mechanical function of two ankle extensors in wild turkeys: shifts from energy production to energy absorption during incline versus decline running. *J Exp Biol* **207**, 2277-88.

Gordon, K. E. and Ferris, D. P. (2007). Learning to walk with a robotic ankle exoskeleton. *J Biomech* **in press**.

Gordon, K. E., Sawicki, G. S. and Ferris, D. P. (2006). Mechanical performance of artificial pneumatic muscles to power an ankle-foot orthosis. *J Biomech* **39**, 1832-41.

Gottschall, J. S. and Kram, R. (2003). Energy cost and muscular activity required for propulsion during walking. *J Appl Physiol* **94**, 1766-72.

Gottschall, J. S. and Kram, R. (2005). Energy cost and muscular activity required for leg swing during walking. *J Appl Physiol* **99**, 23-30.

Grey, M. J., Nielsen, J. B., Mazzaro, N. and Sinkjaer, T. (2007). Positive force feedback in human walking. *J Physiol* **581**, 99-105.

Griffin, T. M., Roberts, T. J. and Kram, R. (2003). Metabolic cost of generating muscular force in human walking: insights from load-carrying and speed experiments. *Journal of Applied Physiology* **95**, 172-83.

Heglund, N. C. and Cavagna, G. A. (1987). Mechanical work, oxygen consumption, and efficiency in isolated frog and rat muscle. *American Journal of Physiology* **253**, C22-29.

Hill, A. V. (1938). The heat of shortening and the dynamic constants of muscle. *Proceedings of the Royal Society of London: Biological Sciences* **B126**, 136-195.

Hill, A. V. (1939). The mechanical efficiency of frog's muscle. *Proceedings of the Royal Society of London: Biological Sciences* **127**, 434-451.

Ishikawa, M., Komi, P. V., Grey, M. J., Lepola, V. and Bruggemann, G. P. (2005). Muscle-tendon interaction and elastic energy usage in human walking. *J Appl Physiol* **99**, 603-8.

Kuo, A. D., Donelan, J. M. and Ruina, A. (2005). Energetic consequences of walking like an inverted pendulum: step-to-step transitions. *Exerc Sport Sci Rev* **33**, 88-97.

Lay, A. N., Hass, C. J. and Gregor, R. J. (2006). The effects of sloped surfaces on locomotion: a kinematic and kinetic analysis. *J Biomech* **39**, 1621-8.

Lay, A. N., Hass, C. J., Richard Nichols, T. and Gregor, R. J. (2007). The effects of sloped surfaces on locomotion: an electromyographic analysis. *J Biomech* **40**, 1276-85.

Leroux, A., Fung, J. and Barbeau, H. (1999). Adaptation of the walking pattern to uphill walking in normal and spinal-cord injured subjects. *Experimental Brain Research* **126**, 359-68.

Lichtwark, G. A. and Wilson, A. M. (2006). Interactions between the human gastrocnemius muscle and the Achilles tendon during incline, level and decline locomotion. *Journal of Experimental Biology* **209**, 4379-88.

Margaria, R. (1938). Sulla fisiologia e specialmente sul consumo energetico della marcia e della corsa a varie velocita ed inclinazioni del terreno. *Atti Accad. Naz. Lincei Memorie, serie VI* **7**, 299-368.

Margaria, R. (1968). Positve and negative work performances and their efficiencies in human locomotion. *Int Z Angew Physiol Einschl Arbeitsphysiol* **25**, 339-351.

Massaad, F., Lejeune, T. M. and Detrembleur, C. (2007). The up and down bobbing of human walking: a compromise between muscle work and efficiency. *J Physiol*.

McGowan, C. P., Baudinette, R. V. and Biewener, A. A. (2007). Modulation of proximal muscle function during level versus incline hopping in tammar wallabies (Macropus eugenii). *J Exp Biol* **210**, 1255-65.

McIntosh, A. S., Beatty, K. T., Dwan, L. N. and Vickers, D. R. (2006). Gait dynamics on an inclined walkway. *J Biomech* **39**, 2491-502.

Minetti, A. E., Ardigo, L. P. and Saibene, F. (1993). Mechanical determinants of gradient walking energetics in man. *Journal of Physiology (London)* **472**, 725-35.

Minetti, A. E., Moia, C., Roi, G. S., Susta, D. and Ferretti, G. (2002). Energy cost of walking and running at extreme uphill and downhill slopes. *J Appl Physiol* **93**, 1039-46.

Poole, D. C., Gaesser, G. A., Hogan, M. C., Knight, D. R. and Wagner, P. D. (1992). Pulmonary and leg VO2 during submaximal exercise: implications for muscular efficiency. *Journal of Applied Physiology* **72**, 805-10.

Ralston, H. J. (1958). Energy-speed relation and optimal speed during level walking. *Int Z Angew Physiol* **17**, 277-83.

Roberts, T. J. and Belliveau, R. A. (2005). Sources of mechanical power for uphill running in humans. *J Exp Biol* **208**, 1963-70.

Roberts, T. J., Marsh, R. L., Weyand, P. G. and Taylor, C. R. (1997). Muscular force in running turkeys: the economy of minimizing work. *Science* **275**, 1113-1115.

Rubenson, J., Henry, H. T., Dimoulas, P. M. and Marsh, R. L. (2006). The cost of running uphill: linking organismal and muscle energy use in guinea fowl (Numida meleagris). *Journal of Experimental Biology* **209**, 2395-408.

Sawicki, G. S. and Ferris, D. P. (2007a). Mechanics and energetics of level walking with powered ankle exoskeletons. *J Exp Biol* **submitted**.

Sawicki, G. S. and Ferris, D. P. (2007b). Metabolic cost of ankle joint work during walking with increasing step length. *J Exp Biol* **submitted**.

Sawicki, G. S., Gordon, K. E. and Ferris, D. P. (2005). Powered lower limb orthoses: applications in motor adaptation and rehabilitation. In *IEEE International Conference on Rehabilitation Robotics*. Chicago, IL: IEEE.

Willems, P. A., Cavagna, G. A. and Heglund, N. C. (1995). External, internal and total work in human locomotion. *Journal of Experimental Biology* **198**, 379-393.

Woledge, R. C. (1985). Energetic aspects of muscle contraction. London: Academic Press.

Chapter V

Conclusion

Accomplishments

The overall goal of this dissertation was to examine the mechanics, energetics and neural control of human walking at the level of the lower-limb joints. I built bilateral ankle exoskeletons powered using artificial pneumatic muscles and controlled with the user's own soleus (an ankle plantar flexor) electromyography (EMG) signal to command torque and drive ankle extension during the push-off phase of walking. I addressed the following questions:

1) Can powered ankle exoskeletons reduce the metabolic cost of level steady speed walking? Just as most new motor skills do, walking with lower-limb robotic exoskeletons requires a period of adaptation and learning. My results (Chapter II) showed that over three thirty minute practice sessions, each separated by three days, subjects progressed from a ~7% increase to a ~10% decrease in net metabolic power during walking with powered ankle exoskeletons. Subjects reduced their metabolic energy consumption by altering soleus EMG to adjust the timing and amplitude of the commanded torque

assistance in order to eliminate negative work performed (energy absorbed) by the exoskeletons over the stride. After practice, exoskeletons transferred distinct bursts of positive power (i.e. 63% of the ankle joint and 22% of the total joint average positive mechanical power) to the users' ankles at push-off. During powered walking, ankle, knee and hip kinematics were close to normal, and ankle extensor EMG was reduced by up to 30% in soleus and up to 10% in medial and lateral gastrocnemius.

2) Is powered assistance more effective at reducing the metabolic cost of walking under conditions of increased workload? Powered exoskeletons could be particularly useful for preventing rapid fatigue during tasks that require high power outputs. I used increasing (1) step length (Chapter III) and (2) surface gradient (Chapter IV) to study how exoskeleton performance changes under conditions of increased external workload. Subjects used exoskeletons to produce similar torques but higher mechanical power outputs during higher workload tasks. This was due to natural changes in joint range of motion and angular velocity. Although absolute reductions in net metabolic cost were larger for higher workloads, relative reductions in net metabolic cost were similar for powered walking with longer steps and on steeper inclines. Reductions in net metabolic power ranged from 8%-13%.

3) What is the 'apparent efficiency' and relative metabolic cost of ankle joint positive mechanical work? Classic experiments on isolated muscle have

established that the efficiency of positive muscle work is ~0.25 ; (Fenn, 1924; Hill, 1939). That is, isolated skeletal muscle consumes 4 Joules of metabolic energy for every 1 Joule of positive mechanical work it generates. The 'apparent efficiency' (or ratio of the average mechanical power input by the exoskeletons to the net metabolic savings of the user) of ankle joint positive mechanical work can be compared with that of isolated muscle to give insight into the underlying mechanical function of the muscle-tendon units spanning a joint. My results indicate that the ankle joint 'apparent efficiency' of positive mechanical work is ~0.5-0.6 for preferred step length walking on level ground at 1.25 m/s. 'Apparent efficiency' values higher than 0.25 suggest an underlying role for passive tendon stretch and recoil. 'Apparent efficiency' values of 0.5-0.6 indicate that the Achilles tendon stores elastic energy and then returns it to produce a portion of the ankle joint positive mechanical power at reduced metabolic cost. We estimate that Achilles tendon performs >50% of the ankle joint push off positive work during level preferred step length walking. Because Achilles tendon work is relative cheap metabolically speaking, the ankle joint can perform 35% of the lower-limb positive mechanical work but consume only 18%-20% of the net metabolic energy for walking at preferred step length on level ground (Chapter II).

Under conditions of increased workload ankle joint 'apparent efficiency' is reduced. For walking between 80%-140% of the preferred step length the 'apparent efficiency' of ankle joint work decreases from 1.39 for the shortest steps to 0.38 for the longest steps. This suggests that muscles rather than the Achilles tendon perform more and more ankle joint positive mechanical work as

the demand for external power is elevated. As a consequence, the net metabolic cost of ankle joint positive mechanical work increases from ~7%-26% as step length increases from 80% to 140% of the preferred step length (Chapter III). Ankle joint 'apparent efficiency' decreases from 0.53 to 0.39 as surface gradient increases from 0%-level to 15%-uphill (Chapter IV).

From a basic science standpoint, these results suggest that the Achilles tendon elastic energy return allows the ankle joint to perform positive mechanical work with very little metabolic energy. Thus, the metabolic cost of walking may be dominated by muscle positive mechanical work at the knee and hip joints.

From an applied science standpoint, these results will help guide the design of powered, wearable robotic devices for reducing metabolic cost of walking. Assisting more proximal joints (e.g. knee, hip) that are less efficient (i.e. where muscles do much and tendons do little positive work) should yield larger reductions net metabolic power of walking.

References

Fenn, W. O. (1924). The relation between the work performed and the energy liberated in muscular contraction. *Journal of Physiology, London* **58**, 373-395.

Hill, A. V. (1939). The mechanical efficiency of frog's muscle. *Proceedings of the Royal Society of London: Biological Sciences* **127**, 434-451.

Appendix

Table A.1. Chapter two subject characteristics.

Subject ID (m/f)	Body Mass (kg)	Height (cm)	Leg Length (cm)	Exoskeleton Mass (kg)	Artificial Muscle Length (cm)	Moment Arm Length (cm)
CA-f	70.3	173	89	1.14	43.0	10.8
FA-f	82.6	174	88	1.20	45.5	9.5
WD-m	89.7	185	98	1.22	48.8	11.0
ME-m	70.3	180	94	1.20	47.3	11.8
AK-f	79.4	180	90	1.16	46.0	11.0
OK-f	72.6	177	91	1.06	45.3	10.8
DM-f	54.4	165	85	1.31	44.3	8.3
OR-m	95.3	196	100	1.48	47.5	11.5
OS-m	85.5	185	98	1.14	46.0	9.0
MEAN ± SD	**77.8 ± 12.4**	**179 ± 9**	**93 ± 5**	**1.21 ± 0.12**	**46.0 ± 1.7**	**10.4 ± 1.2**

Table A.2. Chapter two net metabolic power and statistics.

	METRIC	Unpowered				Powered				STATISTICS	
		Beginning		End		Beginning		End			
		Mean	SE	Mean	SE	Mean	SE	Mean	SE	Condition p-value; THSD	Period p-value; THSD
Session 1	Net Metabolic Power (W/kg)	**3.58**	0.10	**3.52**	0.10	**3.84**	0.30	**3.57**	0.31	p=0.33	p=0.33
Session 2	Net Metabolic Power (W/kg)	**3.40**	0.10	**3.39**	0.08	**3.64**	0.33	**3.23**	0.18	p=0.81	p=0.18
Session 3	Net Metabolic Power (W/kg)	**3.31**	0.11	**3.25**	0.10	**3.22**	0.20	**2.99**	0.17	p=0.03* Powered<Unpowered	p=0.09

	Session p-value; THSD	Period p-value; THSD	Session p-value; THSD	Period p-value; THSD
Net Metabolic Power (W/kg)	p=0.001** S2<S1 S3<S1	p=0.34	p=0.0001** S3<S2 S3<S1	p=0.006** End<Beginning

n=9, See Materials and Methods for calculations.
THSD=Tukey Honestly Significant Difference Test Results; **SE**=Standard Error
Condition: Unpowered, Powered; **Period:** Beginning, End; **Session:** S1,S2,S3
p<0.05 indicates statistical significance.
*** indicates statistical power >0.65; ** indicates statistical power >0.80.**

Table A.3. Chapter two exoskeletons performance metrics and statistics.

METRIC	Powered Session 1				Powered Session 2				Powered Session 3				STATISTICS	
	Beginning		End		Beginning		End		Beginning		End			
	Mean	SE	Mean	SE	Mean	SE	Mean	SE	Mean	SE	Mean	SE	Session p-value; THSD	Period p-value; THSD
Positive Exoskeletons Mechanical Power (W/kg)	**0.29**	0.02	**0.25**	0.02	**0.28**	0.03	**0.26**	0.02	**0.27**	0.03	**0.24**	0.02	p=0.29	p=0.001** End<Beginning
Negative Exoskeletons Mechanical Power (W/kg)	**-0.09**	0.03	**-0.06**	0.03	**-0.07**	0.03	**-0.04**	0.02	**-0.04**	0.01	**-0.03**	0.00	p=0.005** S3<S1	p=0.08
Δ Net Metabolic Power (W/kg)	**0.26**	0.28	**0.00**	0.29	**0.24**	0.29	**-0.18**	0.15	**-0.09**	0.14	**-0.32**	0.12	p=0.04* S3<S1	p=0.007* End<Beginning
Exoskeletons Performance Index (W/kg)	**-0.14**	0.19	**0.13**	0.26	**-0.16**	0.21	**0.21**	0.14	**0.14**	0.14	**0.41**	0.19	p=0.05	p=0.004** End>Beginning

n=9, See Materials and Methods for calculations.

THSD=Tukey Honestly Significant Difference Test Results; **SE**=Standard Error **Δ**=Powered-Unpowered

Session: S1,S2,S3; **Period:** Beginning, End

p<0.05 indicates statistical significance. * indicates statistical power >0.65; ** indicates statistical power >0.80.

Table A.4. Chapter two root mean square electromyography and statistics.

	METRIC	Unpowered				Powered				STATISTICS	
		Beginning		End		Beginning		End			
		Mean	SE	Mean	SE	Mean	SE	Mean	SE	Condition p-value	Period p-value
Session 1	Sol RMS (unitless)	1.00	0.00	0.88	0.03	0.91	0.12	0.74	0.05	p=0.05	p=0.01*
	TA RMS (unitless)	1.00	0.00	1.04	0.06	1.52	0.15	1.27	0.11	p=0.001**	p=0.30
	MG RMS (unitless)	1.00	0.00	0.96	0.04	1.02	0.06	0.92	0.05	p=0.85	p=0.02
	LG RMS (unitless)	1.00	0.00	0.97	0.02	1.06	0.13	0.90	0.06	p=0.93	p=0.15
Session 2	Sol RMS (unitless)	1.00	0.00	0.91	0.04	0.77	0.05	0.69	0.03	p<0.0001**	p=0.007**
	TA RMS (unitless)	1.00	0.00	0.96	0.06	1.38	0.18	1.07	0.06	p=0.02*	p=0.08
	MG RMS (unitless)	1.00	0.00	0.93	0.06	0.93	0.04	0.94	0.06	p=0.45	p=0.43
	LG RMS (unitless)	1.00	0.00	0.95	0.03	1.00	0.10	0.82	0.06	p=0.21	p=0.04
Session 3	Sol RMS (unitless)	1.00	0.00	0.93	0.03	0.78	0.04	0.72	0.03	p<0.0001**	p=0.004**
	TA RMS (unitless)	1.00	0.00	0.97	0.06	1.17	0.08	1.00	0.06	p=0.05	p=0.06
	MG RMS (unitless)	1.00	0.00	0.98	0.03	0.98	0.05	0.96	0.06	p=0.52	p=0.50
	LG RMS (unitless)	1.00	0.00	1.04	0.03	0.97	0.09	0.90	0.06	p=0.09	p=0.83

	Session p-value; THSD	Period p-value; THSD	Session p-value; THSD	Period p-value; THSD
Sol RMS (unitless)	p=0.52	p<0.0001** End<Beginning	p=0.08	p=0.006** End<Beginning
TA RMS (unitless)	p=0.57	p=0.73	p=0.003** S3<S1	p=0.001** End<Beginning
MG RMS (unitless)	p=0.67	p=0.07	p=0.63	p=0.25
LG RMS (unitless)	p=0.10	p=0.47	p=0.33	p=0.002** End<Beginning

n=9, See Materials and Methods for calculations.

Sol=Soleus, **TA**=tibialis anterior, **MG**=medial gastrocnemius, **LG**=lateral gastrocnemius.

Values are root mean square (RMS) average from stance phase only normalized to Unpowered Beginning condition.
THSD=Tukey Honestly Significant Difference Test Results; **SE**=Standard Error

Condition: Unpowered, Powered; **Period:** Beginning, End; **Session:** S1,S2,S3

p<0.05 indicates statistical significance. * indicates statistical power >0.65; ** indicates statistical power >0.80.

Table A.5. Chapter two gait kinematics and statistics.

	METRIC	Unpowered				Powered				STATISTICS	
		Beginning		End		Beginning		End			
		Mean	SE	Mean	SE	Mean	SE	Mean	SE	Condition p-value	Period p-value
Session 1	Step Length (mm)	724	9	741	10	713	10	717	17	p=0.006**	p=0.08
	Step Width (mm)	105	10	100	8	127	8	119	11	p<0.0001**	p=0.10
	Step Period (ms)	573	6	583	7	575	7	580	8	p=0.93	p=0.02*
	Double Support Period (ms)	140	9	141	8	141	6	151	9	p=0.16	p=0.13
Session 2	Step Length (mm)	729	9	729	10	721	12	720	12	p=0.06	p=0.49
	Step Width (mm)	116	7	104	14	135	10	121	17	p=0.002**	p=0.04
	Step Period (ms)	574	8	575	7	577	8	574	9	p=0.56	p=0.98
	Double Support Period (ms)	132	6	135	6	141	6	138	5	p=0.01*	p=0.88
Session 3	Step Length (mm)	732	11	734	9	725	13	717	14	p=0.01*	p=0.93
	Step Width (mm)	123	11	104	9	126	13	120	12	p=0.05	p=0.01*
	Step Period (ms)	575	8	578	7	578	9	575	9	p=0.94	p=0.87
	Double Support Period (ms)	138	6	138	6	140	6	138	5	p=0.47	p=0.38

	Session p-value; THSD	Period p-value; THSD	Session p-value; THSD	Period p-value; THSD
Step Length (mm)	p=0.46	p=0.02* End>Beginning	p=0.48	p=0.79
Step Width (mm)	p=0.01* S3>S1 S2>S1	p=0.002** End<Beginning	p=0.34	p=0.01* End<Beginning
Step Period (ms)	p=0.36	p=0.02* End>Beginning	p=0.97	p=0.94
Double Support Period (ms)	p=0.005** S2<S1	p=0.55	p=0.08	p=0.52

n=9, See Materials and Methods for calculations.

THSD=Tukey Honestly Significant Difference Test Results; **SE**=Standard Error

Condition: Unpowered, Powered; **Period:** Beginning, End; **Session:** S1,S2,S3

p<0.05 indicates statistical significance. * indicates statistical power >0.65; ** indicates statistical power >0.80.

Table A.6. Chapters three and four subject characteristics.

Subject ID (m/f)	Body Mass (kg)	Height (cm)	Leg Length (cm)	Exoskeleton Mass (kg)	Artificial Muscle Length (cm)	Moment Arm Length (cm)
CA-f	70.3	173	89	1.14	43.0	10.8
FA-f	82.6	174	88	1.20	45.5	9.5
TB-m	73.5	170	84	1.04	41.5	11.5
FD-m	109.1	189	100	1.43	47.0	9.8
WD-m	89.7	185	98	1.22	48.8	11.0
ME-m	70.3	180	94	1.20	47.3	11.8
AK-f	79.4	180	90	1.16	46.0	11.0
OK-f	72.6	177	91	1.06	45.3	10.8
OS-m	85.5	185	98	1.14	46.0	9.0
MEAN ± SD	**80.3 ± 14.7**	**179 ± 3**	**92 ± 2**	**1.18 ± 0.11**	**45.6 ± 2.2**	**10.6 ± 0.9**

Table A.7. Chapter three net metabolic power and statistics.

	METRIC	Without		Unpowered		Powered		Condition p-value; THSD
		Mean	SE	**Mean**	SE	**Mean**	SE	
0.8 x Preferred Step Length	**Net Metabolic Power (W/kg)**	**2.49**	0.14	**2.86**	0.07	**2.65**	0.12	p=0.008** Without<Unpowered
1.0 x Preferred Step Length	**Net Metabolic Power (W/kg)**	**3.13**	0.13	**3.39**	0.11	**3.00**	0.10	p=0.001** Without<Unpowered Powered<Unpowered
1.2 x Preferred Step Length	**Net Metabolic Power (W/kg)**	**4.22**	0.18	**4.62**	0.22	**4.04**	0.13	p=0.001** Without<Unpowered Powered<Unpowered
1.4 x Preferred Step Length	**Net Metabolic Power (W/kg)**	**7.18**	0.50	**6.89**	0.32	**6.19**	0.29	p=0.003** Powered<Unpowered, Without
		Gradient p-value; THSD						
	Net Metabolic Power (W/kg)	p<0.0001 1.4>1.2,1.0,0.8 1.2>1.0,0.8 1.0>0.8						

n=9, See Materials and Methods for calculations.

THSD=Tukey Honestly Significant Difference Test Results; **SE**=Standard Error

Condition: Unpowered, Powered; **Step Length:** 0.8xL*, 1.0xL*,1.2xL*,1.4xL*

L* is preferred step length at 1.25 m/s.

p<0.05 indicates statistical significance.

*** indicates statistical power >0.65; ** indicates statistical power >0.80.**

Table A.8. Chapter three exoskeletons performance metrics and statistics.

METRIC	Powered 0.8 x Preferred Step Length		Powered 1.0 x Preferred Step Length		Powered 1.2 x Preferred Step Length		Powered 1.4 x Preferred Step Length		Step Length p-value; THSD
	Mean	SE	**Mean**	SE	**Mean**	SE	**Mean**	SE	
Positive Exoskeletons Mechanical Power (W/kg)	**0.20**	0.02	**0.23**	0.02	**0.25**	0.02	**0.25**	0.02	p=0.01** 1.4>0.8 1.2>0.8
Negative Exoskeletons Mechanical Power (W/kg)	**-0.03**	0.00	**-0.02**	0.00	**-0.02**	0.00	**-0.04**	0.01	p=0.27
ΔNet Metabolic Power (W/kg)	**-0.21**	0.06	**-0.38**	0.07	**-0.57**	0.13	**-0.70**	0.12	p=0.002** 1.4<0.8 1.2<0.8
Exoskeletons Performance Index (W/kg)	**0.18**	0.12	**0.41**	0.06	**0.56**	0.10	**0.65**	0.10	p=0.01 1.4>0.8

n=9, See Materials and Methods for calculations.

THSD=Tukey Honestly Significant Difference Test Results; **SE**=Standard Error

Δ=Powered-Unpowered

Step Length: 0.8xL*, 1.0xL*, 1.2xL*, 1.4xL*; **L*** is preferred step length at 1.25 m/s.

p<0.05 indicates statistical significance.

*** indicates statistical power >0.65; ** indicates statistical power >0.80.**

Table A.9. Chapter three root mean square electromyography and statistics.

METRIC	0.8 x Preferred Step Length				1.0 x Preferred Step Length				1.2 x Preferred Step Length				1.4 x Preferred Step Length				Step Length p-value; THSD
	Unpowered		Powered		Unpowered		Powered		Unpowered		Powered		Unpowered		Powered		
	Mean	SE	Mean	SE	Mean	SE	Mean	SE	Mean	SE	Mean	SE	Mean	SE	Mean	SE	
Sol RMS (unitless)	**0.58**	0.04	**0.52**	0.08	**0.65**	0.02	**0.54**	0.03	**0.83**	0.03	**0.66**	0.02	**1.00**	0.00	**0.81**	0.03	p<0.0001** 1.4>1.2,1.0,0.8 1.2>1.0,0.8 1.0>0.8
TA RMS (unitless)	**0.48**	0.05	**0.55**	0.08	**0.64**	0.04	**0.62**	0.04	**0.85**	0.03	**0.73**	0.04	**1.00**	0.00	**0.87**	0.07	p<0.0001** 1.4>1.2,1.0,0.8 1.2>1.0,0.8 1.0>0.8
MG RMS (unitless)	**0.68**	0.04	**0.64**	0.07	**0.74**	0.03	**0.70**	0.05	**0.82**	0.02	**0.75**	0.02	**1.00**	0.00	**0.87**	0.03	p<0.0001** 1.4>1.2,1.0,0.8 1.2>0.8
LG RMS (unitless)	**0.41**	0.05	**0.37**	0.04	**0.56**	0.05	**0.48**	0.03	**0.71**	0.05	**0.66**	0.04	**1.00**	0.00	**0.87**	0.04	p<0.0001** 1.4>1.2,1.0,0.8 1.2>1.0,0.8 1.0>0.8

	0.8 x Preferred Step Length Condition p-value; THSD	1.0 x Preferred Step Length Condition p-value; THSD	1.2 x Preferred Step Length Condition p-value; THSD	1.4 x Preferred Step Length Condition p-value; THSD
Sol RMS (unitless)	p=0.28	p=0.002** Powered<Unpowered	p<0.0001** Powered<Unpowered	p=0.0001** Powered<Unpowered
TA RMS (unitless)	p=0.22	p=0.46	p=0.003** Powered<Unpowered	p=0.08
MG RMS (unitless)	p=0.32	p=0.35	p=0.009** Powered<Unpowered	p=0.002** Powered<Unpowered
LG RMS (unitless)	p=0.21	p=0.06	p=0.36	p=0.006** Powered<Unpowered

n=9, See Materials and Methods for calculations.

THSD=Tukey Honestly Significant Difference Test Results; **SE**=Standard Error

Sol=Soleus; **TA**=Tibialis Anterior; **MG**=Medial Gastrocnemius; **LG**=Lateral Gastrocnemius;

Values are stance phase root mean square (RMS) amplitude normalized to Unpowered 1.4 x preferred step length
Condition: Unpowered, Powered; **Step Length:** 0.8xL*, 1.0xL*, 1.2xL*, 1.4xL*

L* is preferred step length at 1.25 m/s.

p<0.05 indicates statistical significance. * indicates statistical power >0.65; ** indicates statistical power >0.80.

Table A.10. Chapter three gait kinematics and statistics.

METRIC	0.8 x Preferred Step Length				1.0 x Preferred Step Length				1.2 x Preferred Step Length				1.4 x Preferred Step Length				Step Length p-value; THSD
	Unpowered		Powered		Unpowered		Powered		Unpowered		Powered		Unpowered		Powered		
	Mean	SE	Mean	SE	Mean	SE	Mean	SE	Mean	SE	Mean	SE	Mean	SE	Mean	SE	
Step Length (mm)	**572**	6	**565**	9	**723**	8	**715**	10	**854**	12	**841**	13	**980**	12	**967**	9	p<0.0001** 1.4>1.2,1.0,0.8 1.2>1.0,0.8 1.0>0.8
Step Width (mm)	**123**	8	**127**	12	**111**	10	**111**	12	**107**	6	**113**	10	**123**	11	**125**	9	p=0.002** 1.4>1.2,1.0 1.2<0.8 1.0<0.8
Step Period (ms)	**570**	5	**570**	6	**570**	5	**570**	6	**568**	6	**565**	6	**568**	5	**566**	4	p=0.13
Double Support Period (ms)	**146**	5	**144**	5	**132**	5	**133**	5	**116**	4	**117**	3	**106**	3	**106**	4	p<0.0001** 1.4<1.2,1.0,0.8 1.2<1.0,0.8 1.0<0.8

	0.8 x Preferred Step Length Condition p-value; THSD	1.0 x Preferred Step Length Condition p-value; THSD	1.2 x Preferred Step Length Condition p-value; THSD	1.4 x Preferred Step Length Condition p-value; THSD
Step Length (mm)	p=0.09	p=0.04 Powered<Unpowered	p=0.07	p=0.01
Step Width (mm)	p=0.57	p=0.90	p=0.37	p=0.71
Step Period (ms)	p=1.00	p=0.81	p=0.57	p=0.47
Double Support Period (ms)	p=0.27	p=0.63	p=0.87	p=0.96

n=9, See Materials and Methods for calculations.

THSD=Tukey Honestly Significant Difference Test Results; **SE**=Standard Error

Condition: Unpowered, Powered; **Step Length:** 0.8xL*, 1.0xL*, 1.2xL*, 1.4xL*

L* is preferred step length at 1.25 m/s.

p<0.05 indicates statistical significance. * indicates statistical power >0.65; ** indicates statistical power >0.80.

Table A.11. Chapter four net metabolic power and statistics.

	METRIC	Unpowered		Powered		Condition p-value; THSD
		Mean	SE	**Mean**	SE	
0% Grade	**Net Metabolic Power (W/kg)**	**3.36**	0.13	**2.91**	0.13	p=0.0002** Powered<Unpowered
5% Grade	**Net Metabolic Power (W/kg)**	**5.23**	0.13	**4.65**	0.15	p<0.0001** Powered<Unpowered
10% Grade	**Net Metabolic Power (W/kg)**	**7.41**	0.15	**6.55**	0.19	p<0.0001** Powered<Unpowered
15% Grade	**Net Metabolic Power (W/kg)**	**9.79**	0.23	**8.80**	0.26	p<0.0001** Powered<Unpowered

	Gradient p-value; THSD
Net Metabolic Power (W/kg)	p<0.0001** 15%>10%,5%,0% 10%>5%,0% 5%>0%

n=9, See Materials and Methods for calculations.

THSD=Tukey Honestly Significant Difference Test Results; **SE**=Standard Error

Condition: Unpowered, Powered; **Gradient:** 0%,5%,10%,15%

p<0.05 indicates statistical significance.

*** indicates statistical power >0.65; ** indicates statistical power >0.80.**

Table A.12. Chapter four exoskeletons performance metrics and statistics.

METRIC	Powered 0% Grade		Powered 5% Grade		Powered 10% Grade		Powered 15% Grade		Gradient p-value; THSD
	Mean	SE	**Mean**	SE	**Mean**	SE	**Mean**	SE	
Positive Exoskeletons Mechanical Power (W/kg)	**0.23**	0.02	**0.28**	0.02	**0.33**	0.03	**0.37**	0.03	p<0.0001** 15%>10%,5%,0% 10%>5%,0% 5%>0%
Negative Exoskeletons Mechanical Power (W/kg)	**-0.02**	0.01	**-0.01**	0.00	**-0.03**	0.01	**-0.02**	0.00	p=0.52
ΔNet Metabolic Power (W/kg)	**-0.45**	0.07	**-0.58**	0.07	**-0.86**	0.06	**-0.98**	0.12	p<0.0001** 15%<5%,0% 10%<5%,0%
Exoskeletons Performance Index (W/kg)	**0.47**	0.05	**0.54**	0.06	**0.68**	0.06	**0.66**	0.06	p=0.02* 15%>0% 10%>0%

n=9, See Materials and Methods for calculations.

THSD=Tukey Honestly Significant Difference Test Results; **SE**=Standard Error

Δ=Powered-Unpowered

Gradient: 0%, 5%, 10%, 15%

p<0.05 indicates statistical significance.

*** indicates statistical power >0.65; ** indicates statistical power >0.80.**

Table A.13. Chapter four root mean square electromyography and statistics.

METRIC	0% Grade				5% Grade				10% Grade				15% Grade				Gradient p-value; THSD
	Unpowered		Powered		Unpowered		Powered		Unpowered		Powered		Unpowered		Powered		
	Mean	SE	Mean	SE	Mean	SE	Mean	SE	Mean	SE	Mean	SE	Mean	SE	Mean	SE	
Sol RMS (unitless)	**0.76**	0.04	**0.57**	0.03	**0.86**	0.04	**0.71**	0.02	**0.89**	0.03	**0.75**	0.03	**1.00**	0.00	**0.82**	0.02	p<0.0001** 15%>10%,5%,0% 10%>0% 5%>0%
TA RMS (unitless)	**0.93**	0.13	**0.84**	0.13	**1.04**	0.12	**0.90**	0.10	**1.02**	0.09	**0.94**	0.07	**1.00**	0.00	**0.92**	0.07	p=0.51
MG RMS (unitless)	**0.64**	0.03	**0.60**	0.03	**0.82**	0.04	**0.73**	0.04	**0.93**	0.03	**0.87**	0.03	**1.00**	0.00	**0.95**	0.04	p<0.0001** 15%>10%,5%,0% 10%>5%,0% 5%>0%
LG RMS (unitless)	**0.64**	0.06	**0.48**	0.04	**0.73**	0.03	**0.64**	0.02	**0.85**	0.04	**0.79**	0.04	**1.00**	0.00	**0.85**	0.03	p<0.0001** 15%>10%,5%,0% 10%>5%,0% 5%>0%

	0% Grade Condition p-value; THSD	5% Grade Condition p-value; THSD	10% Grade Condition p-value; THSD	15% Grade Condition p-value; THSD
Sol RMS (unitless)	p=0.0008** Powered<Unpowered	p=0.0007** Powered<Unpowered	p<0.0001** Powered<Unpowered	p<0.0001** Powered<Unpowered
TA RMS (unitless)	p=0.16	p=0.04 Powered<Unpowered	p=0.41	p=0.22
MG RMS (unitless)	p=0.34	p=0.01** Powered<Unpowered	p=0.08	p=0.21
LG RMS (unitless)	p=0.002** Powered<Unpowered	p=0.006** Powered<Unpowered	p=0.07	p=0.001** Powered<Unpowered

n=9, See Materials and Methods for calculations.

THSD=Tukey Honestly Significant Difference Test Results; **SE**=Standard Error

Sol=Soleus; **TA**=Tibialis Anterior; **MG**=Medial Gastrocnemius; **LG**=Lateral Gastrocnemius;

Values are stance phase root mean square (RMS) average amplitude normalized to Unpowered 15%

Condition: Unpowered, Powered; **Gradient:** 0%, 5%, 10%, 15%

p<0.05 indicates statistical significance. * indicates statistical power >0.65; ** indicates statistical power >0.80.

Table A.14. Chapter four gait kinematics and statistics.

METRIC	0% Grade				5% Grade				10% Grade				15% Grade				Gradient p-value; THSD
	Unpowered		Powered		Unpowered		Powered		Unpowered		Powered		Unpowered		Powered		
	Mean	SE	Mean	SE	Mean	SE	Mean	SE	Mean	SE	Mean	SE	Mean	SE	Mean	SE	
Step Length (mm)	**729**	4	**722**	8	**734**	7	**731**	13	**723**	11	**718**	16	**712**	13	**709**	16	p=0.02* 15%<5%
Step Width (mm)	**99**	12	**106**	13	**107**	12	**109**	11	**112**	11	**114**	8	**118**	9	**120**	6	p=0.004** 15%>0%
Step Period (ms)	**573**	3	**574**	5	**575**	6	**576**	9	**570**	9	**572**	12	**559**	11	**562**	12	p=0.04* 15%<5%
Double Support Period (ms)	**136**	4	**136**	5	**137**	4	**137**	6	**138**	5	**137**	6	**135**	5	**138**	6	p=0.90

	0% Grade Condition p-value; THSD	5% Grade Condition p-value; THSD	10% Grade Condition p-value; THSD	15% Grade Condition p-value; THSD
Step Length (mm)	p=0.30	p=0.73	p=0.70	p=0.73
Step Width (mm)	p=0.20	p=0.74	p=0.71	p=0.63
Step Period (ms)	p=0.84	p=0.94	p=0.85	p=0.75
Double Support Period (ms)	p=0.79	p=0.94	p=0.93	p=0.39

n=9, See Materials and Methods for calculations.

THSD=Tukey Honestly Significant Difference Test Results; **SE**=Standard Error

Condition: Unpowered, Powered; **Gradient:** 0%, 5%, 10%, 15%

p<0.05 indicates statistical significance. * indicates statistical power >0.65; ** indicates statistical power >0.80.